UNIVERSITÀ DEGLI STUDI DI MILANO

FACOLTA' DI MEDICINA E CHIRURGIA

CORSO DI DOTTORATO DI RICERCA IN

TRANSLATIONAL MEDICINE

CICLO XXXV

DIPARTIMENTO DI "***Clinical Sciences and Community Health***"

TESI DI DOTTORATO DI RICERCA

Dietary interventions targeting glucose metabolism and hyperinsulinemia: a new translational perspective for the management of Acute Intermittent Porphyria

Settore Scientifico Disciplinare

MED/09

Candidata **Miriam Longo**

Matricola N° **R12620**

TUTOR: **Prof. Irene Motta**

COORDINATORE DEL DOTTORATO: **Prof. Chiarella Sforza**

Anno Accademico (A.A)

2021-2022

Summary

Abstract

Acute Intermittent Porphyria (AIP) represents the most severe form of hepatic porphyrias, an inherited disorder caused by genetic mutations in the *hydroxymethylbilane synthase* (*HMBS*) gene, encoding the porphobilinogen deaminase (PBGD) enzyme and reducing hepatic heme availability. In stressful conditions, as fasting, which stimulates the demand of heme production, the delayed heme biosynthesis leads to the accumulation of porphyrins 'precursors, involved in neurotoxicity, and hyperactivity of ALAS1, the first rate-limiting enzyme of the heme pathway. AIP clinical manifestations presents in 0.5-1% of *HMBS*-mutation carriers and includes severe neurovisceral/neuropsychiatric acute attacks, which are managed with hemin administration and Givosiran, both directed against the hepatic ALAS1 activity. For mild AIP cases, glucose represents an alternative strategy to downregulate ALAS1. Nonetheless, current therapies showed several limitations as biochemical/clinical relapse, raise in transaminases and renal adverse events, thereby encouraging researchers to develop safer therapeutics for the treatment of refractory symptomatology.

Recently, it has emerged that AIP mice developed glucose intolerance and hyperinsulinemia during fasting. In this model, hepatic glycogen storages were not exploited to normalize glycemia and alternative mechanisms as ketogenesis were aberrantly activated to face with energy demand. In addition, AIP patients with clinically stable disease or highly porphyrins' excreters may develop similar metabolic disturbances, which may alter the response to glucidic therapy. In these subset of patients, hyperinsulinemia was associated with a protection against the acute symptomatology, possibly due to the *ALAS1* downregulation mediated by insulin. Despite the protection from the acute episodes, stable AIPs (>90%) did not benefit of any therapeutic treatment albeit they are at risk to develop metabolic-associated disorders, as diabetes, chronic kidney disease and liver cancer due to the high exposure to toxic porphyrins, opening the possibility to introduce insulin-sensitizers as a novel class for AIP management.

Therefore, aims of this study were to assess whether nutritional interventions may correct metabolic dysfunctions observed in AIP, possibly providing the proof-of-concept that metabolic and hepatic assessment of AIP patients, which still do not represent a routine clinical practice, may address towards a personalized medicine. For this purpose, we

tested insulin-sensitizing compounds, which have recently shown attractive results for the management of diabetes and metabolic syndrome in preclinical models and patients.

Firstly, the study deepened the role of an insulin-mimetic, the α-lipoic acid (α-LA), in *PBGD*-silenced hepatocytes and in a genetic AIP murine model, as it showed beneficial effects in porphyria cutanea tarda in previous findings. α-LA enhanced hepatocellular heme pool, glycolysis, and ATP production in *in vitro* model during stressful conditions. Similarly, α-LA administration in AIP mice increased hepatic heme, ATP content and citrate synthase activity during fasting, supporting that this molecule may provide substrates for heme biosynthesis by stimulating Krebs cycle and ameliorate the two major energy-yielding pathways, glycolysis and mitochondrial respiration. Furthermore, it rescued hyperinsulinemia in fasted AIP mice, leading to a great improvement of hepatic glucose metabolism and systemic energetic balance. Indeed, the aberrant activation of insulin signaling, observed during caloric restriction in the livers of AIP mice, was recovered after the α-LA supplementation. Still, AIP+α-LA induced glycogenolysis in fasted state and increased the glucose-sensing Glut2 protein levels in the liver, supporting that α-LA may promote the hepatic glucose export during fasting in order to provide glucidic reserves to the other organs as physiologically occurs. After glucose injection, AIP mice receiving α-LA improved GTT and glucose uptake on PET/CT scans in the liver and brain, skeletal muscle and white adipose tissue (WAT). From PET/CT results, it has emerged that AIP mice enhanced brown adipose tissue (BAT) activation, used as a mean of heat production from glucidic/lipidic sources, after cold stress compared to Wt, probably as an adaptive mechanism to meet whole-body energy requests. Interestingly, AIP+ α-LA did not show a higher BAT metabolic activity, similar to Wt, thus sustaining the improvement of AIP energy status and that the insulin-mimic may avoid energy dissipation attempting to preserve energy reserves.

We then focused on the potential efficacy of probiotics, as dietary consumption of fermented-foods has been proposed as an effective solution to achieve health benefits for common metabolic disorders, in which adiposity represent one of the main risk factors. Nonetheless, their applications in rare disorders has been scarcely investigated. Here, we examined heat-killed probiotic *Bifidobacterium animalis subsp. lactis CECT 8145* (BLP1), the BLP1-derived postbiotic lipoteichoic acid (LTA), which is responsible of many of the BLP1 health cares, and the alive probiotic *Bacillus coagulans* (*B. coagulans*),

whose spores resist to heat temperatures, more than other probiotic strains, during manufacturing processes of fortified foods. These compounds mainly modify intestinal microbial composition and stimulate fat disposal in the liver and WAT. Lipid breakdown and heat dissipation are mediated by BAT, resulting in an improvement of body weight and insulin sensitivity. Here, we found that the use of probiotics (heat-killed or alive) or postbiotic ameliorated glucose tolerance, hyperinsulinemia, lean/mass ratio and muscular energy utilization. However, they boosted a potentially maladaptive BAT activation, which was observed in AIP mice after cold stress, supporting that, although biochemical and glucidic response were improved, a careful monitoring of their energetic status after the prolonged supplementation with these diets need to be considered.

As a translational approach, we firstly provided a metabolic and hepatic characterization in a series of AIP patients (n=14), who were stratified according to recurrence of the attack as following: a) stable AIPs (n=9) who were asymptomatic highly excreters, and b) active AIPs (n=5) who manifested >2 annual attacks. AIP patients underwent bioimpedance analysis, which provided information about energetic status of AIP. We found that stable AIPs had higher % metabolic active cells in skeletal muscle compared to active AIPs, correlating with %lean mass fraction, suggesting that most of the muscle mass in AIP patients pushed their metabolic activity. Similar to AIP models, stable AIPs had altered OGTT curve paralleled by higher insulin levels and HOMA-IR. Therefore, stable AIP patients showed both signs of early hyperinsulinemia and muscle hypermetabolism, possibly being part of an adaptive para-physiologic mechanism to prevent energy substrate deficiency. Mild-moderate fibrosis was non-invasively detected in 5/9 stable AIP cases but not in active ones. Liver stiffness values were significantly correlated with urinary ALA, suggesting a direct role of this porphyrin to induce liver damage, and showed a positive correlation with insulin levels and HOMA-IR, corroborating that metabolic and hepatic screening should be introduced for monitoring and management of AIP.

Introduction

1. Porphyrias: an overview of genetics, diagnosis, and management

Porphyrias refer to a family of rare inherited disorders due to genetic mutations in one of the eight enzymes involved in heme biosynthesis, causing a reduction of the heme production on one side and, on the other side, an excessive accumulation of potentially dangerous heme-derived intermediates (heme precursors or porphyrins and/or porphyrin precursors) in blood, tissues, and urine. Bone marrow and the liver are the major tissues in which heme synthesis occurs [10]. According to the enzyme deficiency and the site of heme precursors' accumulation, porphyrias may be distinguished into two major groups: 1) cutaneous porphyrias (CPs), which are characterized by skin blistering and scarring, pain and/or redness and swelling in sun-exposed areas; 2) acute hepatic porphyrias (AHPs) which involve the nervous system. Some types of porphyria have both neurological and photosensitive symptoms. The CPs include the erythropoietic protoporphyria (EPP), the X-linked protoporphyria (XLP), the congenital erythropoietic porphyria (CEP), the porphyria cutanea tarda (PCT) and its homozygous form, and the hepatoerythropoietic porphyria (HEP), while the δ-aminolaevulinic acid (ALA) dehydratase deficiency porphyria (ALAD), acute intermittent porphyria (AIP), variegate porphyria (VP) and hereditary coproporphyria (HCP) belong to the AHPs group[11,12]. The present thesis will focus on studying AIP, the most common and severe form of AHPs.

The haploinsufficiency of the *hydroxymethylbilane synthase* (HMBS) gene, encoding the porphobilinogen deaminase (PBGD) enzyme, is at the core of the AIP onset. The PBGD half-activity, which catalyzes four consecutive reactions to convert porphobilinogen (PBG) into hydroxymethylbilane (HMB), contributes to the decrease of the hepatic heme availability followed by the loss of the negative feedback exerted by the heme pool on the first rate-limiting enzyme of this via, the 5-aminolevulinic acid synthase-1 (ALAS1). The upregulation of the ALAS1 combined with the slowdown of the heme production participates in increasing the precursors' concentration in the liver, plasma, and urine, which are implicated in the neurotoxicity, tissue damage, and AIP manifestations[13-15].

In most cases, AIP symptomatology is precipitated by endogenous and/or exogenous factors (estrogens, fasting, drugs, infections, alcohol, or physical stress). Precipitating factors share a common mechanism, the increased demand for hepatic heme synthesis, thus promoting the ALAS1 activity and pushing porphyrins and porphyrin precursors'

overproduction and accumulation, especially of 5-aminolevulinic acid (ALA) and porphobilinogen (PBG). Life-threatening acute attacks with gastrointestinal symptoms (abdominal pain, vomiting, nausea, constipation) and neuropsychiatric disorders (seizures, weakness, insomnia, hallucinations, confusion) are the major discomfort which affects AIP patients. In some cases, peripheral motor neuropathy and central nervous system disturbances accompanied by hypertension, hyponatremia, and nephropathy may arise in severe AIP subjects, thereby representing a long-life burden for both patients and relatives[13].

AIP is frequently misdiagnosed for its non-specific, episodic manifestations, and disease surveillance consists of avoiding exposure to precipitating factors. For instance, AIP at-risk patients should not restrict calories and carbohydrate intake, except for short periods and under the supervision of specialists. The first-line strategy to manage and/or prevent acute episodes is represented by hemin infusion. Glucose solution could be alternatively considered for mild cases and in the absence of hemin, although its use in controlled trials led to inconclusive results. Both hemin and carbohydrate loading reduce the hepatic ALAS1 activity, thus providing a transitory alleviation of the symptoms. However, the only curative option is replenishing the defective PBGD to the extent that refractory AIP recipients who underwent liver transplantation (LT) have shown a complete biochemical and clinical remission[16-19]. In 2019, the small interfering RNA (siRNA) molecule targeting the hepatic *ALAS1* mRNA (Givosiran) was approved by the Food and Drug Administration (FDA) for the treatment of adult severe patients affected by AIP due to the positive results obtained by the phase III ENVISION trial (NCT03338816)[2]. Nonetheless, recurrent attacks may affect patient's quality of life and increase the risks of co-morbidities and mortality. Several shortcomings emerged with the abovementioned therapies, encouraging this research branch to develop novel and safer therapeutics. Up to now, new proposals to treat severe AIPs aim at restoring the hepatic PBGD expression and activity, and they include 1) gene therapy, 2) the mRNA-based strategies by which PBGD mRNA is incorporated in lipid nanoparticles (LNP), and 3) the recombinant PBGD protein fused to the liver-directed apolipoprotein A1 (ApoA1)[2,20-23].

Notwithstanding, the larger portion of AIP patients (over 90%), some of whom are high excreters of ALA and PBG (ASHE), remain asymptomatic throughout their life (latent AIP), and they are not eligible to receive any treatment. The 46.4% of these subjects

reported chronic symptoms (abdominal pain, fatigue, muscle pain, and insomnia) and may manifest renal failure and hepatocellular carcinoma (HCC) due to the high exposure to ALA, urging the need to provide careful monitoring of AIP subjects regardless the recurrence of the attack. Interestingly, the characterization of metabolic profiles in AIP experimental models and humans has highlighted that alterations of glucose metabolism, hyperinsulinemia, and mitochondrial bioenergetics may be part of AIP pathophysiology, possibly explaining the low efficacy of glucose-based therapy and offering the possibility to consider insulin and insulin-mimetics for the clinical management of AIP[24-27]. Notably, latent AIPs seem to be highly predisposed to manifest hyperinsulinemia and aberrant glucidic metabolism, which, on one side, may reduce the susceptibility to the acute attack but, on the other side, may increase the risk of dysmetabolic-associated complications[27].

2. Acute intermittent porphyria (AIP): prevalence, penetrance, and genetic traits

AIP is an autosomal dominant disorder caused by inborn errors in the *HMBS* gene, whose prevalence hovers around 1/1700 cases and whose penetrance may vary across geographical areas[28,29]. Although the frequency of the *HMBS* mutations is relatively high, AIP is generally characterized by low and incomplete clinical penetrance, encompassing ~0.5-1% of cases in the general population and presenting in women more than men[28,29]. In a retrospective study, Bauman and collaborators calculated the penetrance from 23 families recorded at the Finnish porphyria registry (n=515 AIP) and showed that penetrance was higher in females compared to males (50% vs.. 17%) and the rate of hospitalization for women reached 41%[28]. Likewise, Lenglet et al. carried out an intra-familial study including 253 AIP families selected from the French reference center of porphyria (CFP). They estimated clinical penetrance in AIP families was 22.9% compared to those observed in the general population [29]. The authors explained this discrepancy as a result of highly harmful genetic traits detected in AIP French descendants combined to environmental factors predisposing them to acute attacks. Among the *HMBS* mutation, it has emerged the p.Ala122Pro, p.Arg167Gln, p.Arg175Gln, p.Arg195Cys, and p.Arg355Gln variants, which encoded an inactive protein, and the p.Glu86Val, p.Arg321His, and p.Asp359Asn mutations which reduced PBGD enzymatic activity to 50%. The presence of null alleles, leading to the complete

loss of function of the PBGD protein, was more frequent than missense mutations in families with AIP and correlated with the severity of disease manifestation[29].

The wide heterogeneity of AIP phenotypic expression is partially explained by the huge variability of mutations detected in the *HMBS* gene. To date, the Human Gene Mutation database (https://www.hgmd.cf.ac.uk/ac/gene/index.php) lists 421 genetic variants affecting the *HMBS* gene of whom the largest portion is represented by missense/nonsense variations (n=171), followed by splicing mutations (n=91), small deletions/insertions (n=125), large deletions/insertions/duplications (n=15), complex rearrangements, mutations in regulatory regions and small indels (n=17).

Two mRNAs, which derive from *HMBS* alternative splicing and differ at the 5'-end, encode two PBGD isozymes: 1) the erythroid-specific isoform is encoded by exons 2–15 and its promoter is positioned at intron 1, whereas 2) the housekeeping isoform is encoded by exon 1 and exons 3–15 with the housekeeping promoter located in the 5' flanking region upstream of exon 1[30]. The majority of patients with AIP carries the *HMBS* mutations in exons 3–15, which affect both PBGD isoforms, while mutations in exon 1 do not influence PBGD functionality in erythrocytes[31]. Additionally, it has been identified that few *HMBS* mutations are relatively more common than others, such as the p.R173W and p.R167Q variants, caused by CpG methylation, and the p.G111R and p.W198X variants, which are most frequent in Argentina and Sweden due to the founder effect[32-34]. The p.W198X alongside c.1073delA, and p.R26C variants were correlated with both higher penetrance and clinical manifestations, while other variants such as p.R167W, p.R225G, and c.G33T were associated with lower penetrance and mild clinical events. Concerning the p.R173W mutation, a reduced penetrance was observed in Finland, whereas it was much higher in Northern Sweden and Spain[35]. A correlation between the presence of p.R116W, p.R173W, p.R149X, p.Q217H, p.G218R, p.A219P, and p.A330P mutations and the severity of AIP manifestations was also predicted through a bioinformatic approach[36]. To conclude, AIP prevalence in the population is high, although its penetrance is exceptionally low, resulting in the difficult identification of asymptomatic individuals with AIP. Moreover, the different penetrance rates of symptomatology in the relatives of French patients with AIP underline that AIP inheritance could be modulated by the environment and other so far unknown genetic factors independently of *HMBS* variations.

3. Heme biosynthesis in the liver and AIP pathogenesis

The heme biosynthesis consists of eight enzymatic steps which take place into the mitochondria and in the cytosol, even if some evidence highlighted that intestinal absorption and intracellular transporters may participate in enhancing its availability[37]. Heme is a prosthetic component of a wide variety of hemoproteins as hemoglobin, myoglobin, catalases, heme peroxidases, respiratory cytochromes, and cytochrome P450 enzymes (CYPs). The erythroid cells account for 80% of daily heme production, followed by the hepatocytes, which mainly exploit it for the CYPs, particularly enriched in the endoplasmic reticulum (ER), and the respiratory chain complexes.

The heme biosynthesis begins in mitochondria. The first enzyme, the ALAS1, condensates the succinyl-CoA, an intermediate derived from the tricarboxylic acid (TCA) cycle, and the amino acid glycine in order to generate ALA. In the second step, two ALA molecules move outside the mitochondria towards the cytosol where the ALA dehydratase (ALAD) converts them into monopyrrole-PBG. Then, the PBGD enzyme provides the polymerization of four PBG molecules in order to synthesize the linear tetrapyrrole HMB. In the fourth step, the uroporphyrinogen (UROgen) III synthase (UROS) converts the HMB into UROgen III, resulting from the cyclization of the tetrapyrrole structure and the formation of the porphyrin ring. Four carboxyl groups are sequentially removed from the carboxymethyl side chains of the UROgen III by the UROgen decarboxylase (UROD), leading to the coproporphyrinogen III (COPROgen) production. At this point, the heme biosynthesis continues and concludes in the mitochondria. The COPROgen III undergoes sequential steps of decarboxylation and oxidation: the first one is performed by the COPROgen III oxidase (CPOX), which removes the carboxyl group and two hydrogens from the COPROgen III, yielding the protoporphyrinogen IX (PROTOgen IX); the second one is caused by the PROTOgen oxidase (PPOX) which removes six atoms of hydrogen thus synthetizing the first colored and fully oxidized tetrapyrrole intermediate, the protoporphyrin IX (PROTO IX). Finally, the ferrochelatase inserts a ferrous ion (Fe^{2+}) into the PROTO IX ring to form the heme[12]. Genetic mutations in the *HMBS* gene lead to a reduction of enzyme PBGD activity, thereby decreasing hepatic heme production. In physiologic conditions, the excess of heme, which is not incorporated in the hemoproteins ‘structure, allosterically inhibits the

ALAS1. Notwithstanding, the shutdown of heme biosynthesis caused by the PBGD haploinsufficiency diminishes the effect of the heme regulatory feedback on ALAS1, resulting in the overproduction and accumulation of ALA and PBG in the liver, circulation, and urine. ALA is the major trigger of neurological damage involved in autonomic, peripheral neuropathy, and encephalopathy. Due to its high structural similarity with the γ-aminobutyric acid (GABA) and glutamate neurotransmitters, ALA may compete for binding to GABA-receptors and may modify the GABAergic system by inhibiting the GABA release from the pre-synaptic terminals[15,27,38].

Moreover, ALA may contribute to the generation of free radicals and reactive oxygen species (ROS) and promote hepatic ROS-induced genomic and mitochondrial DNA damage (mtDNA) which predisposes patients with AIP to a higher risk of developing HCC[39-41]. Although it has been broadly established that the symptoms of acute attacks are mainly attributed to the accumulation of neurotoxic metabolites, there is no conclusive evidence to date about the factors influencing penetrance and the wide variability in clinical manifestations. Indeed, ~90% of patients with AIP remain asymptomatic and/or high excreters of porphyrins (ASHE) throughout their life, suggesting that other hits may be implicated in the pathophysiology of AIP and the precipitation of the acute events[27].

Metabolic alterations were observed in both AIP animal models and patients and have suggested new insights into the pivotal role of the liver in the pathogenesis of the acute attacks. The first evidence was obtained from patients with AIP who improved biochemical and clinical abnormalities after LT[42,43]. Conversely, patients affected by HCC who received livers from donors with AIP developed neurovisceral symptoms with increased ALA and PBG levels[19].

Most recently, AIP experimental models showed impaired glucose metabolism and mitochondrial respiration capacity during acute attacks, while *HMBS*-mutation carriers displayed high body weight, hyperinsulinemia, and alterations in serum lipid profiles combined with IR[24,44,45]. These findings suggest that AIP may be considered a genetic disorder characterized by an umbrella of metabolic dysfunctions, thereby adding additional knowledge about its pathophysiology and, possibly, novel curative strategies. The effect of PBGD haploinsufficiency on heme biosynthesis is represented in **Figure 1**[27].

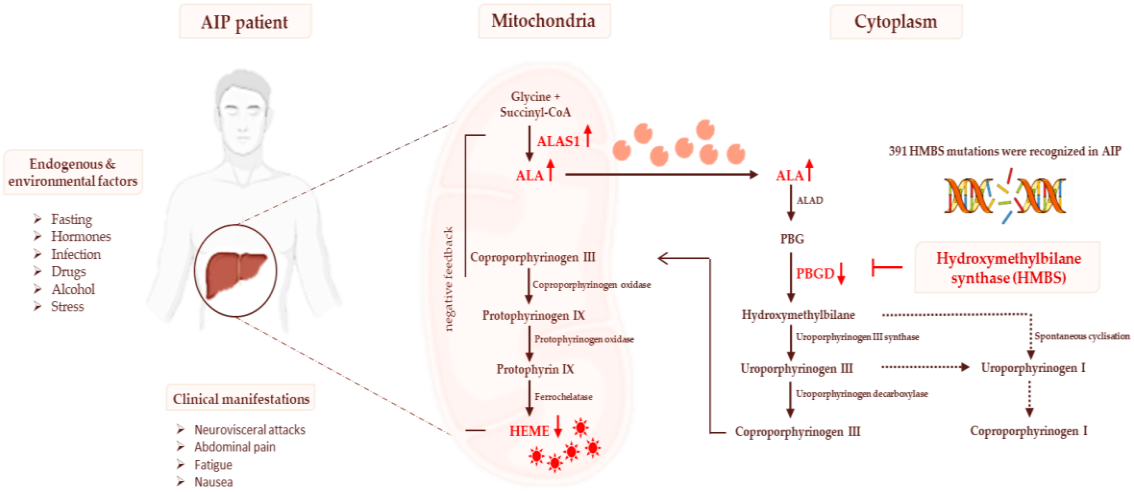

Figure 1: The heme biosynthetic cascade and AIP pathophysiology. Heme biosynthesis starts in mitochondria with the conversion of glycine and succinyl-CoA to δ-aminolaevulinic acid (ALA) through the ALA synthase-1 (ALAS1) enzyme. In the cytoplasm, ALA is converted to porphobilinogen (PBG) up to COPROgen III. The latter is shuttled into mitochondria again for the synthesis of heme, which in turn inhibits ALAS1. The PBGD enzyme deficiency (encoded by the *hydroxymethylbilane synthase* (*HMBS*) gene) causes a reduction in hepatic heme synthesis, leading to the loss of the negative feedback on ALAS1. Precipitating factors may enhance the demand of heme production in the liver, causing the upregulation of the ALAS1 paralleled by the increased levels of porphyrin neurotoxic precursors (ALA and PBG), which accumulate in the liver, blood, and urine. From Longo M., Paolini E Meroni M. and Dongiovanni P.-Biomedicines, 2022.

3.1. Metabolic implications in AIP pathogenesis: the role of glucose homeostasis and hyperinsulinemia

Lifestyle factors such as smoking, alcohol, stress, dieting and caloric restriction are candidate triggers of acute attacks in AIP patients. In 2012, a study carried out by Garcia-Diz et al. suggested that AIP subjects are at high-stakes of malnutrition, showing low consumption of complex carbohydrates, monounsaturated/polyunsaturated fatty acids (MUFAs and PUFAs), and folic acid[46]. In the recent years, it has been shown that high

sugar, fruit juices, and candies intake alongside hyperinsulinemia correlated with less disease activity, to the extent that a well-balanced diet has been recommended in AIP subjects attempting to prevent the symptomatology and glucose infusions have been included for the management of minor symptoms [24,46,47].

Nevertheless, several findings have highlighted that alterations of glucose metabolism, mitochondrial bioenergetics, and hormonal dysregulation may arise in AIP pathophysiology, thus constraining the glucidic-based approaches. Matkovic et al. provided the evidence that glucose metabolism may be modeled by precipitating factors in an inducible model of AIP. They exposed female rats to a combination of 2-allyl-isopropylacetamide (AIA) and 3,5-diethoxycarbonyl-1,4-dihydrocollidine (DCD), two porphyrinogenic drugs, and observed a downregulation of the enzymes involved in the gluconeogenesis and glycogenolysis as phosphoenolpyruvate carboxykinase (PEPCK) and glycogen phosphorylase (GP) by 43-46% compared to the wild-type (Wt)[44]. Carbohydrate deprivation is directly involved in the reduction of heme synthesis and in the susceptibility to the acute events. Low glucose supply limits the availability of TCA cycle intermediates (i.e., succinyl-CoA), reducing equivalents (NADH/FADH2) and ATP levels, thus impairing mitochondrial bioenergetics.

Moreover, in a murine genetic model of AIP, in which hepatic PBGD activity was reduced by 30%, Collantes and collaborators demonstrated that AIP rodents aberrantly responded to caloric restriction. During fasting, Wt mice induced hepatic glycogen catabolism to re-establish glucose homeostasis, while AIP animals activated ketogenesis and gluconeogenesis, increasing ketone bodies as alternative energy sources[45]. Hepatic and muscular glycogen breakdown is hormonally driven by glucagon and insulin in response to blood glucose levels. Interestingly, in both inducible and genetic models of AIP, serum insulin exceeded the physiological range by up to six-fold in case of low glucose concentration. In contrast, glucagon levels were reduced, thus supporting that disturbances of glucose metabolism may occur consequently at hormonal dysregulation[24,25,27,44,45].

Insulin modulates the hepatic ALAS1 activity by inhibiting its translocation from the cytosol into mitochondria via the phosphatidylinositol-3-kinase(PI3K)/Akt pathway[24,47-49]. According to these findings, a case-control study conducted by Fontanellas' team., including 44 AIP Spanish patients and 55 control volunteers, showed a high prevalence

of insulin resistance index (18.2% *vs* 2.3% in the control population). Among eight AIP individuals with high Homeostasis Model Assessment-Insulin Resistance (HOMA-IR) index, five were even affected by obesity (body mass index (BMI)>30 kg/m^2). Interestingly, patients characterized by IR and high serum insulin levels had stable disease, suggesting a protective role for IR against the acute manifestations[24]. In a population-based study, Andersson and collaborators assessed the effects of diabetes on AIP in northerly counties of Sweden. A total of 319 participants were included, among which 16 had developed diabetes. In these patients, the presence of diabetes was not only associated with a complete biochemical remission and ceasing of the acute attacks, but also with the protection against HCC development, possibly due to a normalization of the ALA levels[49,50]. Conversely, it was reported that diabetes mellitus might activate the hepatic ALAS1 in mice, and a case report revealed that the presence of concomitant overt diabetes mellitus in one patient with AIP was paralleled by the late manifestation of acute episodes, supporting that the role of IR in AIP events needs to be elucidated[51,52].

4. Standard treatments and new advancements in precision medicine for AIP management

The prevalence of AIP accounts for approximately 5 in 100.000 in the United States, and it is higher in Europe (1 in 2000), especially in northern countries as Sweden (1 in 1000) due to the founder effect. In addition, AIP diagnosis may be delayed up to a decade after the first onset of the symptomatology due to its characteristic latent phenotype[53]. Several signs may aid in the correct diagnosis, such as the patient's history, abdominal pain located in the epigastric area, weakness, neuropsychiatric symptoms, and the presence of dark-reddish urines. However, the unspecific manifestations which characterize this disorder may delay the diagnosis and the clinical approach. Screening studies include the evaluation of urinary ALA and PBG which may direct towards the diagnosis of acute porphyrias. To identify the subtype of AHP, analysis of porphyrins in the feces and blood may guide to rule out VP and HCP, as well as the identification of disease-causing mutations should be recommended for diagnostic confirmation[27].

The current standard of care to manage acute crises in patients with AIP aims to reduce hepatic ALAS1 activity and porphyrin precursor excretion. The gold standard for treating AIP is hemin administration, even if carbohydrate loading is considered in mild cases.

LT may represent an alternative option for those patients with high disease activity[16,17]. In 2019, the first liver-targeted strategy based on targeting hepatic *ALAS1* mRNA (Givosiran) through a small interfering RNA (siRNA) molecule was approved for the treatment of adult patients with severe AIP by the Food and Drug Administration (FDA) due to the positive results obtained in the phase III ENVISION trial (NCT03338816)[2]. Nonetheless, recurrent attacks may affect patient quality of life and increase the risks of co-morbidities and mortality, as well as several drawbacks emerged with the abovementioned therapies, thereby urging the development of novel, safer therapeutics. Up to now, gene therapy through viral vectors, the newly mRNA-based therapies by which mRNA is incorporated in lipid nanoparticles (LNPs), and the liver-directed recombinant PBGD protein are slowly receiving approval for the treatment of monogenic disorders because they aim to replace the defective proteins and enzymes [23,54]. In addition, the new awareness of AIP pathogenesis is shifting the attention toward introducing insulin or insulin-mimetics to ameliorate metabolic alterations[24,25].

4.1 Hemin, glucose, and liver transplantation: why research is moving towards new therapies

Intravenous hemin infusion (Normosang®, heme-arginate in Europe; Panhematin®, lyophilized hemin in the USA) is the first-line therapy for AIP patients, especially if they recurrently experience hospitalization or the emergency unit[3,13]. Hemin directly inhibits hepatic ALAS1 transcription and dampens its translocation from the cytosol into the mitochondria[13]. Nonetheless, repeated hemin administration has been associated with hepatic inflammation in *Hmbs*$^{-/-}$ mice with the re-activation of *AlAS1* and *Heme oxygenase 1* (*HO-1*), the latter involved in heme catabolism[55]. In a follow-up study including 35 AIP patients, Herrero et al. reported that more than 20% of subjects underwent clinical relapse, reviving acute attacks and with low or no biochemical remission in terms of urinary and circulating porphyrin precursor accumulation[3]. Other restrictions related to chronic hemin regimen include the development of thromboembolic events and infections due to the frequent substitution of central venous catheters and, more so, increased serum ferritin and hepatic iron overload, thus raising the risk of liver fibrosis[4,5]. Concerning the latter point, Willandt and collaborators revealed for the first time that monitoring circulating ferritin could be useful for the risk assessment of secondary hemochromatosis and its complications in patients with refractory AIP. The

authors described the case of a female with AIP with recurrent attacks whose ferritin levels rose up to 1904 μg/L after regular heme administration. At the 5-year follow-up, she developed HCC and underwent partial liver resection, in which excessive iron deposition and advanced fibrosis were observed[5]. Afterward, another follow-up study conducted between 1974 and 2015 in a French cohort that included 602 symptomatic patients with AIP, of whom 46 had regular relapses, showed that the proportion of patients with AIP with recurrent crisis increased from 1995, which coincided with the marketing authorization of hemin[55].

Glucose can downregulate hepatic *ALAS1* transcription by stimulating pancreatic insulin release and, likewise, it may provide substrates for TCA (i.e., acetyl-CoA) and, indirectly, for the heme biosynthesis (i.e. succinyl-CoA)[25,27,56]. Oral or intravenous glucose loading and preventive interventions through dietary carbohydrates for either the AIP prophylaxis or the management of mild attacks, have been proposed. However, their use by clinicians is grounds for scientific debate, on one hand, because glucose-based therapies have shown unclear findings in both experimental models and controlled trials and, on the other hand, because metabolic disturbances related to IR and glucidic homeostasis reported *in vitro*, *in vivo,* and humans may limit the efficacy of these therapies[24,25,27,45,46,56,57]. Clinical guidelines suggest to administer 10% dextrose as a temporizing measure if hemin is not available, although monitoring for glycemia is required to avoid additional neurological complications or the onset of secondary hyponatremia[58]. In the absence of weakness, vomiting, or hyponatremia, high carbohydrate intake two days before a specific treatment is recommended[18]. Nonetheless, most patients with AIP manifest these symptoms during the attack, thus failing to tolerate oral polymer glucose solutions. Therefore, glucose cannot be the substitute for hemin to the extent that the latter needs to be introduced if patients with AIP do not show clinical remission within 1–2 days after glucose therapy or if they run into severe symptomatology[59-61].

Replacement of hepatic PBGD is the only curative option for AIP subjects. In 2004, it was reported that the first successful orthotopic liver transplantation (OLT) normalized porphyrin levels and improved quality of life in a young woman suffering recurrent attacks, thus suggesting to consider the procedure for AIP patients with severe forms of the disease[62]. To date, OLT represents the last chance for AIP patients with disabling,

unmanageable attacks and refractoriness to hemin treatment[10,19,63]. OLT improves both biochemical parameters in urine and plasma (ALA and PBG) and neuropsychiatric manifestations. Although OLT corrects the hepatic PBGD defects and prevents further attacks, recovery of pretransplant neurological deficit is unpredictable. Therefore, a detailed neurological evaluation by a specialist should be obtained to assess the pretransplant neurological status and ideally, OLT should be performed before the onset of permanent neurological damage[19].

Furthermore, pretransplant renal failure is a common AIP complication, which may hasten the decision to proceed with OLT. In some cases, a combined liver-kidney transplant is recommended to preserve renal function[64]. Besides the evaluation of AIP-related comorbidities, OLT presents several constraints including the invasiveness of the procedure itself, the high rates of hepatic artery thrombosis, and comorbidities due to long periods of immunosuppression. In addition, the lack of donors can delay the transplant causing irreversible neurological damage in patients with AIP[42,43,64,65].

4.2 Hepatic ALAS1 inhibitor and PBGD replenishment: an overview on the novel therapeutical proposals

In 2014, Yasuda and collaborators explored the use of RNA interference (RNAi) against the hepatic *Alas1* (Alas1-siRNA) to treat and prevent the acute attack in AIP mice, thus providing a proof-of-concept to develop RNAi-based therapies for AIP clinical management[66]. Over the years, scientific efforts focused on improving the Alas1-siRNA pharmacokinetics, duration, and hepatic delivery by conjugating it to N-acetyl galactosamine (GalNAc), which binds the liver-specific asialoglycoprotein receptor and contains a target sequence well-conserved across the species (ALN-AS1)[21,67]. Subcutaneous ALN-AS1 administration in AIP rodents and non-human primates (NHPs) strongly attenuated *ALAS1* hyperactivity and reduced porphyrin accumulation upon drug-induced attacks. Furthermore, the ALN-AS1 escaped the activation of the immune response, with the advantage of being repeatedly administered without inducing the formation of neutralizing antibodies[22,27,65]. Due to the promising results obtained in pre-clinical studies, the ALAS1-siRNA-GalNAc drug (Givosiran, Alnylam Pharmaceuticals, Inc.) has progressed to clinical trials. The phase I trial (NCT02452372), and phase I-II open-label extension (OLE) study investigated the safety, pharmacokinetics, pharmacodynamics, and outcomes of subcutaneous Givosiran administration in highly

excreters AIP patients or in those with recurrent attacks[68]. The tolerance profile of the Givosiran was acceptable in AIP patients, normalizing both ALAS1 levels and porphyrin accumulation, and it was paralleled by a significant decline of annual hemin use and frequency of the attack[64,65]. In the double-blind placebo-controlled trial (ENVISION, NCT03338816), patients affected by AHP, including n=89 AIP, with at least two acute episodes were enrolled and randomized to receive a monthly dose of Givosiran or placebo for six months. The annual attack rates were reduced by 74% in AIP patients and were accompanied by low ALA/PBG urinary levels, low hemin utilization, and improvement of pain scores, thereby receiving approval from the Food and Drug Administration (FDA) and the European Medical Agency (EMA) for the treatment of adult patients with AIP with active disease and adolescent patients aged ≥12 years with AHP[2,20]. Several queries about the use of Givosiran remain opened. Although it was generally well-tolerated, multiple Givosiran infusions may cause injection-site reactions, nausea, and fatigue. Hepatic and renal adverse events were reported in 15% of the patients under Givosiran regimen, and most of these patients exhibited increased serum creatinine and transaminase levels and reductions in glomerular filtration rates[2]. Hyperhomocysteinemia is a frequent adverse event that could enhance cardiovascular and neurological risk in symptomatic AIP patients, especially those receiving heme therapy[6,7,9]. Finally, the main issue concerns both the high cost of the Givosiran and its long half-life, which could lead to prolonged inhibition of hepatic heme synthesis, thus influencing heme-dependent liver functions[8].

Several shortcomings emerged with the use of the abovementioned therapies and, despite Givosiran has represented a breakthrough for the treatment of severe AIP, the latter is not a definite cure for this disease, thereby urging the need for the development of novel, safer strategies. Up to now, restoring normal PBGD expression and activity in the liver is the best proposal for the resolution of this monogenic disorder, and the new approaches include a) gene therapy (GT), b) mRNA-based therapies, and c) liver-directed recombinant PBGD protein[23,54,69,70].

Concerning the GT, recombinant adeno-associated viruses (rAAV) have been successfully applied in the treatment of inherited disorders. In recent years, they have been optimized to ensure a specific protein's long-term expression, safety, and tissue tropism and to avoid immunogenicity[71-75]. Firstly, the rAAV2 serotype 5 (rAAV2/5)

vector containing human *PBGD* cDNA was developed, which stably sustained hepatic *PBGD* expression and prevented the accumulation of porphyrins during the acute attacks in AIP mice[76]. To optimize the performance of rAAV serotype 5, Pañeda et al. designed a novel cDNA sequence of human PBGD, referred to as human PBGD codon-optimized cDNA (cohPBGD), composed of (a) a Kozak sequence that enhances translational machinery; (b) enrichment of GC content to improve RNA half-life; and (c), the exchange of rarely used codons with those most frequent in humans. The newly engineered rAAV5-cohPBGD was well-tolerated and without side effects in NHPs, showing the highest distribution in the liver compared with the other organs and with a similar efficacy of vector transduction between males and females. In addition, no T-cell responses against AAV capsid proteins or hPBGD were detected in these models after rAAV2/5-cohPBGD injections, thus offering the possibility to be tested in clinical trials[77]. The safety and tolerability profile of rAAV2/5-PBGD administration in eight patients with severe AIP was confirmed in the NCT02082860 clinical trial. Although patients with AIP improved their quality of life and did not develop cellular responses against PBGD after GT, they all showed anti-AAV5 neutralizing antibodies against the vector capsid, which blocked adeno-associated viral vector transduction and had no biochemical remission, probably due to low hepatic PBGD expression. Therefore, new strategies aiming to improve the efficacy of rAAV-mediated GT are under development[78-81]. One approach is the substitution of the constitutive promoter of the AAV vector with an inducible one and the modification of the catalytic site of the PBGD. Serrano-Mendioroz et al. introduced two human ALAS Drug-Responsive Enhancing Sequence (ADRES) motifs upstream from the liver-specific promoter of the AAV vector carrying the *PBGD* gene. The ADRES enhancers were highly responsive to precipitating factors, thereby providing a high expression of PBGD during an induced attack and taking advantage of reducing the effective dose by 10-fold[80]. Moreover, by comparing the consensus protein sequence of 12 mammalian species, they identified two non-human amino-acid substitutions, isoleucine 291 to methionine (I291M) and asparagine 340 to serine (N340S), which improve PBGD stability and generate a hyper-functional isoform conferring full protection on AIP mice against drug-induced attacks[81].

The mRNA-based therapies are a new class of drugs representing a promising treatment for genetic diseases. The mRNA is packaged in LNPs, which, in turn, interact with the

low-density lipoprotein receptor (LDLR) expressed on the hepatocyte surface. Once endocytosed, LNPs are degraded by lysosomes, whereas the mRNA is released into the cytoplasm and translated in the ribosomal machinery into a specific protein[21,22,54]. One of the advantages of mRNA-based therapies includes the possibility to synthesize a protein/enzyme which could localize in any type of subcellular compartment, allowing its natural interactions and post-translational modifications. Moreover, the injections of LNP-encapsuled mRNA avoid genotoxicity as they induce a transient protein replacement, but they may need to be repeatedly administered. Human PBGD (hPBGD) mRNA administration in AIP mice rescued the hepatic PBGD activity over the course of the acute attack, and its stability in hepatic parenchyma was enhanced when PBGD mRNA was conjugated with liver-targeted apolipoprotein A1 (ApoA1), a structural part of high-density lipoprotein (HDL)[23,69,82]. A sustained PBGD genetic correction reduces ALA/PBG accumulation along with alleviating pain, motor discoordination, and disturbances in nerve conduction velocity. Moreover, multiple cycles of hPBGD mRNA injections normalized urinary porphyrin levels in mice, rabbits, and NHPs, which did not show activation of the immune response or aberrations in liver function tests, indicating they are a promising candidate for translatability to humans[23,69,82].

Finally, Córdoba et al. developed a recombinant PBGD protein by binding the ApoA1 to the N-terminal of the human PBGD (rhApoA1-PBGD) or the hyper-functional PBGD carrying the I291M and N340S amino-acid substitutions (rhApoA1-PBGDms). The ApoA1 exploits the centripetal transport of HDL from the periphery to the liver, and it is internalized into hepatocytes by the ApoA1 receptors. Both rhApoA1-PBGD and rhApoA1-PBGDms restored PBGD activity and heme biosynthesis in both the liver and brain tissues, showing the ability to cross the blood–brain barrier. Notably, while the rhApoA1-PBGD prevented the accumulation of ALA/PBG after the drug-induced attack, the rhApoA1-PBGDms provided long-lasting protection against multiple attacks, thereby resulting appealing for the management of patients with recurrent episodes[23]. **Figure 2** obtained by Jericó et al. provides a schematic representation of emerging therapies for PBGD replacement[1].

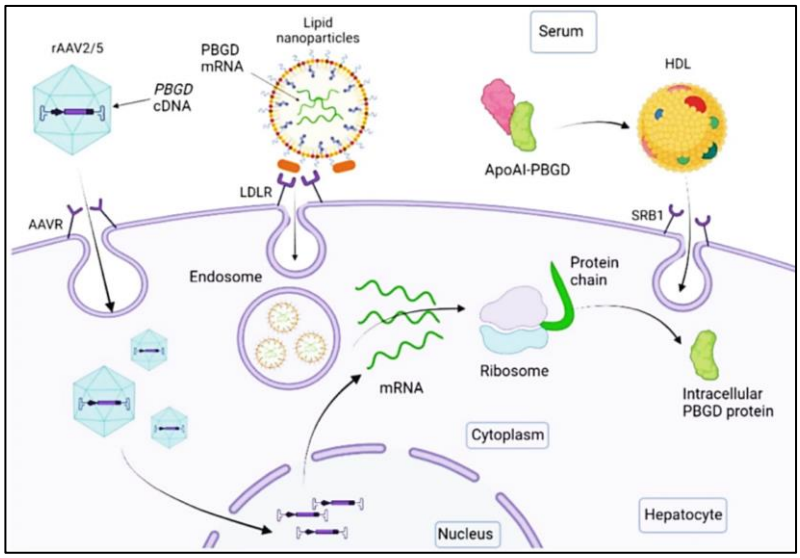

Figure 2. New emerging therapies for increasing PBGD levels in the liver. The recombinant adeno-associated virus 2/5 (rAAV2/5) is the vector used for gene therapy studies. It contains the PBGD complementary DNA sequence (PBGD cDNA) and targets the liver through specific receptors (AAVR). PBGD messenger RNA (PBGD mRNA) formulated in lipid nanoparticles (LNPs) is incorporated into hepatocytes through LDL receptors. The recombinant protein PBGD linked to apolipoprotein AI (ApoAI-PBGD) is transported by HDL particles and internalized in hepatocytes by the centripetal transport of cholesterol through the class B type 1 (SRB1)[1]. From Jericó et al Life 2022.

4.3 Targeting metabolic defects in AIP: who would benefit the most?

The development of new therapeutic interventions for the management of attacks in AIP patients has represented a turning point to curb the recurrence of acute manifestations and improve quality of life. Nevertheless, more than 90% of *HMBS*-mutation carriers present a stable disease, which can be defined as latent AIP or ASHE. These subsets of individuals may manifest sporadic acute attacks and/or chronic symptoms related to AIP pathology and they may be at high-risk to develop renal failure or HCC due to the high accumulation of porphyrins.

In recent years, it has emerged that AIP subjects with stable disease show a higher prevalence of hyperinsulinemia and insulin resistance (IR) compared to either control volunteers, including family members without *HMBS* mutations and porphyrin accumulation, or refractory AIP patients[24,49]. Paradoxically, hyperinsulinemia appeared protective against the recurrence of the acute attacks even though it may increase the susceptibility to develop metabolic disorders and to prime the liver to IR-related pathology[24,49]. Moreover, hyperinsulinemia may limit the efficacy of carbohydrate loading for the treatment of mild AIP cases[7,24,25,47,49]. Oral or intravenous carbohydrate

surplus, leading to an increment in insulin levels, has been associated with low biochemical disease activity in a case-control study including 50 patients with AIP, probably due ALAS1 inhibition mediated by phosphatidylinositol 3-kinase (PI3K)/Akt[7,47]. Accordingly, several studies have reported sustained hyperinsulinemia, excess body weight, or the presence of type 2 diabetes mellitus (T2DM) in stable AIP patients [24,49]. For this category of at-risk patients, no treatments are currently available, and metabolic assessment of AIP subjects has not yet been introduced into clinical practice, thereby opening new perspectives for the development of novel medical care aiming to improve insulin sensitivity.

Recently, it was observed that therapeutic interventions that increased circulating HDL and ApoA1 levels improved hyperglycemia and attenuated IR in *db/db* mice, a genetic model of T2DM[83], thus offering the possibility to consider insulin or insulin-sensitizers to correct metabolic dysfunctions by ameliorating insulin response and enhancing glucose therapy in the AIP context. By comparing the efficacy between a fast-acting insulin (Actrapid®) and a liver-targeted insulin fused to ApoA1 (Ins–ApoA1), both co-administered with glucose, Solares et al. found that both exogenous insulins injected into AIP mice normalized heme biosynthesis, gluconeogenesis, and the levels of circulating triglycerides, probably to promote the synthesis of high-energy molecules. Nonetheless, Actrapid® did not hamper urinary ALA or PBG excretion after a drug challenge, while Ins–ApoA1 sustained hepatic *Alas1* downregulation accompanied by porphyrin reduction. In addition, prophylactic treatment with the Ins–ApoA1 and glucose mixture showed a significant improvement in pain scores and motor coordination in AIP mice, although high ALA/PBG accumulation was maintained[24,84].

Alpha-lipoic acid (α-LA) is an insulin-mimetic tested as a nutraceutical approach in rats in which porphyria was chemically induced with hexachlorobenzene and combined with Vitamin E, in patients affected by PCT, showing interesting results in reducing free radicals and symptoms of PCT[26,85,86]. α-LA is an endogenous antioxidant that acts as co-factor of pyruvate and α-ketoglutarate dehydrogenase complexes, offering the advantage of directly stimulating the TCA to produce substrate for heme biosynthesis[25]. Consistently, lipoate synthesis defects have been associated with low succinyl-CoA availability and heme deficiency[25,26].

α-LA elicits a surprising array of metabolic and clinical effects. In particular, it improves glucose handling in the skeletal muscle by interacting with regulatory components of the insulin signaling cascade, stimulating the translocation of glucose transporter 4 (Glut4) on cell membranes independently of the PI3K/Akt signaling cascade and favoring the utilization of glycogen storages (**Figure 3**). The beneficial effects observed in IR animal models to ameliorate whole-body glucose tolerance and enhance insulin sensitivity have further been translated to clinical trials for patients with type 2 diabetes (T2D). Interestingly, α-LA has provided benefits for patients affected by diabetic neuropathy. Compared to the licensed analgesic drugs, α-LA has shown a safer and well-tolerated profile, improving neuropathic pain and paresthesia, numbness, sensory deficits, and muscle strength[87,88].

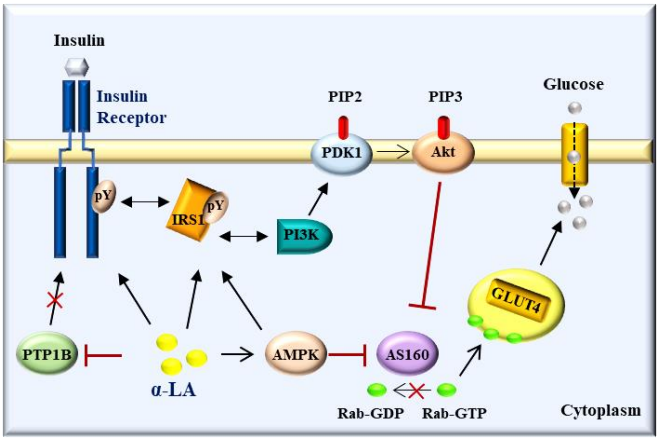

Figure 3. Role of α-LA on glucose uptake in skeletal muscle. α-LA activates peripheral AMPK and induces a) the phosphorylation of insulin receptor substrate 1 (IRS1) paralleled by the activation of the IRS1/PI3K signaling and b) GLUT4 translocation via inactivation of the Akt substrate of 160 kDa (AS160) independently of the IRS1/PI3K/Akt signaling cascade in the skeletal muscle[86,]

However, nobody has investigated its efficacy in AIP and its potential role in the management of metabolic dysfunction in rare disorders need to further elucidated. Therefore, the following PhD project aimed to investigate whether nutritional interventions based on the use of insulin-sensitizing compounds, among which α-LA, may improve disturbances related to glucose metabolism in AIP. Concurrently, the non-invasive assessment of liver pathology and metabolic profile has been carried out in a small cohort of AIP patients attempting to assess whether metabolic and/or hepatic evaluation should be introduced in clinical practice for identification of AIP patients who would benefit from either dietary interventions or canonical therapies.

Aims of the study

Current knowledge about AIP pathogenesis has suggested that alterations of glucose metabolism accompanied by increased insulin levels may arise in response to precipitating factors, such as fasting and porphyrinogenic drugs, as well as they may exist in the subset of patients with latent AIP or ASHE, thereby predisposing them to dysmetabolic-related complications, such as IR and diabetes, and to the adverse effects of porphyrin accumulation as renal failure and HCC development.

Glucose intolerance and hyperinsulinemia associated with AIP pathology may influence the response to both dietary and injectable glucidic therapies. No therapeutic interventions have been approved yet to correct anomalies of sugar metabolism in asymptomatic *HMBS*-mutation carriers who represent the great majority of AIP cases. Recently, Fontanellas et al. showed that AIP mice treated with the fast-acting insulin or, even more, with the liver-targeted Ins-ApoA1 combined with glucose administration improved the hepatic heme biosynthesis, gluconeogenesis, and increased the number of mitochondria and the levels of circulating triglycerides, probably to promote the synthesis of high-energy molecules. Although this field is still at the dawn, the study paved the way for the introduction of liver-targeted insulin and/or its mimicking agents in order to improve the efficacy of glucose therapy and to correct carbohydrate metabolism in AIP.

Therefore, the main aim of this project was to investigate whether α-lipoic acid (α-LA) and other novel therapeutic strategies that may normalize metabolic alterations occurring in the AIP background in both *in vitro* and in *vivo* models, with a particular focus on glucose metabolism and insulin response and looking at the liver and insulin-sensitive tissues (muscle, adipose, and brain). In particular, we aimed:

1. to assess the efficacy of α-LA, an insulin-mimetic molecule with antioxidant and anti-inflammatory properties[19]. Initially, the effects of α-LA on glucose metabolism were evaluated in cultured hepatocytes alone or in combination with glucose.
2. to carry out a pilot study in AIP mice to assess the potential efficacy of α-LA, which was dietary supplemented for a brief period (two weeks), and to compare it with the standard therapies (glucose and hemin).
3. to expand the dietary options for the correction of AIP dysmetabolism. In this part of the project, we prolonged the α-LA administration in AIP mice (from two weeks to 12 weeks) and compared its efficacy with other insulin-sensitizers, which have shown

promising results in the improvement of metabolic syndrome. The new molecules included in the studies were a) the heat-killed probiotic *Bifidobacterium animalis subsp. lactis CECT 8145* (BLP1)[89,90]; b) the BLP1-derived lipoteichoic acid (LTA)[91] and c) the alive probiotic *Bacillus coagulans* (*B. coagulans*)[92]. The effects of the treatments were even compared to the well-proven liver-targeted Ins-ApoA1 and PBGD gene therapy (GT)[24,45].

4. As a translational approach, non-invasive evaluation of metabolic profile (glucose, insulin, transaminases, circulating lipids), body composition (% lean/fat mass), and liver disease was proposed to a small cohort of AIP patients (n=14), followed at the Rare Diseases Unit at the Fondazione IRCCS Cà Granda Ospedale Maggiore Policlinico of Milan. The objective of this part of the study was to identify whether clinical assessment of AIP metabolism may aid the identification of risk categories in clinical practice.

Studies were carried out at the General Medicine, Metabolic and Rare Diseases Unit at the Fondazione IRCCS Cà Granda Ospedale Maggiore Policlinico of Milan in collaboration with the Department of Clinical Sciences and Community Health, University of Milan, Italy, and Hepatology Program, Center for Applied Medical Research (CIMA), University of Navarra, Spain.

Materials and Methods

1. Evaluation of glucose metabolism and α-LA efficacy *in vitro*

1.1 Study design with a commercial PBGD RNA Interference

HepG2 human hepatoma cells, which represent the most used *in vitro* cell line to study liver metabolism and related disorders, were transiently transfected for 48h by pooling 3 different target-specific siRNA oligo duplexes (MyBioSource, Inc., San Diego, CA) of human *HMBS* gene (siPBGD) at a final concentration of 10 µM. Cyclophilin B (10 µM) was used as a scramble negative control (Horizon Discovery, Waterbeach, UK). To mimic fasting, both scramble and siPBGD cells were cultured in Dulbecco's Modified Eagle's Medium (DMEM, Life Technologies-ThermoFisher Scientific, Waltham, United States) with low glucose concentration (1.125 mg/L) for 6h. A cultured medium of siPBGD cells was supplemented with 0.5 mM α-LA alone (siPBGD+α-LA) or in combination with 0.33 mM glucose (α-LA+Gluc) for 24h before inducing fasting. Treatments were freshly prepared and administered when appropriate. The potential efficacy of α-LA alone and α-LA+Gluc were compared to 0.33 mM glucose (siPBGD+Gluc)[25].

1.2 Evaluation of PBGD Enzymatic Activity

siPBGD and scramble cells were lysed in 0.1 M Tris-HCl buffer (pH 8.0) containing 0.2% Triton-X 100. Then, 50 µL cell lysates were incubated with 200 µL 0.1 M Tris-HCl and 25 µL of 1 mM PBG for 1 h at 37 °C in order to evaluate whether PBGD enzyme could convert PBG substrate into uroporphyrin, according to the procedure of Hsiao et al.[93]. After incubation, the enzymatic reaction was stopped through 10% trichloroacetic acid and centrifuged at 13,000 rpm for 10 min. The uroporphyrin fluorescence emission (Ex/Em = 405/655 nm) was measured by a spectrofluorometer (Shimadzu Corporation, Kyoto, Japan), and uroporphyrin concentration was determined using uroporphyrin I standard calibrator (Sigma-Aldrich, St Louis, USA). The PBGD activity (pmol/Uro/h) was normalized to the total amount of proteins (mg) and expressed as percentage of residual activity for each condition.

1.3 Measurement of ATP production

$1x10^6$ HepG2 cells were seeded in 6-well plates and subjected to different treatments. Then the pellets were collected and homogenized in 5% IGEPAL® CA-630 (Sigma Aldrich, USA). To avoid enzymes interfering with the assay, samples were deproteinized

by adding ice cold 1M perchloric acid (PCA). To neutralize PCA-induced acidification and to restore pH range at 6.5-8, 35% of potassium hydroxide (KOH) 2M was added to each sample. The excess of PCA/KOH was precipitated by centrifugating e at 13,000 g for 15 minutes at 4°C. Supernatant were collected and loaded in black walled, clear bottom plates for fluorometric detection (Ex/Em = 535/587 nm).

2. Evaluation of glucose metabolism and α-LA efficacy *in vivo*

2.1 Study design

Three-month-old C57BL/6 wild-type (Wt) and compound heterozygous C57BL/6$^{pbgd1(neo)Uam/obgd2(neo)Uam}$ T1/T2 (AIP) strains were exploited in this study[45,94]. The AIP murine model was generated by the crossbreeding of the homozygous T1 (C57BL/6-$^{pbgdtm1(neo)Uam}$) mice and the heterozygous T2 (C57BL/6-$^{pbgdtm2(neo)Uam}$) as described by Lindberg et al [94]. In both models, the hepatic PBGD activity was decreased to around 55% and they did not show the biochemical characteristics of hepatic porphyria. Conversely, AIP mice bear the 33% of hepatic PBGD activity and resembled both the biochemical and neuropathological features of human pathology. The AIP model was kindly provided by Professor Antonio Fontanellas Romà, University of Navarra, Spain (breeding protocol reference CEEA029c-21 approved the Ethics Committee of the University of Navarra), while the C57BL/6 Wt strain was bought by Charles River-Research Models and Services, Italy. The animals were housed in a ventilated cage system (Tecniplast, Buguggiate, Varese, Italy) at 22±1°C, 55±5% humidity, with a 12h day/night cycle. The experimental protocol was approved by Ministero della Salute (421/2020-PR, code: 568EB.24).

The beneficial effects of α-LA on insulin sensitivity and glucose metabolism have been previously demonstrated in rodents affected by obesity and type 2 diabetes [95], but its role in metabolic rare diseases has not been investigated yet. To avoid wasting animals, we carried out a pilot study in which α-LA was dietary supplemented in water for two weeks and its efficacy on heme pathway was compared to AIP standard therapies (hemin and glucose). In order to trigger metabolic abnormalities, all experimental groups were fasted 14 hours before the sacrifice. Eight experimental groups were included in the study:

1. Wt (n=6) and AIP mice (n=6): control group in fasted condition

2. Wt (n=6) and AIP mice (n=6): received intraperitoneal *(i.p.)* infusion of heme arginate (8 mg/kg) after fasting induction[55]
3. Wt (n=6) and AIP mice (n=6) which received *i.p.* infusion of 30% glucose after fasting induction[96]
4. Wt (n=8) and AIP mice (n=8) received α-LA (100 mg/kg) diluted in water for two weeks[95,97]

All experimental groups were maintained to standard diet (SD) and water *ad libitum*. Once we determined whether α-LA could provide advantages for the heme synthesis, we evaluated its effects on the metabolic abnormalities found in AIP during the fasting-induced stress[45]. We focused on hyperinsulinemia, energy supplies and hepatic glycogenolysis/gluconeogenesis alongside a preliminary evaluation of the effects of α-LA on glucose metabolism in insulin-sensitive organs (muscle, brain, and white adipose tissue).

2.2 Gene Expression Analysis

RNA was extracted from human cell cultures or murine hepatic tissues using Trizol reagent (Life Technologies-ThermoFisher Scientific, Carlsbad, USA). One µg of total RNA was retrotranscribed with a VILO random hexamers synthesis system (Life Technologies-ThermoFisher Scientific, Carlsbad, USA). Quantitative real-time PCR (qRT-PCR) was performed by an ABI 7500 fast thermocycler, using the TaqMan Universal PCR Master Mix (Life Technologies, Carlsbad, USA) or SYBR Green chemistry (Fast SYBR Green Master Mix; Life Technologies, Carlsband, USA. Human Taqman probes included genes involved in heme biosynthesis as *ALAS1* (#Hs00167441_m1) and *PBGD* (#Hs00609297_m1), and genes of glycolysis as *Glucokinase* (*GCK*, #Hs01564555_m1), *Phosphofructokinase*, liver type (*PFK-L*, #Hs01036347_m1), and *Pyruvate kinase* (*PK*, ThermoFisher #Hs00176075_m1). Genes involved in bridging enzymes among glycolysis, glycogenolysis and gluconeogenesis were evaluated in murine livers with the following probes: *Glucose-6-phosphatase* (*G6pc,* #Mm04207416_m1), *Pyruvate carboxylase* (*Pcx,* Mm00500992_m1) and *Phosphoglucomutase 1* (*Pgma1,* Mm00804141_m1). All reactions were delivered in triplicate. Data were normalized to *beta-actin (ACTB)* or glyceraldehyde 3-phosphate dehydrogenase (GAPDH) housekeeping genes and results were expressed as fold increase (Arbitrary units (AU)) or $2^{\wedge-\Delta CT}$ mean value ± standard deviation (SD).

3. Evaluation of glucose metabolism in AIP mice in response to probiotics and insulin-mimetics

3.1 Study design

Three-month-old C57BL/6 wild-type (Wt) and AIP strains were used as described above. The experimental protocol was approved by the Ethics Committee of the University of Navarra (CEEA 023-22), according to the European Council guidelines. In this part of the study, we aim to assess different dietary options with potential insulin-sensitive properties for the correction of metabolic disturbances in AIP. None of the diets have been tested for the management of AIP in previous studies, but they have shown attractive findings in the improvement of nonalcoholic fatty live disease (NALFD), diabetes and metabolic syndrome[89-92].

Wt and AIP mice with a median age of 11 weeks and a median weight of 19 g were randomly assigned to receive the insulin-sensitive compounds, vehicle or no treatment and they were sorted into 10 groups (n=6/cage). All treatments were diluted in water and administered for 12 weeks. Food consumption and weight were weekly monitored. As untreated controls, we included Wt and AIP mice who were maintained to standard diet and drinking water (DW) throughout the course of observation (Wt-DW and AIP-DW). For some treatments, 2mg/ml tapioca maltodextrin (TM), a polysaccharide used as food additive to stabilize certain substances, was used as vehicle. Therefore, other two Wt and AIP groups were exploited as controls receiving daily TM in water (Wt-TM and AIP-TM). Two cohorts of AIP mice were daily supplemented with the heat-killed probiotic *Bifidobacterium animalis subsp. lactis CECT 8145* (BLP1, $2x10^8$ CFU/ml, Biópolis SL, Valencia, Spain) which was isolated from fresh feces of healthy babies undergoing breast-milk feeding[90] or the postbiotic lipoteichoic acid (LTA, Biópolis SL, Valencia, Spain) isolated from BLP1 (1µg/ml), respectively. Both BLP1 and LTA were formulated with TM (TM-BLP1 and LTA-TM). An AIP group was supplied with TM-α-LA (100 mg/kg) to evaluate both the effects of a long-term administration of α-LA and its potential interaction with a sugar (maltodextrin)[89,90,98]. Spores of the bacteria *Bacillus coagulans* (*B. coagulans*) GBI-30 6086 were kindly provided by Ganeden Inc. (Mayfield Heights, OH, USA). The alive bacteria was diluted in water at 7mg/ml without the addition of TM[92]. A cohort of AIP mice (n=6) received a single intravenous (*i.v.*) injection of $5x10^{11}$ genome copies/Kg (gc/Kg) of rAAV5-PBGD vector (TM-GT) four weeks before the start

of the study, while another AIP group (n=6) was subcutaneously injected with the liver-targeted insulin-ApoA1 (TM-Ins) every three days (90 μg/kg). Therefore, TM was daily administered in six out of ten experimental groups. All the analysis were performed after 14 hours fasting.

3.2 Glucose tolerance test (GTT)

Glucose tolerance test (GTT) was performed after 14 hours of fasting and by injecting 2g/kg glucose overload. One week later, a second GTT study was performed following severe hyperglycemia, defined as blood glucose concentration >300 mg/dl, induced by intraperitoneally (*i.p.*) administration of 5g/kg glucose in the same mice. Blood glucose samples were collected from tail vein and glycemia was measured at baseline, 5, 10, 15, 20, 25, 30, 40, 50, 60 and 90 minutes after glucose injection by an Accu-chek glucometer (Roche Diagnostics AVIVA, Mannheim, Germany). Area under the curve (AUC) was calculated as total area post *i.p.* 2g/kg glucose overload or post 1^{st} to 3^{rd} hours post 5g/kg *i.p.* injection. To assess the velocity rate of glucose reduction, we calculated the slope from the glucose peak at 30 up to 90 minutes after *i.p.* 5g/kg glucose injection.

3.3.Serum and hepatic biochemical measurements

Serum insulin levels were measured through a solid-phase sandwich Enzyme-Linked Immunosorbent Assay (ELISA). A target-specific antibody was pre-coated in the wells of a microplate. Serum samples were added into these wells, incubated at 4°C overnight and bound to the immobilized (capture) antibody. The sandwich is formed by the addition of the second (detector) biotin-conjugated antibody for 1 hour at room temperature (RT). Horseradish peroxidase (HRP) conjugated Streptavidin and 3,3',5,5'-Tetramethylbenzidine (TMB) substrate were added to the wells and reacted with the enzyme-antibody-target complex to produce measurable signal. The intensity of this signal is directly proportional to the concentration of insulin present in the original specimen (λ=450).

Serum triglycerides were colorimetrically measured through Triglyceride Quantification Assay Kit (Abcam, Cambridge, UK). Triglycerides were firstly converted into free fatty acids and glycerol after the incubation with a lipase enzyme for 20 minutes at RT. The latter is then oxidized for 60 minutes and the product is read at the spectrophotometer (λ=540).

Hepatic heme, glycogen, ATP, and lactate content were measured in frozen liver samples and in brain, muscle (gastrocnemius) and adipose tissue (gonadal fat fraction) through Heme Assay Kit (Abcam, Cambridge, UK), ATP assay kit (Abcam, Cambridge, UK), Glycogen Assay kit (Sigma-Aldrich, St Luis, MO) and Lactate assay Kit (Sigma-Aldrich, St Luis, MO). Data were normalized on mg of proteins.

3.4 Western Blot Analysis

Proteins were extracted from liver, skeletal muscle (gastrocnemius), brain, white fat tissue (gonadal) and brown adipose tissue (BAT) using RIPA buffer containing 1 mmol/L Na-orthovanadate, 200 mmol/L phenylmethyl sulfonyl fluoride, and 0.02 μg/μL aprotinin. Samples were pooled prior to electrophoretic separation, and all reactions were performed in duplicate. Then, equal amounts of proteins (50 μg) were separated by SDS-PAGE, transferred electrophoretically to nitrocellulose membrane (BioRad, Hercules, CA), and incubated with specific antibodies overnight. At least, three independent lots of freshly extracted proteins were used for experiments. Murine antibodies exploited in this study were: anti-Glut2 (sc-518022), anti-Glut3 (sc-74497), anti-Glut1 (sc-377228), anti-Glut4 (sc-53566), anti-InsRβ (sc-57342), anti-PI 3-kinase p110α (sc-7174), anti-phospho-Akt (S473), anti-phospho-4E-BP1 (T37/46), anti-Akt (pan), anti-4E-BP1 (pan 53H11), anti-Vinculin (EPR8185).

3.5 Quantitative magnetic resonance

For body composition, mice were fasted 14 hours and *in vivo* measurements was performed through EchoMRI-100-700, Echo Medical System, Houston, TX, USA) as previously described[24]. At the end of the experimental period, mice were euthanized and we collected blood samples, liver, kidney, heart, skeletal muscle (gastrocnemius), white adipose tissue (WAT) fractions including gonadal (GON), retroperitoneal (RT), mesenteric (MES) and subcutaneous (SC) and the interscapular brown adipose tissue (BAT).

3.6 In vivo [18F]FDG studies by Micro-Positron Emission Tomography (MicroPET)

Glucose metabolism was *in vivo* studied by MicroPET imaging using the glucose analog [18F]Fluoro-2-deoxy-2-D-glucose ([18F]FDG). Studies were performed in a small animal dedicated tomograph (Mosaic, Philips,Cleveland, OH, USA) followed by a CT image performed

in a U-SPECT6 / E-class (MILabs) scanner to obtain the corresponding anatomical image of the animals.

To perform the PET [18F]FDG images, mice were fasted overnight with ad libitum access to drinking water. On the day of the study, a dose of 9.2 ± 0.9 MBq was injected intravenously in a tail vein. The animals were anesthetized with 2% isoflurane in 100% O_2 gas during the uptake period of 50 min and then were placed prone on the scanner bed for 15-minute image acquisition. A sub-group of animals were exposed to cold stimulation (4ºC) for 1 h before the [18F]FDG injection and also during the uptake period.

All the studies were reconstructed applying dead time, decay, random and scattering corrections into a 128×128 matrix with a 1 mm voxel size. Then, images were exported and analyzed using the PMOD software (PMOD Technologies Ltd., Adliswil, Switzerland) and transformed to standardized uptake value (SUV) units using the formula SUV = [tissue activity concentration (Bq/cm3)/injected dose (Bq)] × body weight (g). For semiquantitative analysis of the images, [18F]FDG uptake by BAT was evaluated drawing spherical volume-of-interest (radius = 2 mm) on PET images over the interscapular BAT (iBAT), brain, heart, liver and hindlimb's muscle. Then, a semi-automatic segmentation was performed including the voxels with a value greater than 50% of the maximum value of the volume. Finally, the average of the SUV values within the semi-automatic VOI was calculated (SUV mean).

3.7 Ex vivo [18F]FDG studies after dissection

Ex vivo quantification of [18F]FDG uptake in some organs/tissues was also measured immediately after PET imaging. For this, animals were sacrificed and organs/tissues were dissected: brain, heart, liver, iBAT and muscle. All tissues were weighed and subjected to radioactivity (Bq) measurement with a gamma counter (Hidex Automatic Gamma Counter). [18F]FDG was expressed as % of ID per gram, correcting the measurement with the calculated radioactive decay of 18-fluorine.

4. Metabolic and hepatic screening in AIP patients

4.1 Acute Intermittent Porphyria cohort: Inclusion and exclusion criteria

The study included patients suffering from AIP (n=14) followed at the General Medicine, Metabolic and Rare Diseases Unit at the Fondazione IRCCS Cà Granda, Ospedale Maggiore Policlinico of Milan, Italy. A written informed consent form was signed by the patient and legally authorized prior to any study-specific procedure being performed. The eligible patients were invited to participate to the study during an initial visit and were

recruited for follow-up visits according to the indications of the clinician. A detailed medical history was collected for the period since the patient's porphyria diagnosis or onset of symptoms, but in general at least 24 months prior to the first visit. At this time, blood samples and urines were withdrawn for identification of disease-causing mutations and measurements of ALA, PBG and total porphyrins. The patients were free to leave the study at any time and for any reason, without incurring any penalty to continuing the medical care. The inclusion criteria were the diagnosis of AIP in adult subjects of any age made by a porphyria specialist with at least one of the following documented molecular confirmation:

a) identification of disease-causing mutation in the HMBS gene.

b) decreased PBGD activity and increased urinary porphyrins

Exclusion criteria included diagnosis of diabetes mellitus 1 and 2, metabolic syndrome according to NCEP ATP III criteria99, viral hepatitis (HCV, HBV) and infection (HIV), liver disorders with a different etiology (NAFLD, ALD). Patients who chronically consumed drugs which may predispose to IR (corticosteroids, thiazide diuretics, non-selective β-blockers) and alcohol abusers (>20g/day for women, >30g/day for men) were even excluded.

AIP patients were stratified according to the frequency of the attacks as previously reported24. Demographic, anthropometric, and clinical features of AIP cohort are reported in Table 1. Our cohort mainly consisted of clinically stable AIP participants (n=9, Stable AIP), who presented the highest concentration of urinary porphyrins (total porphyrins≥150 μmol/mol creatinine, ALA≥5 μmol/mol creatinine, PBG≥1.5 μmol/mol creatinine), of whom 3 had only one sporadic attack throughout their life, and AIP subjects who experienced >2 annual acute events (n=5, Stable AIP) according to European Porphyria Network (EPNET) criteria.

4.2 Metabolic and hepatic assessment in AIP cohort

For biochemical evaluation, serum samples were collected from AIP patient in order to measure markers of glucidic/lipidic metabolism (insulin, triglycerides, cholesterols) and of liver damage as alanine and aspartate aminotransferases (ALT and AST). For oral glucose tolerance test (OGTT), basal glycemia was measured in fasted AIP patients and after 60- and 120-minutes post 75g glucose overload. Homeostatic Model Assessment for

Insulin Resistance (HOMA-IR) was used as index to identify IR. HOMA-IR values between 1.9 and 2.5 were defined as early IR, while HOMA>2.5 indicated overt IR.

Metabolism rate and body composition in AIP patients were estimated with the bioimpedance analysis performed through BIA-Dex, which allowed to determine the basal metabolic rate (BMR), %fat mass (FM), %free fat mass (FFM or lean mass), body cellular mass (%BCM, which represent the metabolically active muscular cells), total body water (TBW) and intracellular/extracellular water (ICW, ECW), based on the conductive or insulating capacities of biological tissues.

AIP patients underwent instrumental assessment of hepatopathy by performing upper abdominal ultrasound and hepatic elastosonography (Fibroscan). Particular attention was given to the evaluation of the liver parenchyma with regard to the presence or absence of ultrasonographic signs of hepatopathy. The presence or absence of steatosis was assessed at Fibroscan using the CAP (Controlled Attenuation Parameter) index, since ultrasound is not an accurate method especially in detecting milder forms. A CAP index ≥ 248 (Db/m), adjusted according to BMI, was used as indicative of the presence of at least mild steatosis (≥ S1). Concerning liver fibrosis, A M-type probe was used, according to patient's body mass index (BMI). To determine liver fibrosis degree, the cut-offs used for nonalcoholic steatohepatitis (NASH) were taken as a reference: in detail, an index ≥7 kPa indicative of clinically significant fibrosis (F2/F3/F4), on the contrary, an index <7 kPa indicative of clinically insignificant fibrosis (F0-F1).

4.3 Statistical Analysis

Differences between two groups were calculated by one-way ANOVA, followed by post hoc *t-test* (two-tailed). Differences among multiple groups were analyzed by one-way ANOVA followed by two-stage linear step-up procedure of Benjamini, Krieger, and Yekutieli, which corrects for the number of comparisons and controls the False Discovery Rate (FDR). For skewed variables which were log transformed, one-way parametric ANOVA was exploited and followed by Bonferroni correction. Adjusted (adj) p values < 0.05 were considered statistically significant. Statistical analyses were performed using JMP 16.0 (SAS, Cary, NC) and Prism software (version 9.1, GraphPad Software).

Results

1. Evaluation of glucose metabolism and α-LA efficacy *in vitro*

1.1 α-LA improves heme content in siPBGD Cells

At baseline, PBGD silencing reduced both *PBGD* mRNA levels by 60% ($p<0.0001$ at ANOVA; adj $p<0.0001$ *vs.* scramble; **Figure 1A**) and its enzymatic activity by 42% ($p=0.0001$ at ANOVA; adj $p=0.001$ *vs*. scramble; **Figure 1B**). siPBGD cells showed lower *ALAS1* expression ($p=0.003$ at ANOVA; $p=0.01$ *vs.* scramble; **Figure 1C**) and intracellular heme content ($p<0.0001$ at ANOVA; adj $p<0.0001$ *vs.* scramble; **Figure 1D**) compared to the scramble probably due to the delay in the heme biosynthetic pathway induced by PBGD downregulation.

Fasting further reduced PBGD activity ($p=0.0001$ at ANOVA; adj $p=0.04$ *vs.* siPBGD untreated (NT) and *vs.* fasted scramble; **Figure 1B**) and promoted ALAS1 upregulation without increasing heme content ($p=0.003$ at ANOVA; $p=0.03$ *vs.* siPBGD-NT; **Figure 1C-D**), as occurs in AIP subjects during a stress-induced attack.

To assess the potential efficacy of α-LA as prophylactic treatment, we exposed siPBGD cells to α-LA 0.5 mM for 24h before fasting, and its efficacy was compared to glucose supplementation (0.33 mM) at the same timing. Additionally, we explored whether α-LA could enhance glucose efficacy by evaluating the potential synergism between the two treatments.

In low-glucose condition, α-LA treatment alone hampered the siRNA-induced PBGD downregulation in terms of both mRNA levels ($p=0.0005$ at ANOVA; adj $p=0.0003$; **Figure 1E**) and protein activity ($p=0.03$ at ANOVA; $p=0.005$ *vs.* fasted siPBGD cells; **Figure 1F**) paralleled by increased hepatocellular heme concentration ($p<0.0001$ at ANOVA; adj $p<0.0001$; **Figure 1G**). Moreover, α-LA showed greater ability than glucose to promote heme biosynthesis by rising PBGD levels ($p<0.0001$ at ANOVA; adj $p=0.0002$; **Figure 1E-F**) and the amount of heme ($p<0.0001$ at ANOVA; adj $p=0.0004$; **Figure 1G**).

Although α-LA+Gluc treatment ameliorated PBGD expression ($p=0.0005$ at ANOVA; adj $p=0.0002$ *vs.* fasted siPBGD cells; adj $p=0.0005$ *vs.* siPBGD+Gluc, **Figure 1E**), enzymatic performance ($p=0.03$ at ANOVA; adj $p=0.005$ *vs.* fasted siPBGD cells; **Figure 1F**), and intracellular heme synthesis *($p<0.0001$* at ANOVA; adj $p<0.0001$ *vs.* fasted siPBGD+Gluc; adj $p=0.002$ *vs.* fasted siPBGD+α-LA; **Figure 1G**), the effect was quite

comparable to those induced by α-LA alone, thus supporting that it may efficiently rescue heme content in fasted hepatocytes.

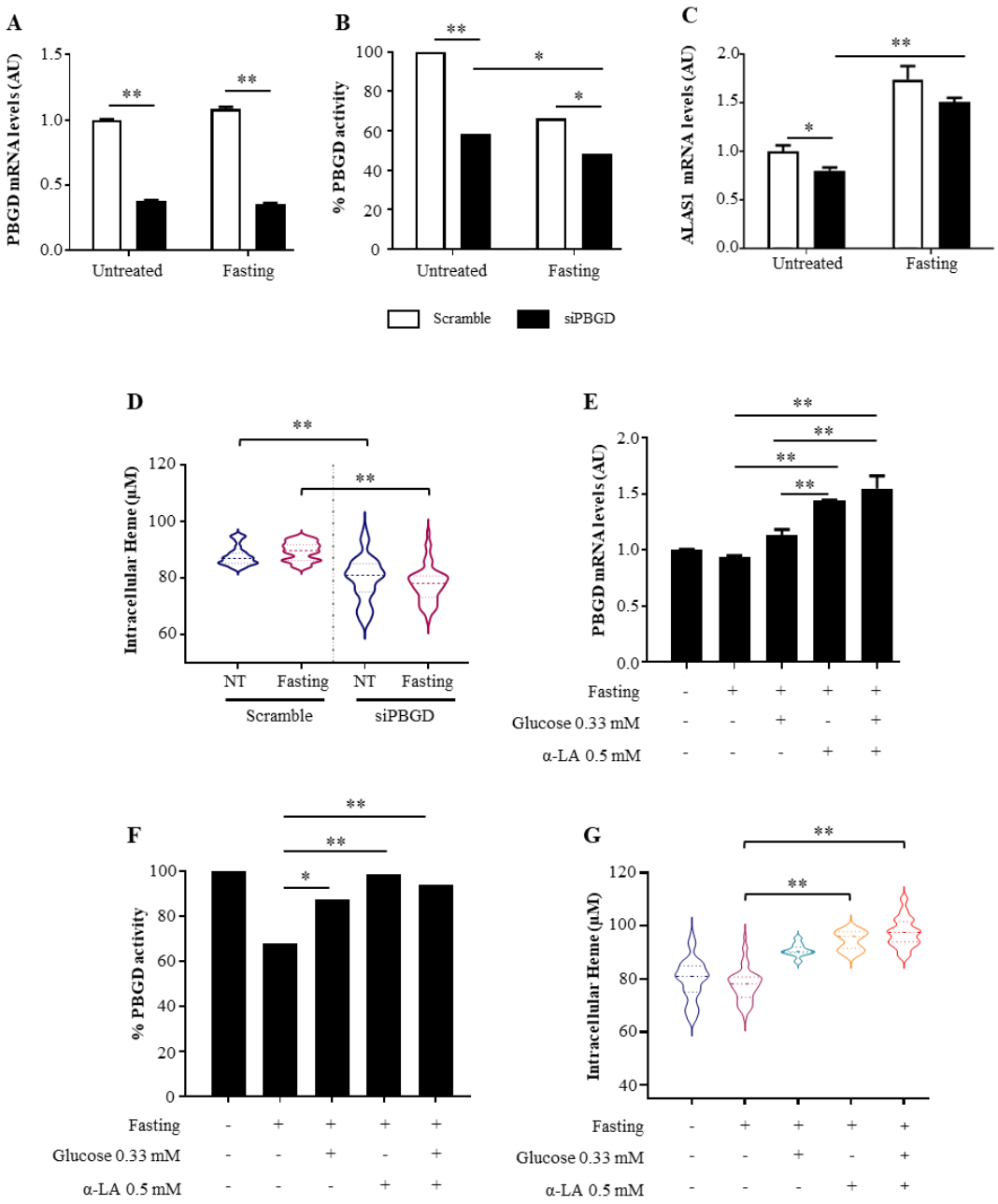

Figure 1. α-LA rescued heme biosynthesis in PBGD-silenced HepG2 cells. A) PBGD mRNA expression was assessed by qRT-PCR in scramble and siPBGD cells at baseline and after fasting. **B**) PBGD enzymatic activity was measured in both scramble and siPBGD cells with or without fasting. Data were normalized to mg of proteins and expressed as % of PBGD residual activity. **C**) ALAS1 mRNA levels were assessed by qRT-PCR in scramble and siPBGD cells at baseline and after fasting. **D**) Violin plot showed intracellular heme content (µM), which was colorimetrically measured in cell lysates following the manufacturer's instruction. **E**) The mRNA expression of PBGD was evaluated by qRT-PCR in siPBGD cells at baseline, after fasting and in the presence of glucose, α-LA, or both treatments. **F**) The percentage of PBGD residual activity was assessed in siPBGD cells at baseline, after fasting and in the presence of glucose, α-LA, or both treatments. **G**) Heme concentration (µM) was determined in siPBGD cells and compared to fasting, siPBGD+Gluc, siPBGD+α-LA, and to siPBGD plus α-LA+Gluc. For gene expression, data were normalized to *ACTB* housekeeping gene and expressed as fold increase (Arbitrary Unit-AU) compared to control group. For violin plot, data were expressed as median concentration (thick dashed lines) and interquartile range (dotted lines). At least three independent experiments were conducted. Adjusted *p<0.05 and **p<0.01

1.2 α-LA stimulates glucose utilization and provides energy supplies during fasting

Alterations in glucose metabolism might precipitate the AIP acute attack and compromise the efficacy of glucose therapy. However, metabolic aberrancies occurring in hepatocytes at baseline have not been described yet, and whether they could be refrained through an insulin-mimic agent has not been reported in previous studies.

In siPBGD cells, the expression of *Glucokinase* (*GCK*, p=0.009 at ANOVA; adj p=0.04, **Figure 2A**), *Phosphofructokinase* (*PFK-L*, p<0.0001 at ANOVA; adj p<0.0001; **Figure 2B**) and *Pyruvate Kinase* (*PK*, p<0.0001 at ANOVA; adj p=0.005, **Figure 2C**), genes involved in different steps of glycolysis, was lower compared to scramble. Accordingly, total ATP levels were reduced by ≈40% in siPBGD cells (p<0.0001 at ANOVA; adj p<0.001; **Figure 2D**).

Starving state further delayed glycolysis in siPBGD cells by dramatically downregulating *GCK* (p=0.009 at ANOVA; adj p=0.009, **Figure 2A**), *PFK-L* (p<0.0001 at ANOVA; adj p<0.001; **Figure 2B**), and *PK* expression (p<0.001 at ANOVA; adj p<0.001, **Figure 2C**) and by even inducing ATP shortfall (p<0.001 at ANOVA; adj p<0.001 *vs.* scramble fasted cells; adj p=0.0017 *vs.* siPBGD; **Figure 2D**).

As expected, glucose administration upregulated the expression of *GCK* (p=0.004 at ANOVA; adj p=0.02 *vs.* fasted siPBGD cells, **Figure 2E**), *PFK-L* (p=0.0002 at ANOVA, adj p=0.0001 *vs.* fasted siPBGD cells; **Figure 2F**), and *PK* (p<0.0001 at ANOVA, adj p<0.0001 *vs.* fasted siPBGD cells; **Figure 2G**), although it was ineffective at promoting ATP production, whose levels matched with those produced in siPBGD cells at baseline (p<0.0001 at ANOVA; adj p=0.0009 *vs.* fasted siPBGD cells; **Figure 2H**), thereby supporting that alterations of glucose metabolism occur in the presence of *PBGD* downregulation.

Interestingly, pre-treatment with α-LA alone not only upregulated *GCK* (p=0.004 at ANOVA; adj p=0.004 *vs.* fasted siPBGD cells; **Figure 2E**), *PFK-L* (p<0.0001 at ANOVA, adj p<0.0001 *vs.* fasted siPBGD cells; **Figure 2F**), and *PK* mRNA levels (p=0.0002 at ANOVA, adj p=0.03 *vs.* fasted siPBGD cells; **Figure 2G**), but also it hugely raised the total ATP compared to either fasted siPBGD cells or to siPBGD+Gluc ones (p<0.0001 at ANOVA; adj p<0.0001; **Figure 2H**).

The combined α-LA+Gluc supplementation additively participated in promoting the gene expression of glycolytic enzymes (p=0.004 at ANOVA; adj p=0.0001 *vs.* fasted siPBGD

cells, adj p=0.004 *vs.* siPBGD+Gluc, p=0.02 *vs.* siPBGD+α-LA; p<0.0001 at ANOVA, adj p=0.0001 *vs.* fasted siPBGD cells, p=0.001 *vs.* siPBGD+ α-LA; p<0.0001 at ANOVA, adj p<0.0001 *vs.* fasted siPBGD, siPBGD+Gluc and siPBGD+α-LA; **Figure 2E–G**). Compared to the single treatments, α-LA+Gluc administration enriched the siPBGD cells of ATP resources (p<0.0001 at ANOVA, adj p<0.0001 *vs.* fasted siPBGD, siPBGD+Gluc and siPBGD+α-LA; **Figure 2H**) and enhanced triglyceride secretion (p<0.0001 at ANOVA; p<0.0001 *vs.* fasted siPBGD, siPBGD+Gluc and siPBGD+α-LA; **Figure 2I**). Therefore, it could be speculated that α-LA administration may supply *PBDG*-silenced hepatocytes with energy fuels during energy shortage by possibly improving glucose utilization.

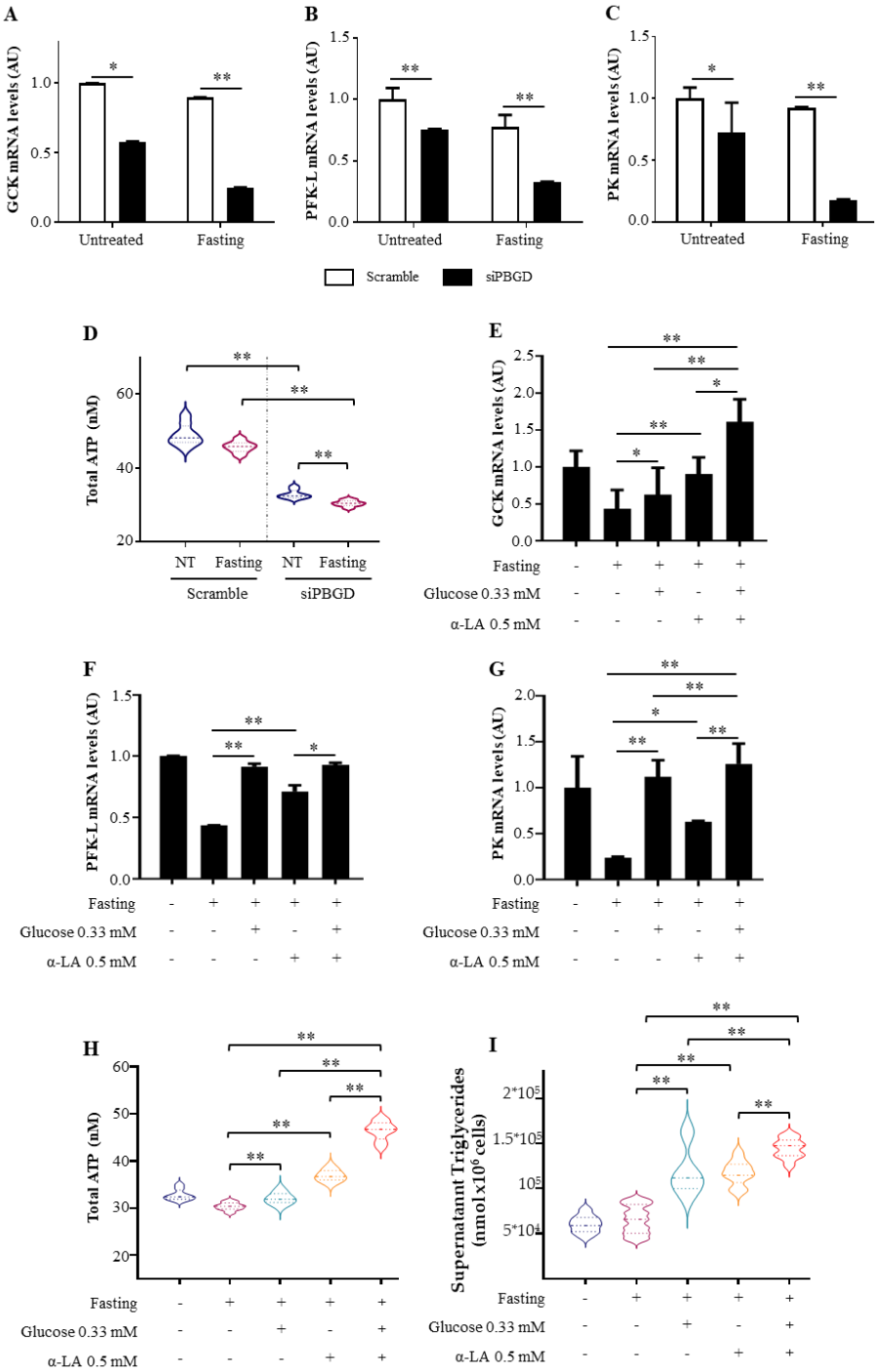

Figure 2. α-LA improved glucose utilization in PBGD-silenced HepG2 cells. **A-C**) GCK, PFK-L and PK mRNA levels were assessed by qRT-PCR in scramble and siPBGD cells at baseline and after fasting. **D**) ATP concentration was quantified in cell lysates through a fluorometric assay. **E-G**) GCK, PFK-L and PK mRNA expression was measured in siPBGD cells at baseline, after fasting and in presence of glucose, α-LA or both treatments. **H**) Intracellular ATP was measured in siPBGD cells and compared to fasting, siPBGD+Gluc, siPBGD+α-LA and to the combined treatment according to manufacturer 'instruction. **I**) Measurement of triglyceride secreted in cell supernatants of siPBGD cells with or without fasting and pre-treated with glucose, α-LA and α-LA+Gluc. For gene expression, data were normalized to *ACTB* housekeeping gene and expressed as fold increase (Arbitrary Unit-AU) compared to control group. For violin plot, data were expressed as median concentration (thick dashed lines) and interquartile range (dotted lines). At least three independent experiments were conducted. Adjusted *p<0.05 and **p<0.01

2. Evaluation of glucose metabolism and α-LA efficacy *in vivo*

2.1 α-LA sustains heme biosynthesis in AIP mice

Since preliminary results have shown that α-LA could improve heme biosynthesis, glucose utilization and mitochondrial bioenergetics in PBGD-silenced hepatocytes, we carried out a pilot study in AIP mice in which α-LA was administered for a short-term and compared to hemin and glucose standard treatments after fasting challenge.

As expected, AIP mice showed less PBGD activity in the liver and a lower amount of heme than Wt animals (adj p<0.0001 *vs.* Wt, **Figure 3A-B**). Upon acute hemin or glucose *i.p.* infusion, hepatic PBGD activity showed a further reduction in both Wt and AIP mice (adj p<0.0001 and adj p=0.02 *vs.* fasting, **Figure 3A**), probably because both treatments induced the ALAS1 downregulation which spills over into the slowdown of the heme synthesis. Conversely, AIP mice who received dietary supplementation with α-LA for two weeks did not show a downregulation of the hepatic PBGD activity but rather an upward trend (p=0.07 *vs.* AIP fasted, **Figure 3A**), resembling the data obtained *in vitro*.

Precipitating factors have in common the increased demand of heme production. However, AIP livers cannot meet the energy demand in response to stressful conditions. Therefore, we hypothesized that the steady, but not downregulated, hepatic PBGD activity in AIP mice treated with α-LA was paralleled by a sustained synthesis of the heme as the α-LA may directly provide TCA intermediates for the heme biosynthesis. Consistently, the hepatic heme concentration was increased in AIP mice after α-LA supplementation either against fasted AIP or AIP mice who received glucose injection (adj p=0.002 *vs.* AIP fasted and adj p=0.009 *vs.* AIP+Gluc, respectively, **Figure 3B**). Still, no difference in heme content was found between AIP+α-LA and AIP+hemin (**Figure 3B**), thus supporting that α-LA may promote the heme production in the liver.

AIP serum porphyrins usually increase during stress. To assess whether the amelioration of heme via was even accompanied by an improvement of biochemical anomalies during fasting, we measured serum porphyrins in AIP mice at the spectrofluorometer. We found that both hemin and glucose infusions reduced porphyrin peak during fasting, with the lowest levels observed in AIP animals who received hemin (adj p<0.0001 and adj p=0.004 *vs.* fasted AIP, **Figure 3C**). Unexpectedly, even the AIP+α-LA group showed lower porphyrin levels compared to fasted AIP mice (p=0.008 *vs.* fasted AIP, **Figure 3C**), displaying similar changes to AIP model after glucose injection.

Therefore, unlike hemin and glucose standard treatments whose acute administration aims to reduce the ALAS1 hyperactivity during a stressogenic factor, our findings suggest that α-LA may sustain the heme biosynthesis over time thereby maintaining the hepatic, albeit low, PBGD activity in AIP mice exposed to fasting. Surprisingly, α-LA supplementation has shown a partial efficacy at reducing serum porphyrins' peak.

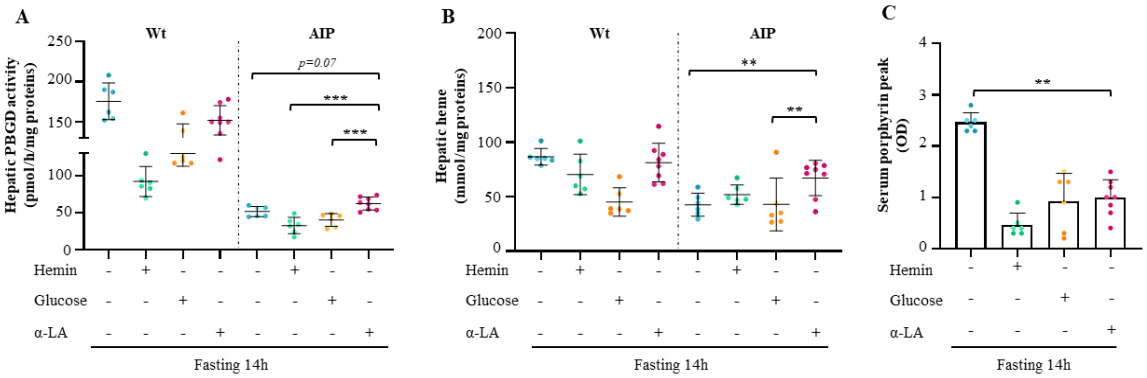

Figure 3. Short-term α-LA supplementation improved heme synthesis in AIP mice. **A**) PBGD activity was assessed in the livers of Wt and AIP mice. Data were normalized on hepatic mg of proteins and expressed as pmol/h. **B**) Box plot showed intracellular heme content (mmol), which was colorimetrically measured in frozen livers. Data were normalized on hepatic mg of proteins. **C**) Serum porphyrins' peak was measured in AIP mice through the Nanodrop spectrofluorometer. All experimental groups were fasted 14 hours before the sacrifice.

2.2 The effects of α-LA on serum metabolic profile and hepatic glucose metabolism in AIP mice

The results from *in vitro* and *in vivo* models have suggested that pre-treatment with α-LA alone may recover heme production in the liver thus preventing a complete decompensation of this *via* and partially limiting the serum porphyrins' accumulation during a stressful event.

AIP mice are characterized by metabolic disturbances during fasting such as hyperinsulinemia, the inability to utilize the hepatic carbohydrate-derived energy stores and bioenergetic imbalance. Indeed, it has been shown that lipids from the adipose tissues, instead of sugars, become the primary energy source in AIP mice in fasted condition[24]. Therefore, we investigated whether the α-LA supplementation may improve glucose metabolism in mice with the hepatic PBGD deficiency under caloric restriction.

AIP mice showed a status of hyperglycemia compared to Wt group (median:153.5 mg/dl, IQR [145.5-172.75] *vs.* median:110.5 mg/dl, IQR [94.75-118], p=0.0003 at ANOVA; adj p=0.004 *vs.* Wt, **Figure 4A**). Conversely, AIP mice supplemented with α-LA presented similar blood glucose levels to those observed in the Wt animals (median: 95.5 mg/dl,

IQR [87.75-105]; p=0.0003 at ANOVA; adj p=0.0001 *vs.* fasted AIP**, Figure 4A**). Furthermore, at GTT analysis, AIP group developed a higher glycemic peak within 30 minutes after glucose overload with a delayed decline over time compared to Wt (**Figure 4B**). α-LA administration improved GTT curve, resembling the trend of Wt controls (**Figure 4B**). Through the calculation of the AUC, we confirmed that AIP animals maintained higher glycemic levels than controls (p=0.01 at ANOVA, p=0.03 *vs.* Wt, **Figure 4C**) and that they were normalized in those treated with α-LA (p=0.01 at ANOVA, p=0.009 *vs.* fasted AIP, **Figure 4C**), thus indicating that α-LA may improve glucose tolerance.

In line with previous findings[24], hyperinsulinemia was detected in fasted AIP rodents (median:195.39 µlU/ml, IQR [162.79-255.34] *vs.* median:109.36 µlU/ml, IQR [86.91-112.69], p=0.002 at ANOVA, p=0.001 *vs.* Wt, **Figure 4D**), accompanied by less circulating triglycerides (p=0.04 at ANOVA, p=0.04 *vs.* Wt, **Figure 4E**), supporting the need of AIP mice to use alternative energy sources to glucose[24]. α-LA significantly reduced serum insulin levels by around 70% in AIP mice (median: 134.36 µlU/ml, IQR [105.73-186.07], p=0.002 at ANOVA, p=0.03 *vs.* fasted AIP, **Figure 4D**) and enhanced triglyceride release (p=0.04 at ANOVA, p=0.02 *vs.* fasted AIP, **Figure 4E**), thereby mirroring the effects observed in the siPBGD cells after α-LA exposure (**Figure 2I**).

From GTT and biochemical analysis, it has emerged that α-LA ameliorates glucose tolerance, and insulin response and increases the secretion of high-energy molecules (triglycerides), likely due to beneficial effects on hepatic glucose metabolism. In order to validate this hypothesis, we aimed to evaluate specific aspects which were altered in the liver of AIP models and which were related to insulin sensitivity and energetic balance linked to sugars metabolism.

At the hepatic level, an aberrant phosphorylation of phosphatidylinositol 3-kinases (PI3K) p85α, Akt (Ser473) and 4E-BP1 (Thr37/46), intracellular mediators of insulin signaling, were detected in AIP mice (**Figure 4F**), probably caused by the high insulin levels found in this group in a starved state. AIP mice exposed to α-LA showed an increase in hepatic insulin receptor β (InsRβ) chain and of PI3K p85α phosphorylation, although serum insulin was reduced in these animals (**Figure 4F**). Nevertheless, we found that Akt and 4E-BP1 were significantly less phosphorylated at Ser473 and Thr37/46 residues (**Figure 4F**). Such findings may suggest that AIP mice supplemented with α-LA

and in fasted condition did not develop a paradoxical insulin activation within the hepatic tissue since the phosphorylation of PI3K p85α was not followed by the activation of downstream mediators of the insulin signaling. Additionally, glucose transporter 2 (Glut2), which mediates glucose-dependent transport into the blood during fasting (**Figure 2F**), was increased in AIP+α-LA mice, thereby indicating a possible activation of glycogenolysis and gluconeogenesis within the liver.

In fasted AIP mice, ATP levels were lower than Wt ones (p=0.02 at ANOVA, p=0.03 *vs.* Wt, **Figure 4G**), while the total lactate amount was increased during fasting (p=0.006 at ANOVA, p=0.008 *vs.* Wt, **Figure 4H**). Reduced citrate synthase activity was even found in the liver of AIP mice (p=0.02 at ANOVA, p=0.01 *vs.* Wt, **Figure 4I**), supporting that the impairment of mitochondrial bioenergetics and the two major energy-yielding pathways, glycolysis and mitochondrial respiration, occurs in AIP pathology. Moreover, AIP mice are unable to exploit glycogen storages and gluconeogenesis during fasting, shifting the energy provision towards ketone bodies production[45,58], a metabolic anomaly that we even found in our experimental setting (p<0.0001 at ANOVA, p<0.0001 *vs.* Wt, **Figure 4J**). Notably, AIP mice which consumed dietary α-LA showed a significant raise of ATP content in the liver (p=0.02 at ANOVA, p=0.04 *vs.* fasted AIP, **Figure 4G**), paralleled by a decrease of hepatic lactate levels (p=0.006 at ANOVA, p=0.01 *vs.* fasted AIP, **Figure 4H**) and high citrate synthase (p=0.02 at ANOVA, p=0.02 *vs.* fasted AIP, **Figure 4I**). Consistent with the elevated ATP levels, AIP+α-LA group improved glycogen utilization during fasting (p<0.0001 at ANOVA, p<0.0001 *vs.* fasted AIP, **Figure 4J**) and showed higher levels of genes involved in different steps of gluconeogenesis (p=0.0005 at ANOVA, p=0.03 and p=0.004 *vs.* fasted AIP, **Figure 4K**).

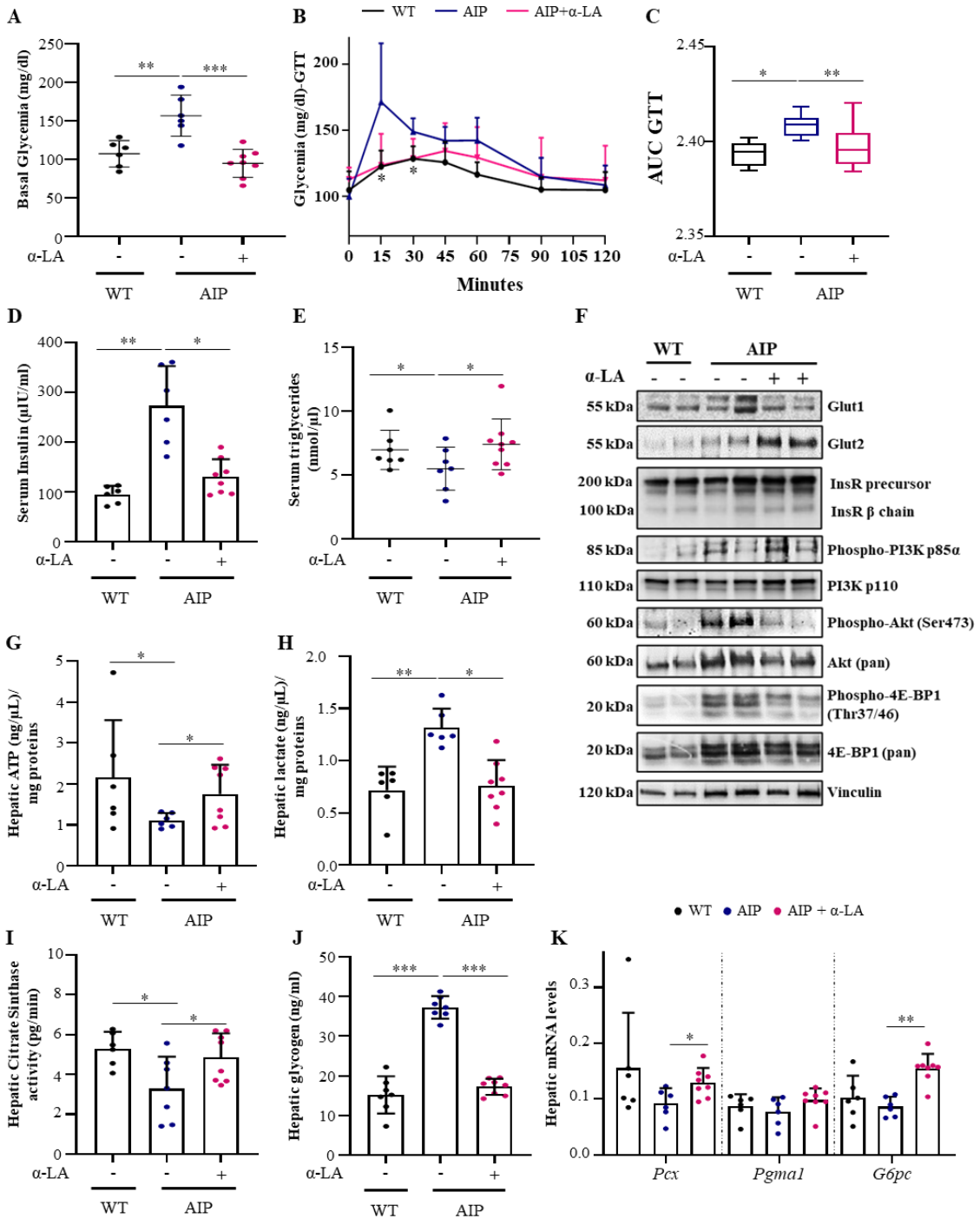

Figure 4. Improvement of metabolic profile, hepatic insulin sensitivity and glucose homeostasis in AIP mice supplemented with α-LA. **A**) Basal glycemia (mg/dl) was measured through Accu-chek Active blood glucose glucometer in Wt and AIP mice (n=6/group), and AIP+α-LA ones (n=8). **B-C**) GTT curve performed from 0 to 120 minutes after 2g/kg glucose i.p. injection and AUC was calculated to evaluate the blood glucose variations over time. **D-E**) Insulin concentration and triglycerides were colorimetrically measured in murine serum. *F*) Western blot analysis of insulin signaling and glucose transporters was evaluated in the livers of Wt, AIP and AIP+α-LA groups. Hepatic proteins were pooled and Vinculin was used as housekeeping gene. **G-J**) Hepatic ATP, lactate and citrate synthase and glycogen content was colorimetrically determined in frozen livers and normalized on hepatic mg of proteins. **K**) *pyruvate carboxylase* (*Pcx*), *phosphoglucomutase 1* (*Pgma1*) and *glucose-6-phosphatase catalytic subunit 1* (*G6pc*) mRNA levels were assessed through RT-PCR and normalized on *β-actin* housekeeping gene.

2.3 Evaluation of α-LA efficacy on insulin-sensitive tissues

As the liver, the energetic balance of insulin-sensitive tissues (muscle, brain and white visceral adipose tissues (wVAT)) may be affected by hyperinsulinemia. Therefore, we preliminarily explored whether energy reserves and insulin-sensitive glucose transporters (Glut) may be influenced by α-LA treatment during starvation.

In the skeletal muscle of fasted AIP mice, we observed a significant accumulation of glycogen storages (p=0.0007 at ANOVA, p=0.003 *vs.* Wt, **Figure 5A**), possibly implying that the inability to utilize glucidic supplies is also extended in other organs, which was mobilized in those receiving α-LA supplementation (p=0.0007 at ANOVA, p=0.0002 *vs.* fasted AIP, **Figure 5A**).

As concerns tissue-specific Glut, we found that Glut4 was upregulated in AIP+α-LA under the fasted condition in both skeletal muscle (p=0.01 *vs.* fasted AIP at two-tailed student *t*-test, **Figure 5B-C**) and even more, in wVAT (p<0.0001 *vs.* fasted AIP at two-tailed student *t* test, **Figure 5B-C**). Similarly, Glut3 was strongly induced in the brain of AIP mice treated with α-LA and (p=0.03 *vs.* fasted AIP at two-tailed student *t* test, **Figure 5B-D**), probably supporting that α-LA may sustain glucose uptake in targeted organs. InsRβ chain protein levels were not modified by α-LA treatment in the skeletal muscle or brain (**Figure 5E**). Conversely, the expression InsR precursor and the InsRβ chain was higher in the wVAT of AIP+α-LA mice compared to fasted AIP ones (p=0.03 *vs.* fasted AIP at two-tailed student *t* test, **Figure 5B-E**), showing a similar effect to that observed in the liver (**Figure 2F**).

Although Glut transporters were increased in muscle, brain and white adipose tissues, only the latter showed a significant increase of ATP levels in AIP+α-LA mice compared to fasted AIP ones (p=0.004 at ANOVA, p=0.002 *vs.* fasted AIP, **Figure 5F**), possibly suggesting that α-LA may enhance energy expenditure by the fat tissue to provide lipid sources during glucose deprivation.

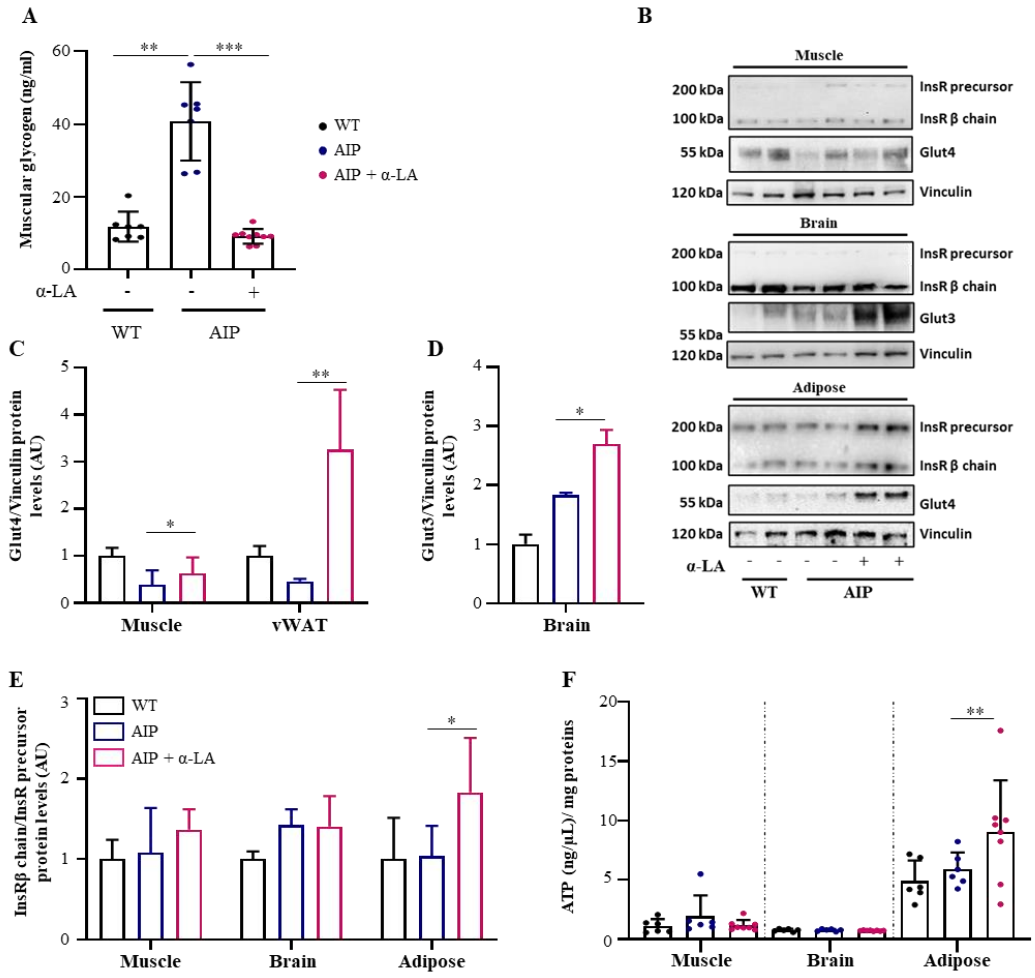

Figure 5. α-LA improved insulin-sensitive Gluts and improved ATP content in wVAT of fasted AIP mice. A) Glycogen was colorimetrically measured in skeletal muscle (*gastrocnemium*) and normalized of mg of proteins. **B-E**) Western blot images and protein quantification assessing the InsR and Gluts in *gastrocnemium*, brain and gonadal fat of Wt, AIP and AIP+α-LA groups. Proteins were pooled and Vinculin was used as housekeeping gene. Data are shown as fold increase (Arbitrary Unit-AU). **F**) ATP content was colorimetrically quantified in *gastrocnemius*, brain, and gonadal fat of Wt, AIP and AIP+α-LA groups. ATP levels were normalized on mg of proteins.

3. Expanding the insulin-sensitizing and dietary options for the correction of AIP dysmetabolic features

In the first part of this project, we have introduced the concept that an insulin-mimetic may ameliorate the metabolic disturbances in *PBGD*-silenced hepatocytes and in AIP mice under a fasted regimen, by improving both biochemical and hepatic defects. Since the results obtained were promising, we have broadened the experimental design by investigating the effects of other insulin-sensitive compounds already exploited in animal models of metabolic syndrome. All treatments were diluted in water and were

administered for a long-term period (12 weeks) as previously described[89-92]. The novel treatments included the heat-shocked probiotic (BLP1) and one of its by-products (LTA), which were both formulated with tapioca maltodextrin (TM), and the alive probiotic *B. coagulans*, which did not require the addition of TM. The new compounds were compared with TM-α-LA in order to evaluate both the long-term efficacy of α-LA and the potential combination with a carbohydrate, and the recently reported liver-targeted Ins-ApoA1 (Ins-TM)[24]. As disease control, a cohort of AIP mice (n=6) received the rAAV-PBGD gene therapy (TM-GT). As negative controls, we included both Wt and AIP mice (n=6/group) in which the vehicle TM was supplemented with water (Wt-TM, AIP-TM) throughout the 12 weeks and Wt and AIP mice (n=6/group) which received neither treatments nor TM (Wt-DW, AIP-DW). Given the large number of animals and data we had to deal with, we selectively reported specific targets related to glucose metabolism in this thesis.

3.1 LTA, α-LA and B. coagulans showed the best response to high glucose overload and hyperinsulinemia

At the end of the 12 weeks, the first parameter we focused on was the response to *i.p.* glucose overload. We carried out two types of GTT tests consisting of moderate to high glucose dose (2g/Kg and 5g/kg, respectively), attempting to investigate whether the treatments improved glucose tolerance in AIP mice and whether their efficacy persisted in a condition of severe hyperglycemia (≥300mg/dl). Therefore, mice were fasted 14 hours and the following morning, 2g/kg or 5g/kg of glucose was *i.p.* injected.

At GTT with 2g/Kg, AIP mice supplemented with TM-BLP-1, TM-LTA and TM-α-LA showed the best response to moderate glucose overload when compared to AIP with vehicle or drinking water (measured as total AUC after glucose *i.p.* injection; p=0.009 at ANOVA: p=0.01 and p=0.003 TM-BLP-1 *vs.* AIP-TM or AIP-DW; p=0.03 and p=0.007 TM-LTA *vs.* AIP-TM or AIP-DW; p=0.04 and p<0.01 TM-α-LA *vs.* AIP-TM or AIP-DW, data not shown), and against the TM-Ins and TM-GT groups (p=0.009 at ANOVA: p=0.03 and p=0.01 TM-BLP-1 *vs.* TM-Ins or TM-GT; p=0.04 and p=0.02 TM-LTA *vs.* TM-Ins or TM-GT; p=0.02 and p=0.04 TM-α-LA *vs.* TM-Ins or TM-GT, data not shown). Conversely, *B. coagulans* showed a lower but not significant reduction of the AUC compared to both AIP-TM and AIP-DW (data not shown).

As expected, after increasing the glucose dose up to 5g/Kg, severe hyperglycemia arose in all experimental groups (median blood glucose levels: 420.25 mg/dl IQR [389.37-474.87], measured at the peak ranging from 25-45' after *i.p.* glucose injection, **Figure 6A-B**). The AUC, calculated from 1st to 3rd hours post 5g/kg *i.p.* glucose overload, confirmed that AIP mice with or without TM delayed the reduction of hyperglycemia compared to Wt-TM and Wt-DW (p=0.0001 at ANOVA, p=0.03 AIP-TM *vs.* Wt-TM, p=0.004 AIP-DW *vs.* Wt-DW, **Figure 6C**). At such high concentration, TM-BLP1 was less effective at restoring normal blood glucose levels (p=0.33 *vs.* AIP-TM and AIP-DW, **Figure 6A-C**). Conversely, TM-LTA and TM-α-LA showed the strongest effect at improving hyperglycemia compared to both AIP-TM and AIP-DW (p=0.02 at ANOVA: p=0.009 and p=0.001 TM-LTA *vs.* AIP-TM or AIP-DW; p=0.02 and p=0.005 TM-α-LA *vs.* TM-Ins or TM-GT, **Figure 6A-C**), likely due to the fact that the effect of probiotics is closely related to changes in the gut microbiota and it may take longer to be effective, whereas LTA and α-LA molecules may directly influence the glucose uptake ability in insulin-sensitive organs.

No remarkable differences were found in AIP mice receiving either TM-Ins or TM-GT compared to AIP-TM on reduction of the AUC (**Figure 6C**), despite a downward trend in the AUC was observed against the AIP-DW group (p=0.07 *vs.* AIP-DW, **Figure 6C**), possibly suggesting that the addition of TM in water may slightly modify the effects of Ins and GT on AUC. Although glucose peak did not significantly decrease in TM-Ins and TM-GT treated mice, we investigated whether the two treatments may ameliorate hyperglycemia by improving glucose uptake rate. Therefore, we measured the slope from the glucose peak at 30 up to 90 minutes after *i.p.* 5g/kg glucose injection. We found that both experimental groups showed a rapid decline of glycemia after 30' of glucose overload compared to both AIP-TM and AIP-DW (p=0.003 at ANOVA: p=0.008 and p=0.01 TM-Ins *vs.* AIP-TM or AIP-DW; p=0.02 and p=0.04 TM-GT *vs.* AIP-TM or AIP-DW, **Figure 6D**). Notably, AIP mice supplemented with *B. coagulans* not only showed a dramatic decline of glucose peak after 30' (**Figure 6B**), with a significant reduction of AUC (p=0.02 at ANOVA, p=0.01 *vs.* AIP-DW, **Figure 6C**), but it was also paralleled by higher velocity to restore basal glycemia compared to AIP-TM and AIP-DW (p=0.003 at ANOVA, p=0.002 and p=0.005 *B. coagulans* vs. AIP-TM or AIP-DW). In sum, findings support that TM-BLP1 may improve glucose tolerance at moderate dose but it resulted

ineffective against high blood sugars levels. TM-LTA and TM-α-LA molecules may exert a systemic effect on glucose uptake resulting in an overall reduction of blood sugar levels at both moderate and high glucose overload, while the liver-targeted therapies may rapidly enhance the glucose uptake, probably by directly acting on the liver. Interestingly, the alive probiotic *B. coagulans* presented both effects showed by TM-LTA and TM-α-LA diets as well as the liver-targeted therapies, as it improved the AUC in case of severe hyperglycemia coupled with a rapid reduction of glycemic peak.

As in the pilot study, we explored the effects of the diets on insulin levels during caloric restriction. Higher serum insulin was detected in AIP-DW mice (median: 160.44 µlU/ml, IQR [130.35-261.42] *vs.* median: 126.29 µlU/ml, IQR [121.64-132.49], p=0.02 *vs.* Wt-DW, **Figure 6F**) and, even more, in those with vehicle (median: 191.19 µlU/ml, IQR [129.02-428.77] *vs.* median: 152.08 µlU/ml, IQR [139.29-166.15], p=0.02 *vs.* Wt-TM, **Figure 6F**). Thus, the paradoxical high levels observed in untreated AIP mice during fasting suggest that AIP pathogenesis may be associated with abnormal insulin secretion, further exacerbated by the addition of TM in water.

Elevated insulin levels were even observed in TM-Ins (median: 192.25 µlU/ml, IQR [107.69-483.48], **Figure 6F**), and TM-GT (median: 219.64 µlU/ml, IQR [156.23-486.94], **Figure 6F**), thereby suggesting that the liver-targeted treatments did not confer a great protection against pathologic hyperinsulinemia.

AIP mice supplemented with TM-BLP1 showed lower but not significant trend of reduction of serum insulin compared to AIP-TM (median: 162.85 µlU/ml, IQR [124.09-257.59], p=0.03 at ANOVA, p=0.08 *vs.* AIP-TM, **Figure 6F**), while the TM-LTA diet displayed a greater effect than BLP1 to ameliorate insulin levels in AIP fasted mice (median: 138.91 µlU/ml, IQR [114.22-167.40], p=0.03 at ANOVA, p=0.04 *vs.* AIP-TM, **Figure 6F**). Likewise, TM-α-LA improved hyperinsulinemia, showing the lowest insulin levels among all the AIP experimental groups (median: 113.40 µlU/ml, IQR [107.25-150.47], p=0.03 at ANOVA, p=0.01 *vs.* AIP-TM, **Figure 6F**) and resembling the results obtained during the short-term exposure (**Figure 4D**). Although TM-BLP1, TM-LTA and TM-α-LA treated mice reduced insulin levels compared to AIP-TM, their effects on hyperinsulinemia were not appreciable against the AIP-DW group, which, on one side had higher insulin levels compared to Wt-DW, but on the other side serum insulin was less elevated than those observed in AIP-TM mice probably due to the absence of TM in

water. Finally, AIP mice receiving the alive bacteria *B. coagulans* restored serum insulin to the same levels as those found in WT mice during fasting (median: 133.96 µlU/ml, IQR [111.76-166.16], p=0.04 *vs.* AIP-DW, **Figure 6F**), thereby resulting effective to improve both glycemic and insulinemic indexes.

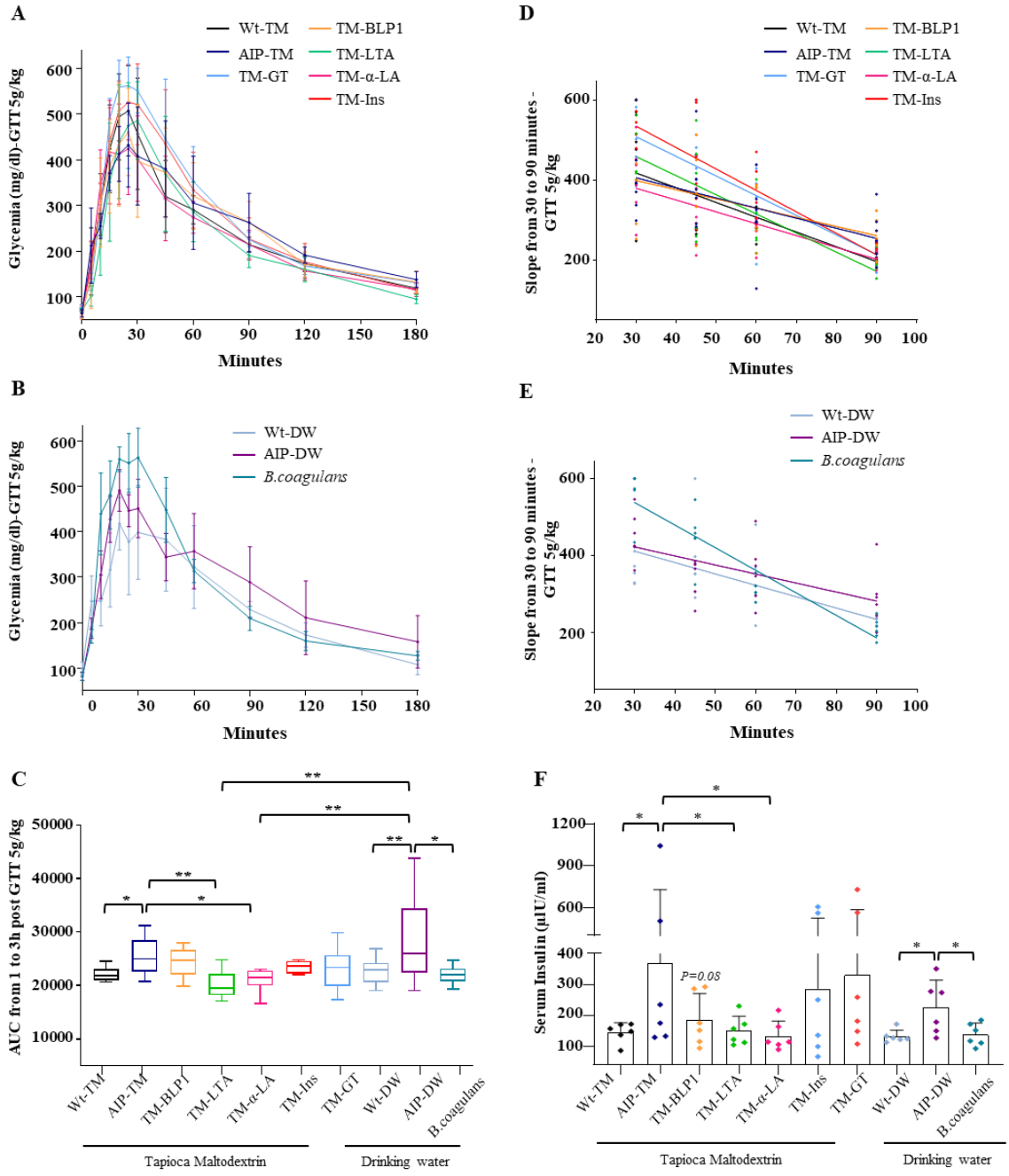

Figure 6. AIP mice feeding LTA, α-LA and B. coagulans diets ameliorated GTT and hyperinsulinemia. A-B) GTT curves performed after 5g/kg i.p. glucose overload to induce severe hyperglycemia. Blood glucose was measured from 0 to 180 minutes after glucose injection**. C)** Box plot showing the AUC calculated from 1st to 3rd hours post 5g/kg i.p. glucose overload. D-E) Analysis of the slope was carried out from the glycemic peak at 30' up to 90' minutes after carbohydrate loading**. F)** Insulin levels were measured in the serum samples of Wt and AIP mice with or without treatments. All experimental groups were fasted 14hrs before GTT and insulin measurements. Data are shown as average and standard deviation (SD). Comparisons were performed by one-way ANOVA followed by Bonferroni post-test.

3.2 LTA, α-LA and B. coagulans reduced body fat fraction and increased lean mass in AIP mice

Throughout the experimental trial, we monitored weekly food intake and body weight attempting to evaluate whether diets may modify nutritional habits, energy expenditure (measured as weight gain (g)/Kg weekly food ingested) and body composition. Weight gain (or loss) is directly linked to energy expenditure, physical activity or the need to replenish energy with food. If energy consumption is more than food ingested, animals will tend to lose weight, whereas if energy consumption is less than food intake, animals will tend to gain weight.

The median food ingested was the same between Wt-DW and Wt-TM mice (103.05g and 103.8g, respectively, **Figure 7A**), and it was associated with no alterations in food yield (**Figure 7B**), supporting that TM did not alter energy expenditure in Wt condition. Conversely, lower weekly food intake was observed in AIP-TM compared to AIP-DW (96.1g *vs.* 107.86g, respectively, **Figure 7A**). Similar weekly food consumption was detected in TM-BLP1 (95.0g), TM-LTA (91.35g), TM-α-LA (90.65g), TM-Ins (95.1g) and TM-GT (99.45g) groups compared to AIP-TM (96.1g), while significant differences emerged by comparing AIP-DW mice to those supplemented with either TM-α-LA (90.65g *vs.* 107.86g, p=0.0004 at ANOVA, p=0.02 *vs.* AIP-DW, **Figure 7A**) or *B.coagulans*, which showed the lowest food intake probably due to the poor palatability of the diet (82.74g *vs.* 107.86g, p=0.0004 at ANOVA, p=0.01 *vs.* AIP-DW, **Figure 7A**). With the same amount of food eaten, AIP-DW mice and, even more, those receiving TM, were featured by less weight gain compared to Wt groups (p=0.001 at ANOVA, p=0.008 AIP-TM *vs.* Wt-TM; **Figure 7B**), supporting that AIP mice run into high energy expenditure to possibly face energy demand. Reduced weight gain was furtherly detected in AIP plus either TM-BLP1 or TM-α-LA diets compared to AIP-TM and it became significant against the AIP-DW group (p=0.001 at ANOVA, p=0.003 TM-BLP1 *vs.* AIP-DW; p=0.01 TM-α-LA *vs.* AIP-DW; **Figure 7B**). Low weight gain was even estimated in AIP mice with the addition of TM-LTA and *B.coagulans* diets or with the liver-targeted treatments compared to AIP-DW, although no significance arose among multiple comparisons analysis, but not compared to AIP-TM (**Figure 7B**), thus suggesting that the presence of TM in water may enhance energy consumption in AIP mice and the latter may be exacerbated with the heat-shocked BLP1 bacteria and α-LA.

Attempting to investigate whether weight loss was associated with changes in the body composition, we performed EchoMRI-100-700 (Echo Medical Systems, Houston, TX, USA) in *in vivo* animals, which provided a precise measurement of fat and lean mass, measured as % on body weight (BW). We found no difference in both fat and lean/fat ratio among AIP groups and Wt ones with or without TM (**Figure 7C-D**). Despite TM-BLP1 treated AIP mice reduced weight gain over the 12 weeks of treatment, the % of both fat and lean mass was not different from those observed in both Wt and AIP mice (**Figure 7C-D**). Otherwise, low weight gain observed in TM-LTA, TM-α-LA, TM-Ins and TM-GT groups were paralleled by a lesser % of fat mass by 25.6%, 18.64%, 18.86% and 12.83%, respectively (p=0.003 at ANOVA, p=0.01 TM-LTA *vs.* AIP-TM, p=0.03 TM-α-LA, TM-Ins and TM-GT *vs.* AIP-TM, **Figure 7C**), and the largest effect on fat composition was observed in AIP mice supplemented with *B.coagulans* which reduced %fat by 30% (p=0.003 at ANOVA, p=0.009 vs. AIP-DW, **Figure 7C**). Interestingly, in parallel to lower fat content, a significant improvement of lean/fat ratio was found in TM-LTA and TM-α-LA mice by 33.8% and 22.7%, respectively (p=0.005 at ANOVA, p=0.01 TM-LTA *vs.* AIP-TM, p=0.02 TM-α-LA *vs.* AIP-TM, **Figure 7D**), while it did not reach the significance in TM-Ins and TM-GT treated groups (p=0.005 at ANOVA, p=0.07 TM-Ins and TM-GT *vs.* AIP-TM, **Figure 7D**). Finally, *B.coagulans* supplemented mice showed the highest lean/fat ratio, increasing by around 46.28% compared to AIP-DW (p=0.005 at ANOVA, p=0.0.04 vs. AIP-DW, **Figure 7D**).

Therefore, such findings have suggested that diets did not or slightly modify weekly food intake in AIP mice. Overall, AIP mice weight less than Wt ones, even though the minor BW was not associated to alterations of body composition, in terms of both fat and mass percentage, but rather to a higher energy consumption. Lower weight gain combined to reduced % of fat composition was observed in all experimental AIP groups in which diets were added to the drinking water. However, treatments that significantly induced changes in %fat/BW paralleled by a concomitant increased in lean mass were TM-LTA, TM-α-LA and *B.coagulans*, supporting that the high energy expenditure were accompanied by an improved muscle mass tone.

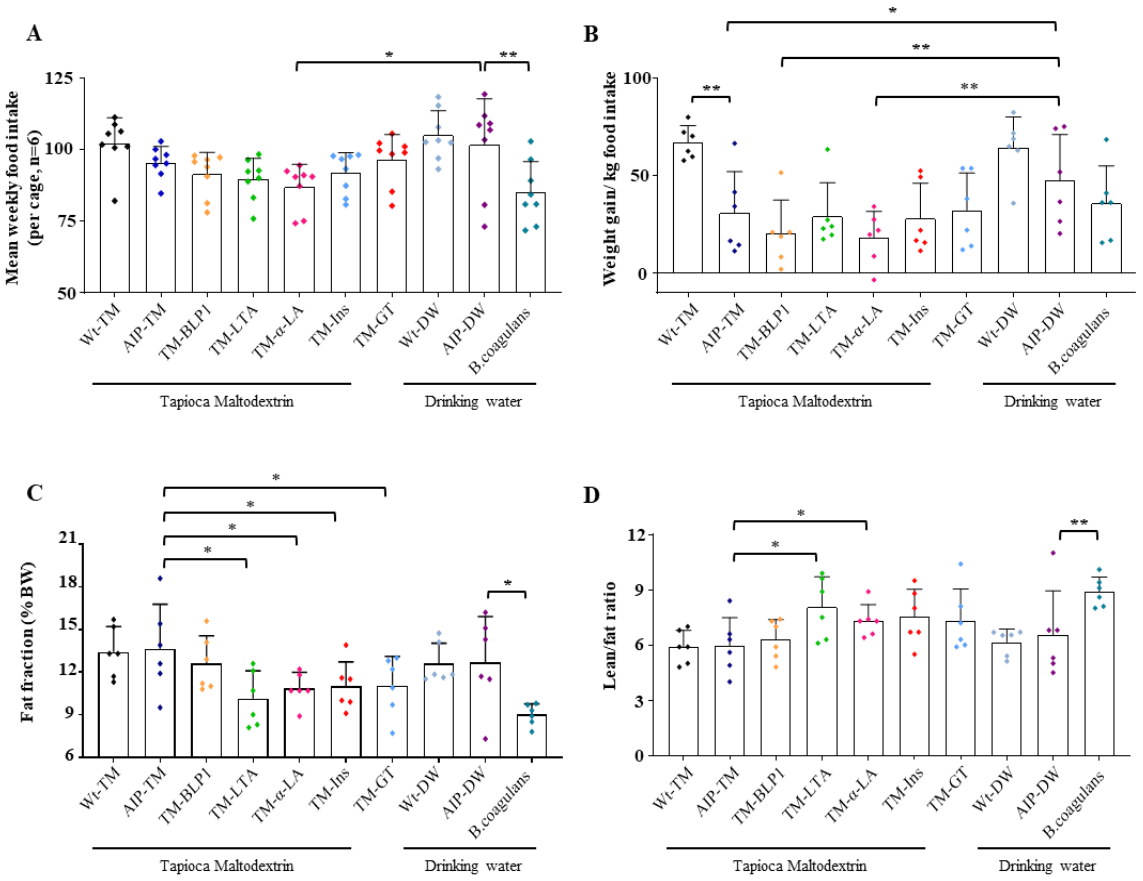

Figure 7. LTA, α-LA and B.coagulans diets induced weight loss accompanied by higher lean/fat ratio. A) Food consumption was measured every 3 days/week and weekly food consumption was calculated as the mean of the three measurements. **B)** Body weight was weekly measured in mice and normalized on kg of weekly food ingested. **C-D)** Body fat composition (%) and lean mass were assessed by EchoMRI-100-700 (Echo Medical Systems, Houston, TX, USA). Data are shown as average and standard deviation (SD). Comparisons were performed by one-way ANOVA followed by Bonferroni post-test.

3.3 The probiotics BLP1 and B.coagulans, more than LTA and α-LA, contribute to raise heme content in AIP mice

As outlined above, AIP mice carry hepatic PGD deficiency coupled with reduced heme biosynthesis. Therefore, the first parameter we explored was whether treatments might modify hepatic heme content. As expected, TM-Ins and TM-GT improved heme content in AIP mice (p=0.001 at ANOVA, p<0.001 TM-Ins *vs.* AIP-TM and AIP-DW; p<0.001 and p=0.03 TM-GT *vs.* AIP-TM and AIP-DW, **Figure 8A**). TM-LTA and TM-α-LA diets increased heme levels in the livers of AIP mice compared to AIP-TM (p<0.001 at ANOVA, p=0.004 TM-LTA *vs.* AIP-TM; p=0.01 TM-α-LA *vs.* AIP-TM, **Figure 8A**), mirroring what observed in the pilot study (**Figure 4B**). Surprisingly, the largest effects

on hepatic heme content was observed in AIP mice treated with the heat-shocked and alive bacteria, which showed a hepatic heme content equal to the concentration found in Wt mice ($p<0.001$ at ANOVA, $p<0.001$ TM-BLP1 *vs.* AIP-TM and AIP-DW; $p<0.01$ B.coagulans *vs.* AIP-TM and AIP-DW, **Figure 8A**), suggesting that the hepatic heme availability may be enhanced by the gut-liver crosstalk.

3.4 Insulin-sensitizing compounds regulate glucose transporters and insulin receptors, but slightly modify glucose uptake in the liver and the brain

Once determined that diets aid to increase the heme content in the liver, we looked at glucose handling by combining an anatomical-functional analysis (PET/CT) to the evaluation of Glut transporters and InsR in the liver and insulin-sensitive tissues. [18F]FDG was injected in fasted animals and, to ensure a precise measurements of its uptake, we measured [18F]FDG radioactivity *ex vivo*.

Several studies have reported that sugars may modify the [18F]FDG uptake in the liver and other organs like the brain cortex[100]. Here, we found that TM reduced hepatic glucose uptake of Wt-TM mice *vs.* Wt-DW ($p<0.001$ at ANOVA, $p<0.001$ Wt-TM *vs.* Wt-DW, **Figure 8B**). AIP mice with or without vehicle showed lower [18F]FDG uptake in the liver compared to Wt-DW animals ($p<0.001$ at ANOVA, $p<0.001$ AIP-TM *vs.* Wt-DW; $p<0.001$ AIP-DW *vs.* Wt-DW; **Figure 8B**). Such findings were consistent with both the condition of hyperinsulinemia observed in AIP animals during caloric restriction and supported the concept that the latter are poorly capable of internalizing glucose. TM-BLP1, TM-LTA and TM-α-LA, but not *B.coagulans*, attempted to counteract the hepatic inability of AIP mice to absorb [18F]FDG, showing slightly better effects of that induced with TM-Ins and TM-GT therapies, albeit none of the dietary treatments reached the statistical significance ($p<0.001$ at ANOVA, $p=0.06$ TM-BLP1 *vs.* AIP-TM; p=ns TM-LTA *vs.* AIP-TM; $p=0.06$ TM-α-LA *vs.* AIP-TM, **Figure 8B**). Paralleling the PET/CT results, we found that, the TM-Ins and TM-GT showed the strongest effect at enhancing Glut1/2 protein expression in AIP livers, followed by TM-BLP1 diet (**Figure 8C**). TM-LTA and *B.coagulans* did not improve Glut1/2 levels, while the addition of TM to α-LA appeared to not have an additive effects of Glut1/2 expression (**Figure 8C**). Conversely, both exogenous TM-Ins and the analogue TM-α-LA induced the InsRβ chain expression, whose levels were reduced in AIP-DW mice, thereby resembling the trend obtained in the pilot study (**Figure 8C**).

Likewise, the highest levels of [18F]FDG absorption were found in the brain of Wt-DW mice, which were lowered by the presence of TM ($p=0.001$ at ANOVA, $p<0.001$ Wt-DW *vs.* Wt-TM, **Figure 8D-E**). Less [18F]FDG signal was even traced in both AIP-DW and AIP-TM mice compared to Wt-DW ($p=0.001$ at ANOVA, $p<0.001$ Wt-DW *vs.* AIP-DW, $p=0.003$ Wt-DW *vs. A*IP-TM, **Figure 8D-E**), possibly suggesting that the reduced glucose uptake rate may be extended to the organs involved in AIP symptomatology. No increasing[18F]FDG radioactivity was found with TM-Ins and TM-GT, probably as their efficacy is best elicited in the liver. TM-BLP1, TM-LTA and *B.coagulans* did not show an increment of cerebral [18F]FDG tracer compared to both AIP mice with or without the vehicle, while TM-α-LA resulted in the only treatment in which [18F]FDG was ~20% more than AIP-DW and AIP-TM groups even if no statistical differences arise with the multiple comparisons probably due to the lack of statistical power (**Figure 8D-E**). Although a low efficacy in glucose uptake was detected in the brain, dietary and non-dietary supplements still provided an advantage in inducing the expression of tissue-specific Glut transporters and InsRβ chain as observed in the livers. Specifically, AIP mice treated with TM-Ins showed the largest expression of Glut1 and Glut3, followed by the TM-BLP1 and *B.coagulans* bacteria (**Figure 8F**). The latter even enhanced the InsR β chain protein levels (**Figure 8F**), suggesting that the gut microbiota may stimulate factors involved in carbohydrate metabolism. TM-LTA resulted in the lowest efficacy at improving [18F]FDG absorption and Glut1/Glut3/InsRβ chain proteins in the brain. In contrast, AIP mice supplemented with TM-α-LA did not further modify the expression of glucose channels and insulin receptor despite the higher [18F]FDG uptake (**Figure 8F**), possibly due to a partial bias of TM on the effects of α-LA administration.

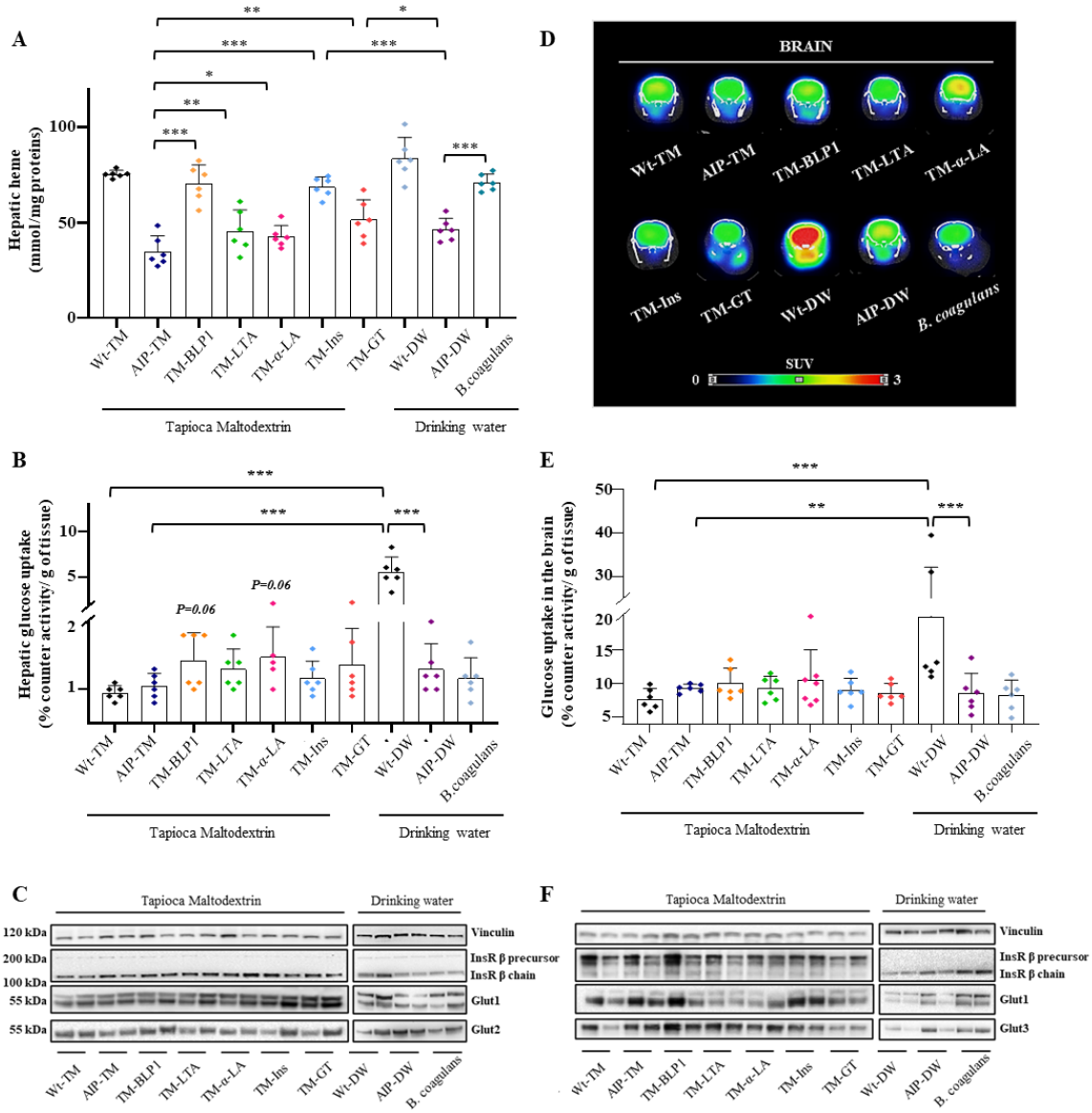

Figure 8. The effects of insulin-sensitizing compounds on [18F]FDG uptake and glucose transporters in the liver and brain. **A)** Bar graph showed heme content (mmol), which was colorimetrically measured in frozen livers. Data were normalized on hepatic mg of proteins. All experimental groups were fasted 14 hours before the sacrifice. **B)** [18F]FDG radioactivity measured ex vivo in murine livers. **C)** Hepatic Glut1/2 and InsRβ chain analyzed through WB. **D-E)** Representative PET/CT in vivo images (axial plane) performed after 1h of [18F]FDG injection in fasted mice and ex vivo quantification of [18F]FDG radiotracer of brain tissues. **F)** Glut1/2 and InsRβ chain analyzed through WB assessed in brain tissues. *Ex vivo* quantification data were normalized on [18F]FDG injected volume and tissue weight (g).Values are shown as average and standard deviation (SD). Comparisons were performed by one-way ANOVA followed by Bonferroni post-test.

3.5 TM-BLP1, TM-α-LA and B.coagulans enhance glucose absorption in skeletal muscle

In skeletal muscle, AIP-DW and AIP-TM mice displayed a higher but not significant glucose uptake than Wt animals (**Figure 9A-B**), possibly due to a pathologic energy expenditure. We previously reported that both AIP groups were characterized by hyperinsulinemia during caloric restriction (**Figure 6F**), thereby suggesting that the higher rate of [18F]FDG uptake in AIP skeletal muscles may result from an aberrant response to elevated insulin levels which stimulate glucose utilization in peripheral tissues. Similarly, TM-Ins and TM-GT did not significantly improve insulin and lean/fat mass ratio. In TM-Ins mice, we did not find differences in [18F]FDG absorption, while TM-GT muscles behave as AIP-DW and AIP-TM groups (**Figure 9A-B**). Conversely, lower serum insulin combined to an improvement of lean/fat mass ratio (**Figure 6F** and **7F**) were detected in AIP mice receiving TM-BLP1, TM-LTA, TM-α-LA and *B.coagulans*. Here, we found that [18F]FDG signal was higher in TM-LTA treated mice, but the effect was not statistically significant (p=0.003 at ANOVA, p=0.34 and p=0.05 TM-LTA *vs.* AIP-TM or AIP-DW, **Figure 9A-B**). In the skeletal muscle of AIP mice supplemented with TM-BLP1, TM-α-LA and *B.coagulans,* the higher [18F]FDG uptake reached the significance against the AIP-TM (p=0.003 at ANOVA, p=0.04 TM-BLP1 *vs.* AIP-TM; p=0.04 TM-α-LA *vs.* AIP-TM; **Figure 9A-B**) and, even more, against the AIP-DW (p=0.003 at ANOVA, p=0.006 TM-BLP1 *vs.* AIP-DW; p=0.006 TM-α-LA *vs.* AIP-DW; p=0.04 *B.coagulans vs.* AIP-DW; **Figure 9A-B**).

Attempting to evaluate the fold increase in the rate of glucose uptake, we calculated the average [18F]FDG signal in AIP-DW and AIP-TM skeletal muscles and compared it with those of significant treated groups, (TM-BLP1, TM-α-LA and *B.coagulans*). We observed that [18F]FDG absorption in skeletal muscles increased by 82.3%, 86% and 60% in AIP mice supplemented with TM-BLP1, TM-α-LA and *B.coagulans*, respectively, confirming previous data which indicated that the improvement of biochemical abnormalities and muscle mass was associated with an ameliorated energy utilization.

Moreover, as in the other organs, treatments may regulate the expression of glucose channels and this stimulation not always matched with their ability to improve [18F]FDG uptake but it could rather be related to a transcriptional/translational regulation. For

instance, a higher signal of the insulin-sensitive Glut4 emerged in striated muscle of AIP mice with TM-LTA (**Figure 9C**). Glut1 and Glut4 were mostly induced by the TM-BLP1 and *B.coagulans* treatment compared to either AIP-TM or AIP-DW (**Figure 9C**). *B.coagulans* even enhanced InsR β chain protein levels, thereby suggesting that contribution of gut microbiota at stimulating factors involved in carbohydrate metabolism is extended at systemic level. In AIP mice supplemented with TM-α-LA, Glut1/4 expression was higher compared to AIP-DW mice but not versus the AIP-TM group (**Figure 9C**), reinforcing the concept that TM did not enhance α-LA effects on glucose transporters.

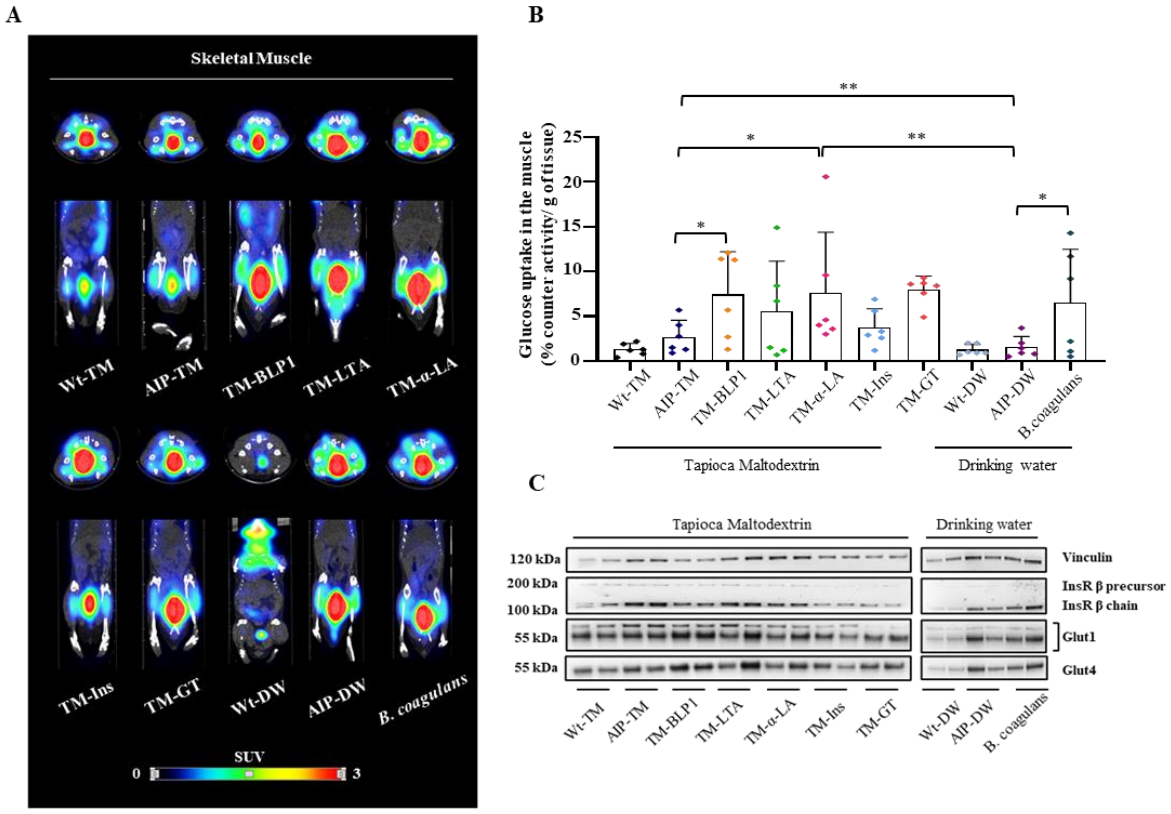

Figure 9. The effects of insulin-sensitizing compounds on [18F]FDG uptake and glucose transporters in skeletal muscle. A) Representative PET/CT in vivo images of the skeletal muscle (tibial anterior, on top: axial plane; on bottom: coronal plane) performed after 1h of [18F]FDG injection in fasted mice. **B)** *Ex vivo* quantification of [18F]FDG radiotracer measured in the skeletal muscles. Data were normalized on [18F]FDG injected volume and tissue weight (g). **C)** Glut1/2 and InsRβ chain analyzed through WB assessed in skeletal muscles. Values are shown as average and standard deviation (SD). Comparisons were performed by one-way ANOVA followed by Bonferroni post-test.

3.6 Glucose absorption in AIP mice: the role of white and brown fat

As aforementioned, it has been demonstrated that AIP mice are leaner than Wt ones since they exploit white fat deposits (WAT) more than glucidic reserves as alternative source of energy[24,45]. Moreover, brown adipose tissue (BAT) activity has been associated with loss of body weight and improved muscle contractility, whereas its decline with reduced insulin sensitivity, glucose homeostasis and T2DM development[101]. Therefore, we investigated the role of metabolic active white and brown fat in AIP, a field that needs to be elucidated. To this aim, [18F]FDG was injected in half of AIP and Wt mice with or without diets and liver-targeted treatments (n=3/group) which were kept in warm condition, while the other half underwent cold for 1 hour before [18F]FDG injection in order to activate BAT (n=3/group). All experimental groups were fasted 14 hours before the PET/CT and the *ex-vivo* analysis.

Compared to AIP-DW and AIP-TM, a higher basal [18F]FDG signal was found in Wt-DW and Wt-TM mice during the *in vivo* PET/CT imaging (**Figure 10A**), which was exacerbated by the presence of TM in drinking water by 3-fold ($p<0.001$ at ANOVA, $p=0.02$ Wt-DW *vs.* Wt-TM **Figure 10A-B**). Similarly, AIP mice treated with TM-GT showed an increased glucose uptake in the BAT at RT compared to AIP mice (**Figure 10A**), which was not greatly influenced by cold exposure, suggesting that less energy dissipation may occur after the re-establishment of hepatic PBGD activity.

As outlined above, both AIP mice had lower BAT activation compared to Wt groups (**Figure 10A**) and the rate of glucose uptake between AIP-DW and AIP-TM groups was not modified by the presence of TM. Under cold *stimulus*, [18F]FDG was internalized in the BAT with an increase of 2-fold, even if the statistical significance was not reached probably due to the lack of statistical power ($p<0.001$ at ANOVA, $p=0.07$ AIP-DW at RT *vs.* AIP-DW RT at 4°C; $p=0.06$ AIP-TM at RT *vs.* AIP-TM RT at 4°C; **Figure 10B**). Thus, AIP mice are featured by low BAT metabolic activity at baseline, which is consistent with the aberrant glucose metabolism and hyperinsulinemia, and they need to dissipate heat more than Wt after cold exposure probably to regulate energy balance. AIP mice under the TM-BLP1 and TM-LTA regimen showed the highest metabolic activation of BAT as they induced a [18F]FDG absorption by more than 4-fold after cold compared to their counterpart at RT ($p<0.001$ at ANOVA, $p<0.001$ TM-BLP1 at RT *vs.* TM-BLP1 RT at 4°C; $p<0.001$ TM-LTA at RT *vs.* TM-LTA RT at 4°C, **Figure 10B**). Likewise, AIP

mice receiving *B.coagulans* enhanced glucose absorption in the BAT after being out in the cold condition ($p<0.001$ at ANOVA, $p=0.005$ *B.coagulans* at RT *vs. B.coagulans* RT at 4°C, **Figure 10B**), albeit the response was less effective than those induced by TM-BLP1 and TM-LTA. Such data may suggest that compounds involving gut microbiota or its derivatives intensified the activity of the BAT in dissipating energy during fasting. Conversely, with both TM-α-LA and TM-Ins, [18F]FDG levels were not changed among warm and cold status, showing a similar effect of those observed in Wt-DW, Wt-TM and AIP plus TM-GT (**Figure 10A-B**), thereby suggesting that both treatments may preserve energy reserves during caloric restriction.

In order to evaluate glucose uptake in WAT, we collected visceral WAT which included mesenteric (MES), gonadal (GON) and retroperitoneal (RT), and subcutaneous fat (SC). AIP-DW mice showed less ability to capture [18F]FDG in WAT compared to Wt-DW ($p<0.001$ at ANOVA, $p=0.0002$ AIP-DW *vs.* WT-DW, **Figure 10C**), whilst those receiving TM enhanced [18F]FDG uptake ($p<0.001$ at ANOVA, $p=0.01$ AIP-TM *vs.* AIP-DW, **Figure 10C**). In AIP mice supplemented with TM-BLP1 and TM-LTA or in those receiving TM-Ins and TM-GT injection, a higher radiotracer signal was detected compared to AIP-DW, but the effect seemed to be driven mostly by TM than by the treatments (**Figure 10C**). Conversely, AIP mice supplied with *B.coagulans* increased [18F]FDG absorption in WAT ($p<0.001$ at ANOVA, $p=0.04$ *B.coagulans vs.* AIP-DW; **Figure 10C**) and those consuming TM-α-LA displayed the major glucose internalization in WAT compared to AIP-DW ($p<0.001$ at ANOVA, $p=0.003$ TM-α-LA *vs.* AIP-DW, **Figure 10C**), especially in GON fat pad ($p<0.001$ at ANOVA, $p=0.03$ and $p=0.007$ TM-α-LA *vs.* AIP-TM or AIP-DW, **Figure 10C**), RT ($p<0.001$ at ANOVA, $p=0.0008$ TM-α-LA *vs.* AIP-DW, **Figure 10C**) and SC ($p<0.001$ at ANOVA, $p=0.01$ TM-α-LA *vs.* AIP-DW, **Figure 10C**).

Concerning the expression of glucose transporters in adipose tissues, we pooled BAT and WAT proteins according to the temperature (warm or cold) to which animals were exposed (n=3 mice/group). We found that AIP mice who have ingested TM-BLP1, TM-LTA and *B.coagulans* diets presents higher expression of Glut1 and Glut4 in brown but not white adipose tissue when they were challenged with cold, suggesting that the high [18F]FDG absorption in the BAT was coupled by enhanced expression of glucose transporters (**Figure 10D-E**). In AIP mice treated with TM-α-LA, TM-Ins or TM-GT,

which dissipated less energy under fasting and cold conditions, we observed differences between cold and room temperature only in the BAT of those receiving TM-α-LA (**Figure 10D-E**), probably due to the intrinsic ability of this compound to induce Glut transporters on membrane surface. However, its effects in inducing Glut4 in the WAT did not emerge as in the pilot study and despite this treatment was the only one which increased glucose uptake in white adipocytes. Likely, the presence of TM may mask the α-LA functions on targeted organs, thereby corroborating the hypothesis that it may be supplemented without this sugar.

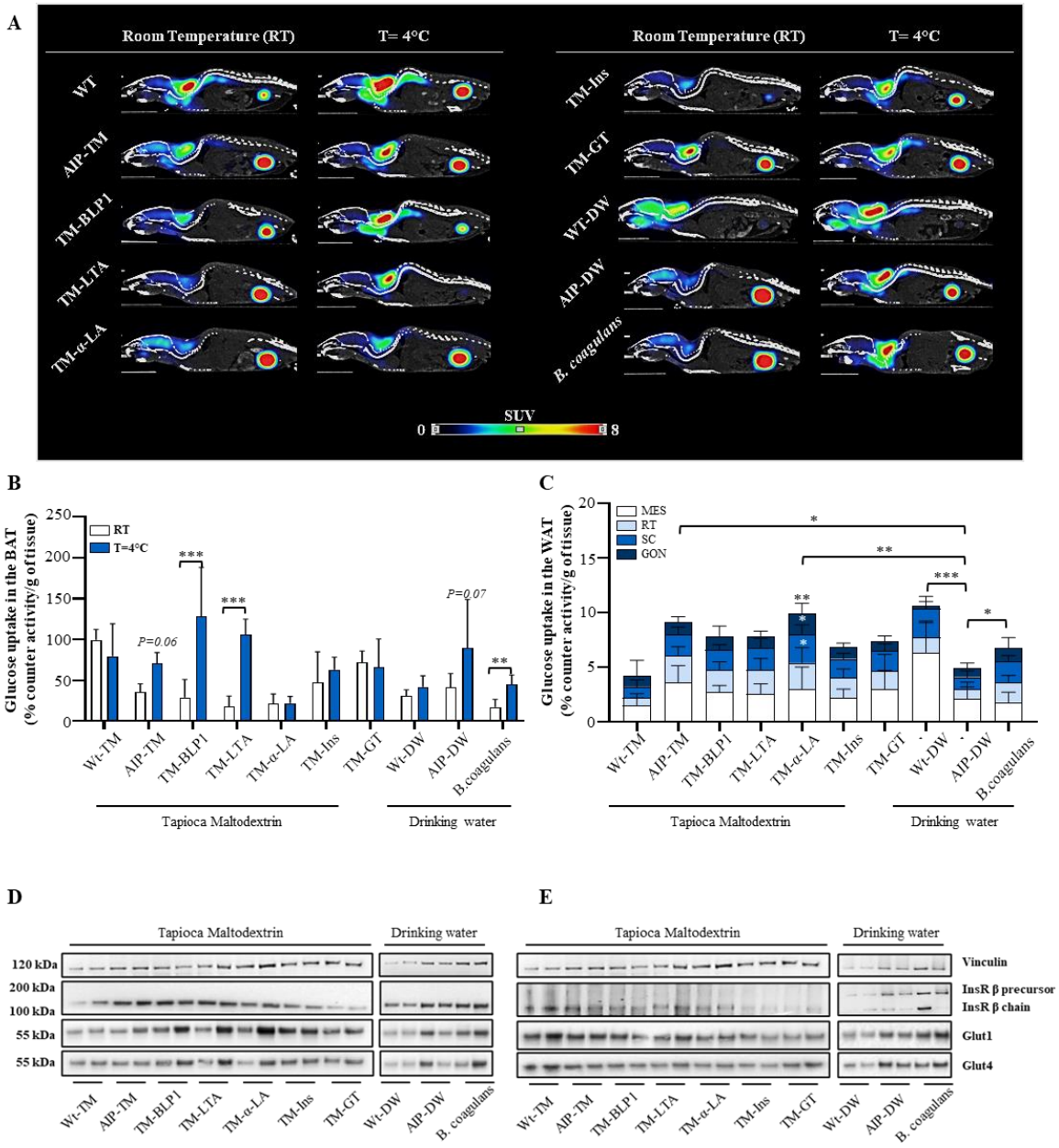

Figure 10. [18F]FDG uptake and glucose transporters white and brown adipose tissues. A) Representative PET/CT in vivo images of [18F]FDG uptake in BAT (interscapular space, sagittal plane) performed at RT and 4°C in fasted mice. **B-C)** *Ex vivo* quantification of [18F]FDG radiotracer measured in BAT and white fat pads (mesenteric, gonadal, retroperitoneal, and subcutaneous). Data were normalized on [18F]FDG injected volume and tissue weight (g). **D-E)** Glut1/2 and InsRβ chain analyzed through WB assessed in BAT and WAT (gonadal fat). Values are shown as average and standard deviation (SD). Comparisons were performed by one-way ANOVA followed by Bonferroni post-test.

4. Metabolic profile and evaluation of liver pathology in AIP patients

Hyperinsulinemia and high HOMA-IR have been described in AIP subjects with a stable disease who, although they are protected against the recurrence of the acute attacks, may manifest chronic symptoms due to porphyrin accumulation and metabolic disturbances.

Nevertheless, evaluation of metabolic profile and its hepatic manifestations are not yet part of clinical practice, either because AIP is often underestimated and/or misdiagnosed or because the identification of at-risk categories is becoming an emerging issue.

Therefore, we recruited n=14 AIP patients, who are followed by the Rare Diseases Unit at the Fondazione IRCCS Cà Granda Ospedale Maggiore Policlinico of Milan. AIP individuals with informed consent were screened for the metabolic and hepatic profile at the General Medicine and Metabolic Disease Department at the Fondazione IRCCS Cà Granda Ospedale Maggiore Policlinico of Milan.

Firstly, AIP patients were stratified according to the frequency of the attacks as previously reported[24]. Demographic, anthropometric, and clinical features of the AIP cohort are reported in **Table 1**. Due to the low number of study participants, our cohort mainly consisted of asymptomatic AIP subjects, who presented the highest concentration of urinary porphyrins, plus AIP individuals who have had one sporadic attack (n=9, **Stable AIP**) and AIP with recurrent acute events (n=5, **Active AIP**).

	Stable AIP (n=9)	**Active AIP (n=5)**	***P value***
Sex, F	7 (77.77)	5 (100)	/
Age, years	42.77±12.16	44.80±6.87	0.53
ALA, µmol/mmol creatinine	5.25 {4.26-9.76}	3.99 {2.83-8.23}	0.31
PBG, µmol/mmol creatinine	9.15 {2.20-14.14}	10.7 {7.41-14.45}	0.33
Urinary porphyrins, µg/L	411.5 {254.2-978.5}	243 {109-531}	**0.04**
Glycemia, mg/dL	86.44±5.70	82.60±5.12	0.11
Insulin, IU/mL	10.88±5.84	9.16±3.44	0.28
HOMA-IR	2.38±1.37	1.89±0.76	0.30
BMI, kg/m^2	23.77±4.28	25.90±2.72	0.17
ALT, U/L	22.5 {21.25-23.75}	28 {24-33]	0.06
AST, U/L	23 {23-25}	33 {32.5-33.5}	0.07
GTT, U/L	10 {10-10.75}	11 {10-15}	0.14
Triglycerides, mg/dL	75.75±22.77	86.8±22.23	0.20
Total Cholesterol, mg/dL	191.22±30.62	202.4±21.75	0.24
Steatosis, yes	3 (33.33%)	0	/
Fibroscan >7 kPa, yes	5 (55.55%)	0	/
• kPa values	8.42±1.80	5.28±1.38	**0.03**

Table 1. Demographic, anthropometric, and clinical features of AIP patients (n=14), stratified according to the frequency of acute episodes. Values are reported as means ± SD, number (%), or median {interquartile range}, as appropriate. Comparisons among AIP with stable (n=9) or active (n=5) disease were performed through unpaired nonparametric Mann-Whitney test. ALA, aminolaevulinic acid; PBG, porphobilinogen; ALT, alanine aminotransferase; AST, aspartate aminotransferase; GTT, γ-glutamyl transferase, BMI, body mass index, HOMA-IR, homeostasis model assessment-estimated insulin resistance.

AIP patients with stable and active disease showed similar levels of basal glycemia. Higher serum insulin levels at baseline were found in stable AIPs (**Figure 11A**), thereby resembling the results obtained by Solares et al[24]. HOMA-IR values were greater than 1.9 in stable AIPs but less than 2.5, thus suggesting that patients did not experience overt IR but rather they are in early IR condition (**Figure 11B**). Stable AIP were leaner compared to patients with active disease (**Table 1**), and albeit the difference among the two groups did not reach the statistical significance, they were even characterized by less triglycerides and cholesterol levels, possibly reminding the trend observed in AIP mice in which metabolic disturbance were induced by fasting and suggesting that body fat may be mostly utilized by the category of patients with stable AIP (**Table 1**). Attempting to assess energy expenditure capacity, AIP patients underwent impedance testing, which measures the % lean mass, % fat mass and the % of metabolic active muscle cells (BCM). We found that stable AIP had lower % of body fat compared to active AIPs (mean: 25.96% *vs.* 34.78%, p=0.02 at Mann-Whitney, **Figure 11C**). Conversely, %lean mass and %BCM were higher in stable AIP (mean: 74.08% *vs.* 65.22 %, p=0.03 at Mann-Whitney; mean: 42.52% *vs.* 31.84%, p=0.002 at Mann-Whitney, **Figure 11D-E**), and we found a significant positive correlation among the %BCM and %lean mass (p=0.007; **Figure 11F**), thus suggesting that skeletal muscle participates to mechanisms of metabolic compensation in order to meet energy demand, mirroring the PET/CT results obtained in AIP mice, and this phenomenon mainly involves the stable AIP subgroup.

Moreover, we performed OGTT in AIP subjects and evaluated glycemic fluctuations at baseline, 1hour and after 2 hours. At the same timing, serum insulin was monitored in blood samples to assess both glucose and insulin response. At OGTT, stable AIPs showed higher glycemic peak at 1 hour and blood glucose levels remained higher after 2 hours of glucose overload compared to subjects with active disease (**Figure 11G**). Differences between stable and active AIPs were statistically significant at AUC calculated post glucose loading (p=0.02 at Mann-Whitney, **Figure 11H**). Serum insulin reached the peak at 1 hours, the same interval in which we observed the glycemic peak in stable AIPs. According to HOMA-IR results, serum insulin decreased after 2 hours albeit blood glucose concentration remained higher at the same timepoint, thus corroborating that the pre-IR condition may provide a partial response to insulin secretion at re-establishing normoglycemia (**Figure 11I**).

Finally, the role of the liver in AIP pathogenesis is well-established. However, clinical assessment of liver pathology is not a routine healthcare practice for patients monitoring. IR and glucose intolerance may prime the liver to develop related disorders, such as hepatic steatosis, inflammation, fibrosis and, in a less percentage of cases, HCC. Here, we proposed the non-invasive evaluation of hepatic fat accumulation and fibrosis through echography/elastography ultrasound and *Fibroscan*, respectively, which are commonly used in patients affected by obesity, T2DM and NAFLD in order to bypass liver biopsy. Neither steatosis nor fibrosis were detected in AIP patients with active disease, thus supporting that they were less predisposed to metabolic alterations than stable subjects (**Table 1**). 3 out of 9 stable AIPs (33.33%) had mild steatosis, including one with mild fibrosis (kPa=7.5). However, the prevalence of hepatic steatosis worldwide hovers around 30% of the general population, suggesting that the presence of fatty liver in these subjects may reflect the natural epidemiology of this disorder. Noteworthy, 5/9 stable AIPs (55.55%) showed a liver stiffness ranging between 7.3 and 11.6 kPa, which denoted the presence of low-moderate to significative fibrosis (mean: 8.42±1.80 *vs.* 5.28±1.38, p=0.03 at Mann-Whitney, **Table 1**). Attempting to evaluate whether hepatic fibrosis may be related to metabolic alterations, we correlated liver stiffness values with biochemical measurements. We found a significant correlation between urinary ALA and liver stiffness (p=0.01, **Figure 11J**) but not with urinary PBG and total porphyrins, suggesting that although stable AIP patients did not present acute symptoms, they are exposed to a chronic and silent liver damage induced by ALA accumulation. Additionally, a positive correlation with a trend towards significance was found among serum insulin levels, HOMA-IR index, and liver stiffness (p=0.07 and p=0.06, **Figure 11K-L**), thus suggesting that early IR may be even contribute to liver damage.

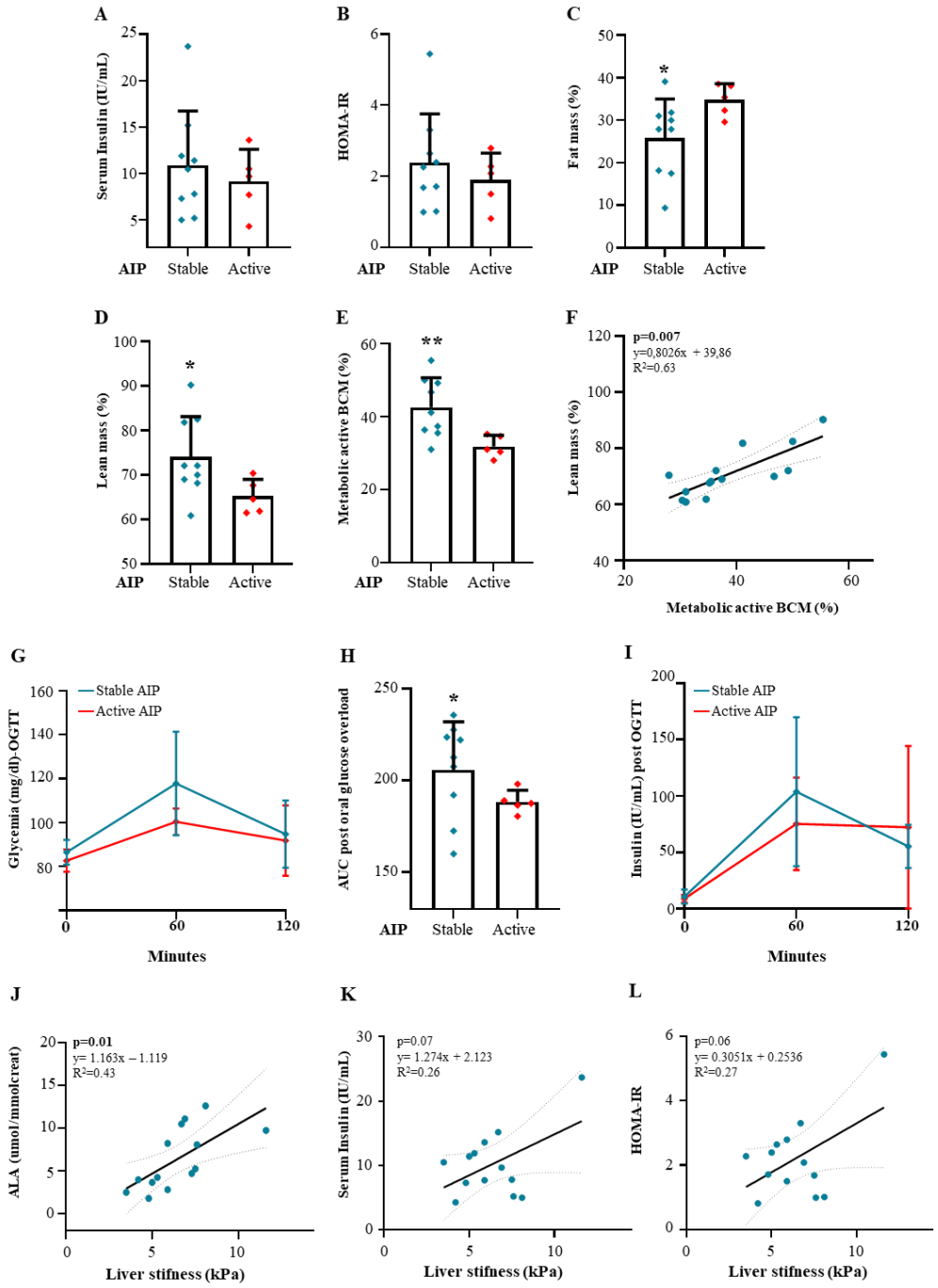

Figure 11. Non-invasive evaluation of metabolic profile and liver disease in AIP patients. A-B) Basal insulinemia and HOMA-IR assessed in AIP patients stratified according to the recurrence of acute symptomatology. **C-E)** Bioimpedancemetric data showing % fat mass, %lean mass and %BCM. F) Simple linear regression correlating %BCM with %lean mass. **G-I)** OGTT, AUC calculation from OGTT curve and ITT measured at baseline, 1h and 2h after 75g glucose overload. **J-L)** Simple linear regression correlating liver stifness values (kPa) with ALA, insulin and HOMA-IR. Data are shown as average and standard deviation (SD). Comparisons between AIP categories were performed through Mann-Whitney nonparametric test.

Discussion

AIP is the most common and severe form of AHPs, a congenital disorder affecting 1/2000 cases in the general population and caused by pathogenic mutations in the *HMBS* gene. Clinical penetrance hovers around 1% *HMBS*-mutation carriers, who may experience the burden of life-threatening and recurrent attacks, which represents a growing life-long discomfort for both patients and relatives[13-15]. Old and new therapeutic approaches, including hemin, glucose in mild cases and givosiran aimed to reduce hepatic ALAS1 activity during the attacks or to prevent the occurrence of the acute episodes. However, several shortcomings emerged with these therapies, including biochemical/clinical relapse, raise in transaminases levels and renal disease[2-9], thereby moving the research towards new frontiers. In particular, the first liver transplantations in AIP patients, who were refractory to treatments, led to two relevant conclusions: 1) the liver exerts a pivotal role in the pathogenesis of AIP and 2) replenishment of normal PBGD activity results in a complete clinical and biochemical remission[10,19,62,63]. Therefore, therapies based on the replacement of *HMBS* genetic defect, PBGD mRNA or protein are under development or refining and they currently represent the breakthrough for AIP care[23,54,69,70].

Despite the medical advances, a new issue is emerging which involves the identification of patients who may benefit from the current therapies, mainly AIP with an active acute symptomatology, and of those who have no treatment available. The larger portion of *HMBS*-mutation carriers (>90%) are asymptomatic or high porphyrin excreters (ASHE), referred to as stable AIP subjects, and, recently, it has been described that stable AIP patients may manifest metabolic alterations related to glucose tolerance and lower insulin sensitivity. Stable AIP subset is not symptom-free as they may present myalgia, abdominal pain, and sleep disorders as well as they may run into chronic kidney disease and HCC, despite being less susceptible to manifest acute attacks. The protection against the acute symptomatology seems to be conferred by hyperinsulinemia as insulin is an endogenous and transcriptional inhibitor of ALAS1[7,24-27,47,84]. Nevertheless, metabolic evaluation of insulin sensitivity and its hepatic implications does not represent a routine clinical practice for AIP management, and its underestimation may lead to the development of IR and related disorders in the long-term[24,49]. Moreover, hyperinsulinemia may limit the efficacy of carbohydrate loading for the treatment of mild or sporadic AIP cases[7,24,25,47,49]. Therefore, throughout the three-years PhD program, the

study focused on elucidating the role of glucidic metabolism and insulin response in *PBGD*-silenced hepatocytes, AIP mice and a small cohort of AIP patients, and to investigate whether the introduction of insulin-sensitizing compounds may be considered as a potential strategy for the correction of metabolic aberrancies in AIP.

In the first part of the study, carried out in human HepG2 cells in which PBGD was transiently silenced and in AIP mice, we assessed the potential efficacy of α-LA on heme biosynthesis, glucose metabolism and insulin sensitivity. Then, we widened the study by assessing a panel of different dietary options with insulin-sensitizing effects, testing both probiotics (alive and heat-killed) and their derivatives, and attempting to provide additional information about the use of insulin-sensitizers in AIP.

Dietary supplementation of α-LA was already tested in diabetic mice and in clinical trials for the treatment of diabetes as it ameliorates glucose homeostasis, insulin sensitivity and glucose uptake in skeletal muscle[86,87]. Moreover, in another type of porphyria (PCT), α-LA had shown antioxidant properties accompanied by reduced symptomatology[26,85,86]. Still, our group has demonstrated that α-LA improved mitochondrial bioenergetics and its turnover in *PBGD*-silenced hepatocytes[25], thereby opening the possibility to deepen α-LA effects even in the field of hepatic porphyrias. Here, we showed that treatment with α-LA either alone or in combination with glucose improved hepatocellular heme content, glycolysis, ATP production and triglyceride release in *PBGD*-silenced hepatocytes. The study *in vitro* highlighted that some of the effects, as the increased heme content, were amenable to α-LA administration alone, and the addition of glucose to cultured medium allowed to determine that it improved glucidic response, thus resembling the results obtained with the treatment with the liver-targeted Ins-ApoA1 in AIP mice by Solares et al[24]. These findings were then corroborated by the *in vivo* studies, in which we observed an increase of heme availability in the liver, possibly due to the direct effect of α-LA at providing substrates for heme synthesis from TCA cycle. Consistent with this hypothesis, in AIP mice drinking α-LA, we found a significant improvement of hepatic citrate synthase activity and ATP content, supporting that the treatment enhanced mitochondrial bioenergetics and respiration.

As previously reported, AIP metabolic and hepatic profile was altered after a stressful condition induced by fasting[45]. Glucose intolerance, hyperinsulinemia, and inability to catabolize hepatic glycogen were observed in fasted AIP mice and even occurred in our

experimental setting. It has been hypothesized that these aberrancies may be attributed to peripheral IR, although none has investigated the hepatic insulin cascade. Here, we demonstrated that hyperinsulinemia, but not hepatic IR, occurs in AIP mice. The high insulin levels detected in the serum of AIP mice was associated with an aberrant activation of insulin signaling during caloric restriction, which may possibly explain the lack of glycogen breakdown to provide glucidic sources, and it cannot be ruled out that the effect of hyperinsulinemia may contribute to the development of IR in the long-term as shown in AIP patients who had developed IR and diabetes[24,49,50].

α-LA treatment in fasted AIP mice showed a great efficacy in normalizing serum insulin levels and it was paralleled by a reduction of fasted glycemia and an improvement of response to moderate/high glucose overload. The re-establishment of eu-insulinemia was followed by the inhibition of the hepatic insulin signaling, suggesting that α-LA fixed the hormonal dysregulation occurring in AIP mice during fasting. Since it has been shown that α-LA improve Glut trafficking in cell membranes of skeletal muscle, we assessed whether hepatic Glut2 expression, which mediates glucose uptake and release according to blood glucose concentration, changed in response to α-LA treatment. We found a strong induction of Glut2 in AIP+α-LA mice and, notably, it was accompanied by an increased glycogenolysis and upregulation of genes involved in gluconeogenesis, thus supporting that Glut2 may respond to low glucose levels in the attempt to enhance glucose export from the liver into the blood during fasting[102]. Additionally, our data has suggested that α-LA ameliorates the ability of AIP to exploit intrahepatic glucidic reserves. Consistent with this hypothesis, the abovementioned high ATP content paralleled by lower lactate levels may be markers of enhanced glycolysis and mitochondrial respiration. Augmented glycolysis and, possibly TCA, may provide acetyl-coA for synthesis of other energy reserves as triglycerides, whose levels were reduced in AIP mice probably as they exploited them as alternative source of energy. In AIP+α-LA, increasing serum triglyceride release, reaching the same values of Wt, has been detected, thereby resembling previous findings obtained with the treatment of the liver-targeted insulin in AIP mice[24]. Moreover, anatomic-functional PET/CT analysis has outlined that AIP mice receiving neither treatments nor vehicle showed defects at internalizing glucose within the liver after the *i.v* injection with the [18F]FDG radiotracer. α-LA tended to increase hepatic glucose absorption, supporting the data obtained with the GTT curves, even

though it did not reach the statistical significance. However, a relevant issue should be mentioned: sugars may alter the ability to pick up [18F]FDG in the liver and brain[100]. In the long-term evaluation of α-LA efficacy, TM was used as vehicle for all dietary compounds, except for *B.coagulans*, and we observed that the Wt hepatic ability to absorb [18F]FDG was lower in those receiving TM, thus suggesting that an important bias in terms of efficacy in glucose uptake needs to be taken into account for the PET/CT analysis. Still, the combination of TM with α-LA did not enhance the efficacy of this molecule at inducing Glut transporters in both the liver and the other insulin-sensitizing organs, alike the additive effects of glucose and α-LA observed *in vitro*, but nevertheless supports that AIP mice with metabolic aberrancies may still benefit of α-LA properties when it is administered alone.

Metabolic disturbances related to hyperinsulinemia and glucidic intolerance may involve the liver and peripheral tissues. Previously, it has been demonstrated that fasted AIP mice exploit white fat reserves in order to provide molecules with high-energy content[24]. Nevertheless, the role of fat deposits as well as of the insulin-responsive organs (as brain and muscle) need to be elucidated and whether insulin-sensitizers may provide beneficial effects even in these tissues has never been explored in AIP context. We performed a preliminary assessment regarding glucose metabolism, body composition, and [18F]FDG uptake in the brain, skeletal muscle, and white/brown adipose tissues. In the pilot study, we found that glycogen accumulated in AIP mice with no treatment, resembling what was observed in the liver, and lipid droplets deposits within the skeletal muscle have been detected in these mice (data not shown), supporting that alterations in glycogen disposal during fasting is also extended to other organs. AIP mice drinking α-LA reduced muscular glycogen stocks and showed higher Glut4 expression, according to the improvement of glucose handling reported in successfully treated T2DM mice[86,87]. The insulin-sensitive Glut3, expressed in the brain, and Glut4 in WAT/BAT, were even induced in AIP+α-LA rodents. In skeletal muscle, the Glut4 translocation in cell membranes, mediated by α-LA, is an insulin-independent mechanism, involving AMPK signal[86] and, due to the high similarity of Gluts structure, it could be speculated that α-LA may act in a similar fashion in inducing tissue-specific Gluts even in the other insulin-sensitive organs. Moreover, these findings may agree with both data from GTT and with those concerning the glucose export from the liver to the other organs: after glucose overload, α-LA may act at systemic

levels by stimulating Glut channels in order to restore normoglycemia, while in fasted state, the improved glucose export from the liver may be distributed to muscle, brain and WAT as physiologically occurs.

Accordingly, at PET/CT analysis, α-LA resulted in the only treatment which enhanced glucose signal by around 20% in the brain, despite the adverse effects induced by TM on [18F]FDG absorption, and it strongly promoted the metabolic activity of skeletal muscle and WAT, but not in BAT. Monitoring of weekly food consumption and BW has supported that AIP mice weigh less than Wt, although they consumed the same amount of food and their fat and lean mass (%/BW) is similar to those detected in Wt, supporting that the reduced weight gain may by justified by high energy expenditure. Even AIP mice drinking α-LA reduced weight gain. Nonetheless, analysis of body composition has shown that this compound reduced the %fat/BW and improved muscular mass (%), arguing that the amelioration of muscle flanked the improvement of energy utilization observed at PET/CT.

Notably, α-LA turned out to be peculiar in its effects on adipose tissues. Despite AIP mice plus α-LA reduced %fat/BW, [18F]FDG signal and ATP content resulted elevated in the WAT, supporting that α-LA stimulates its metabolic activity. Enhanced glucose uptake in WAT is usually associated with anabolic activities including glycolysis, energy production and lipid stocks. Interestingly, after a cold stimulus, α-LA did not increase [18F]FDG uptake in the BAT, likely resulting in less energy dissipation and reflecting the trend observed in Wt groups and in AIP treated with GT. BAT is the principal organ which mediates the dissipation of stored lipids as heat and stimulation of its activity improved body weight and insulin sensitivity in T2DM models, in which visceral adiposity represents one of the most relevant risk factor[101]. According to these findings, AIP mice displayed low BAT activity at baseline probably due to glucose intolerance and hyperinsulinemia. However, they are lean and waste a lot of energy to the extent that BAT responded to cold by increasing its activity more than Wt likely to regulate energy balance. Based on this evidence, the non-activation of the BAT in AIP mice receiving α-LA, similar to what we observed in Wt mice, sustains the improvement of AIP energy status, and it may suggest that this compound avoids energy dissipation from white fat storages attempting to preserve them as energy stocks.

Interesting findings emerged with the use of probiotics and/or their derivatives. In this study, we included three compounds (the heat-killed BLP1, LTA and alive *B. coagulans*) which have shown relevant results for treating metabolic syndrome. BLP1 (CECT 8145 strain) formulated with TM has been exploited in Wistar rats, in which metabolic syndrome was induced by obesogenic cafeteria (CAF) diet and its intake ameliorated insulin sensitivity, dyslipidemia and increased energy expenditure and lean mass. A great efficacy at improving visceral adiposity was found in both CAF dietary model and genetic Zucker fatty rats receiving the CEPT 8145 strain as well as in a randomized controlled trial including obese subjects[90,98,103]. In our experimental setting, AIP mice under BLP1 regimen showed a downward trend of serum insulin levels during caloric restriction which was paralleled by reduced glycemia after a moderate glucose injection (2g/kg) and with no effect after doubling sugar load. Supporting the data from GTT 2g/kg, [18F]FDG signal and Glut2 expression were higher in the livers of BLP1-treated AIP mice, suggestive that BLP1 may improve hepatic glucose absorption. Conversely, in the brain, [18F]FDG had the same traceability as that detected in AIP mice, even if the treatment improved the tissue-specific Glut3. In skeletal muscle, AIP mice receiving BLP1 had strong muscular metabolic activity, evaluated as [18F]FDG uptake, alongside Glut1/4 induction. [18F]FDG signal in the BAT after cold showed the highest levels compared to the other experimental groups, possibly supporting the increased utilization of white lipid deposits to deal with energy request. The enhancement of BAT activity in AIP mice induced by BLP1 may in this case represent a marker of partial improvement when compared to α-LA, as this may represent an adaptive, compensatory mechanism for the provision of energy substrates during stress which may, in the long-term, refuel a vicious cycle leading to maladaptation and new metabolic alterations. Supporting this hypothesis, the improved glucose absorption was not accompanied by changes of lean/fat mass composition, suggesting that BLP1 intake may provide benefits for glucose uptake and biochemical abnormalities, but with only a partial effect on energy expenditure and systemic metabolism.

LTA is one of the cell wall polymers of gram-positive bacteria. Balaguer et al. have recently purified LTA from BLP1 (alive and heat-killed), *Bifidobacterium longum* ES1 and *Bifidobacterium animalis* BB12 and they found that LTA isolated from BLP1 better reduced fat accumulation in *Caenorhabditis elegans*, suggesting that many of the fat-

reducing properties of BLP1 may be attributed to LTA[91]. Therefore, LTA from BLP1 has been proposed as a potential postbiotic treatment for metabolic disorders, although the evaluation of its effectiveness in more complex experimental models is still missing. Here, we first provided the proof of dietary use of LTA in an AIP murine model as we found that it exhibited a greater efficacy to reduce severe hyperglycemia and serum insulin than the bacteria from which it derived. Probably, this discrepancy between LTA and BLP1 efficacy may be explained by the fact that BLP1 may require longer time to modify gut microbiota composition, while LTA (as well as α-LA molecule) may directly act on its target organs to normalize glycemia after glucose overload. At PET/CT, [18F]FDG radioactivity resulted similar between BLP1 and LTA in both the liver and with no changes in the brain tissues, whereas it was strongly internalized in the skeletal muscle. Moreover, LTA enhanced the mechanism of adaptative glucose uptake in the BAT after cold, showing a similar effect of that induced by BLP1. Nonetheless, compared to BLP1, the ability of LTA to induce tissue-specific Gluts was less relevant, suggestive that the effects on Gluts channels may be amenable to other components of the heat-shocked bacteria. Furthermore, reduced weight gain combined to a higher lean/fat mass ratio was found in LTA-treated AIP mice but not in BLP1-treated ones, thus partially resembling the outcomes observed with α-LA on improvement of skeletal muscle energy utilization.

Modifications of gut bacteria diversity have been associated with amelioration of obesity and NAFLD to the extent that dietary consumption of fermented-foods has been proposed as an effective solution to achieve health benefits. *Bifidobacterium* and *Lactobacillus* are the most studied microorganisms used to control body weight and reduce hepatic fat accumulation. However, these strains hardly tolerate the heat and production processes of fortified-foods. Emerging studies have highlighted that *Bacillus* species may confer health advantages and their spores can survive to severe processing conditions. Among them, *B. coagulans* has shown anti-obesity effects and protected against metabolic disturbances induced by high-fat diet in mice[92]. However, the use of *Bacillus* strains is still recent in common disorders and its applications in porphyrias has never been explored. We firstly revealed that *B. coagulans* has a strong effect at restoring fasted serum insulin and it showed the highest rate to re-establish normoglycemia after a severe dose of glucose injection, mirroring the effects obtained with the liver-targeted insulin

and gene therapy. Nevertheless, PET/CT analysis did not highligh changes of hepatic [18F]FDG absorption and Glut1/2 expression, possibly supporting that glucose may be rapidly internalized by the other organs. Reduced weight gain combined to lower fat fraction and higher lean mass fraction were observed in AIP mice drinking the alive bacteria, even if it was associated to lower food weekly consumption probably due to the bad palatability of this diet. According to the increase of lean/fat mass ratio, [18F]FDG tracer was greatly uptaken in the skeletal muscle and it was accompanied by a higher expression of Glut4, thus suggesting that *B. coagulans* ameliorated glucose utilization in this tissue. Concerning energy dissipation, AIP mice treated with *B. coagulans* showed a partial response to cold stress in the BAT and higher glucose absorption in WAT paralleled by the induction of Glut channels in both adipose tissues. Therefore, *B. coagulans* attempted to reduce the adaptive mechanism of BAT and to improve glucose utilization from WAT, without inducing the increase in body weight, possibly to maintain lipid reserves.

Finally, despite AIP has been recognized as a metabolic and hepatic disorder, its diagnosis is often hampered by disease unrecognizability due to aspecific symptoms at the presentation. Hence, the identification of AIP patients and their stratification according to severity of acute manifestation represent a clinical challenge. Only in recent years, it has emerged that these patients should undergo metabolic and hepatic evaluation in order to identify subjects at risk of recurrent acute attacks and those with metabolic abnormalities attempting to address them towards a personalized therapeutic approach. Early studies have reported an abnormal OGTT and hyperinsulinemia in patients with AIP and, in an observational case-control-study, Fontanellas and collaborators have described the presence of IR in AIP patients with clinically stable disease[24,45,104,105]. We also provided a clinical assessment of metabolic features and combined the evaluation of liver disease with non-invasive methods in a small cohort of AIP subjects (n=14), who were stratified according to stable or active acute symptomatology. Paralleling metabolic profile, AIP patients underwent bioimpedance analysis, which has shown interesting findings as concerns their energetic balance. As observed in AIP mice, which showed a great muscular energy expenditure without changes in % of lean and fat mass, a higher % metabolic active cells in skeletal muscle, correlating with %lean mass fraction, was found in stable AIP patients compared to those with acute attacks, suggesting that most

of the muscle mass in AIP patients pushed their metabolic activity compared to those with active AIP. Similarly, stable AIPs were characterized by a condition of early IR, as they presented altered OGTT curve paralleled by higher insulin levels and HOMA-IR. Therefore, stable AIP patients showed both signs of early hyperinsulinemia and muscle hypermetabolism, possibly being part of an adaptive para-physiologic mechanism to prevent energy substrate deficiency and neurotoxins' accumulation associated with acute attacks. Despite hyperinsulinemia, overt IR was not found in our case series, probably due to the low number of cases. This hypothesis is consistent with data obtained in the AIP murine model, in which hyperinsulinemia, but not peripheral IR, was detected. Likely, development of IR may require chronic stimulations with triggers of metabolic dysfunction in mice (as fasting) or other factors as aging. Notably, hepatic evaluation with Fibroscan has highlighted the presence of mild-moderate fibrosis in 5 out of 9 stable AIP cases but not in active ones. Liver stiffness values were significantly correlated with urinary ALA, suggesting a direct role of this porphyrin to induce liver damage, and showed a positive correlation with insulin levels and HOMA-IR, corroborating that metabolic and hepatic screening should be introduced for monitoring and management of AIP.

Conclusions and future perspectives

In sum, the study shed light on the role of insulin-mimetics compounds in the context of AIP. First, we deeply investigated the role of α-LA in AIP, a safe, well-tolerated molecule which has shown attractive properties for the treatment of metabolic dysfunction. α-LA was proposed for the treatment of hepatic porphyrias in one study (specifically in PCT), but further analyses were required to characterize its functions. Briefly, we demonstrated that α-LA improved glucose metabolism, hyperinsulinemia and hepatic dysfunction occurring in AIP upon caloric restriction, ameliorating glucose uptake in insulin-sensitive organs and protecting them against the excessive energy expenditure.

Food supplementation with several probiotic strains and/or their structural components are widely used strategies which may provide health benefits in metabolic disorders, especially those where the increased adiposity represents the major risk factor (obesity, T2DM, NAFLD). These compounds mainly modify intestinal microbial composition and stimulate fat disposal in both the liver and WAT. Lipid breakdown may be mediated by lipolysis mechanisms or be dissipated as heat by BAT, resulting in an improvement of body mass index and insulin sensitivity. Here, we found that the use of probiotics (heat-killed or alive) or postbiotic ameliorated glucose tolerance and insulinemia and they boosted BAT activation, an adaptive mechanism observed in AIP mice after cold stress, but not in Wt ones, probably to meet energy requests. Nonetheless, AIP mice are neither obese nor diabetic, and, although biochemical and glucidic response were improved, a careful monitoring of their energetic status after the prolonged supplementation with these diets should be considered.

Further analysis and issues concerning this study need to be elucidated. One of them will be the evaluation of thermogenesis and metabolic utilization of nutritional substrates in order to increase the knowledge about the contribution of BAT in AIP pathogenesis. As for the liver, an extensive analysis of insulin signaling should be provided for the other organs attempting to assess whether the aberrant activation of insulin signaling even arose in the peripheral tissues and to deepen the mechanisms of action of the diets. Furthermore, over the course of the treatments, we collected fresh feces for the analysis of gut microbiome, a field that has never been described in AIP, in the attempt to evaluate whether dietary treatments induced relevant changes of intestinal bacteria composition.

Limitations of the study mostly include the low number of AIP patients who have been enrolled for the evaluation of metabolic/hepatic profile. Nonetheless, bioimpedance analysis and GTT curve have provided interesting differences among stable AIP patients, which showed signs of early IR associated to a high % of muscle activity, and active AIP subjects. Moreover, liver fibrosis was non-invasively identified in more than half of stable AIP patients, opening up the clinical perspective of proposing metabolic assessment to these patients for a personalized therapy. To conclude, the translatability of these results into a clinical trial, combining the assessment of systemic metabolism focusing on glucidic one and energetic balance, with the goal to identify AIP patients at metabolic risk, and the use of dietary interventions, does seem achievable in the foreseeable future.

References

1 Jericó, D. *et al.* Recent Insights into the Pathogenesis of Acute Porphyria Attacks and Increasing Hepatic PBGD as an Etiological Treatment. *Life* **12** (2022).

2 Balwani, M. *et al.* Phase 3 Trial of RNAi Therapeutic Givosiran for Acute Intermittent Porphyria. *The New England journal of medicine* **382**, 2289-2301, doi:10.1056/NEJMoa1913147 (2020).

3 Herrero, C., Badenas, C., Aguilera, P. & To-Figueras, J. [Acute intermittent porphyria: Long-term follow up of 35 patients]. *Medicina clinica* **145**, 332-337, doi:10.1016/j.medcli.2014.06.012 (2015).

4 Kuo, H.-C., Lin, C.-N. & Tang, Y.-F. Prophylactic Heme Arginate Infusion for Acute Intermittent Porphyria. *Frontiers in pharmacology* **12**, doi:10.3389/fphar.2021.712305 (2021).

5 Willandt, B. *et al.* Liver Fibrosis Associated with Iron Accumulation Due to Long-Term Heme-Arginate Treatment in Acute Intermittent Porphyria: A Case Series. *JIMD reports* **25**, 77-81, doi:10.1007/8904_2015_458 (2016).

6 To-Figueras, J. *et al.* Dysregulation of homocysteine homeostasis in acute intermittent porphyria patients receiving heme arginate or givosiran. *Journal of inherited metabolic disease* **44**, 961-971, doi:10.1002/jimd.12391 (2021).

7 Di Pierro, E. & Granata, F. Nutrients and Porphyria: An Intriguing Crosstalk. **21**, doi:10.3390/ijms21103462 (2020).

8 Fontanellas, A., Ávila, M. A., Arranz, E., Enríquez de Salamanca, R. & Morales-Conejo, M. Acute intermittent porphyria, givosiran, and homocysteine. *Journal of inherited metabolic disease* **44**, 790-791, doi:10.1002/jimd.12411 (2021).

9 Ventura, P. *et al.* Hyperhomocysteinemia in patients with acute porphyrias: A potentially dangerous metabolic crossroad? *European journal of internal medicine* **79**, 101-107, doi:10.1016/j.ejim.2020.04.002 (2020).

10 Balwani, M. *et al.* Acute hepatic porphyrias: Recommendations for evaluation and long-term management. *Hepatology* **66**, 1314-1322, doi:10.1002/hep.29313 (2017).

11 Stein, P. E., Badminton, M. N. & Rees, D. C. Update review of the acute porphyrias. *British journal of haematology* **176**, 527-538, doi:https://doi.org/10.1111/bjh.14459 (2017).

12 Phillips, J. D. Heme biosynthesis and the porphyrias. *Molecular genetics and metabolism* **128**, 164-177, doi:10.1016/j.ymgme.2019.04.008 (2019).

13 Bonkovs.ky, H. L. *et al.* Acute porphyrias in the USA: features of 108 subjects from porphyrias consortium. *Am J Med* **127**, 1233-1241, doi:10.1016/j.amjmed.2014.06.036 (2014).

14 Kauppinen, R. Porphyrias. *Lancet (London, England)* **365**, 241-252, doi:10.1016/s0140-6736(05)17744-7 (2005).

15 Puy, H., Gouya, L. & Deybach, J. C. Porphyrias. *Lancet (London, England)* **375**, 924-937, doi:10.1016/s0140-6736(09)61925-5 (2010).

16 Frei, P. *et al.* Liver Transplantation because of Acute Liver Failure due to Heme Arginate Overdose in a Patient with Acute Intermittent Porphyria. *Case Reports in Gastroenterology* **6**, 190-196, doi:10.1159/000338354 (2012).

17 Soonawalla, Z. F. *et al.* Liver transplantation as a cure for acute intermittent porphyria. *Lancet (London, England)* **363**, 705-706, doi:10.1016/s0140-6736(04)15646-8 (2004).

18 Stein, P., Badminton, M., Barth, J., Rees, D. & Stewart, M. F. Best practice guidelines on clinical management of acute attacks of porphyria and their complications. *Annals of Clinical Biochemistry* **50**, 217-223, doi:10.1177/0004563212474555 (2013).

19 Singal, A. K. *et al.* Liver transplantation in the management of porphyria. *Hepatology (Baltimore, Md.)* **60**, 1082-1089, doi:10.1002/hep.27086 (2014).

20 Honor, A., Rudnick, S. R. & Bonkovs.ky, H. L. Givosiran to treat acute porphyria. *Drugs of today (Barcelona, Spain : 1998)* **57**, 47-59, doi:10.1358/dot.2021.57.1.3230207 (2021).

21 Fontanellas, A., Ávila, M. A., Anderson, K. E. & Deybach, J. C. Current and innovative emerging therapies for porphyrias with hepatic involvement. *Journal of hepatology* **71**, 422-433, doi:10.1016/j.jhep.2019.05.003 (2019).

22 Fontanellas, A., Ávila, M. A. & Berraondo, P. Emerging therapies for acute intermittent porphyria. *Expert reviews in molecular medicine* **18**, e17, doi:10.1017/erm.2016.18 (2016).

23 Córdoba, K. M. & Serrano-Mendioroz, I. Recombinant porphobilinogen deaminase targeted to the liver corrects enzymopenia in a mouse model of acute intermittent porphyria. **14**, eabc0700, doi:10.1126/scitranslmed.abc0700 (2022).

24 Solares, I. *et al.* High Prevalence of Insulin Resistance in Asymptomatic Patients with Acute Intermittent Porphyria and Liver-Targeted Insulin as a Novel Therapeutic Approach. *Biomedicines* **9**, 255 (2021).

25 Longo, M. *et al.* α-Lipoic Acid Improves Hepatic Metabolic Dysfunctions in Acute Intermittent Porphyria: A Proof-of-Concept Study. *Diagnostics* **11**, doi:10.3390/diagnostics11091628 (2021).

26 Vilas, G. L., Aldonatti, C., San Martín de Viale, L. C. & Ríos de Molina, M. C. Effect of alpha lipoic acid amide on hexachlorobenzene porphyria. *Biochemistry and molecular biology international* **47**, 815-823, doi:10.1080/15216549900201903 (1999).

27 Longo, M., Paolini, E., Meroni, M. & Dongiovanni, P. Cutting-Edge Therapies and Novel Strategies for Acute Intermittent Porphyria: Step-by-Step towards the Solution. *Biomedicines* **10**, 648 (2022).

28 Baumann, K. & Kauppinen, R. Penetrance and predictive value of genetic screening in acute porphyria. *Molecular genetics and metabolism* **130**, 87-99, doi:10.1016/j.ymgme.2020.02.003 (2020).

29 Lenglet, H. *et al.* From a dominant to an oligogenic model of inheritance with environmental modifiers in acute intermittent porphyria. *Human molecular genetics* **27**, 1164-1173, doi:10.1093/hmg/ddy030 (2018).

30 Chretien, S. *et al.* Alternative transcription and splicing of the human porphobilinogen deaminase gene result either in tissue-specific or in housekeeping expression. *Proceedings of the National Academy of Sciences of the United States of America* **85**, 6-10, doi:10.1073/pnas.85.1.6 (1988).

31 Chen, C. H., Astrin, K. H., Lee, G., Anderson, K. E. & Desnick, R. J. Acute intermittent porphyria: identification and expression of exonic mutations in the hydroxymethylbilane synthase gene. An initiation codon missense mutation in the housekeeping transcript causes "variant acute intermittent porphyria" with normal expression of the erythroid-specific enzyme. *The Journal of clinical investigation* **94**, 1927-1937, doi:10.1172/jci117543 (1994).

32 Petersen, N. E. *et al.* Mutation screening by denaturing gradient gel electrophoresis in North American patients with acute intermittent porphyria. *Clinical chemistry* **44**, 1766-1768 (1998).

33 De Siervi, A. *et al.* Identification and characterization of hydroxymethylbilane synthase mutations causing acute intermittent porphyria: evidence for an ancestral founder of the common G111R mutation. *American journal of medical genetics* **86**, 366-375 (1999).

34 Ma, L., Tian, Y., Peng, C., Zhang, Y. & Zhang, S. Recent advances in the epidemiology and genetics of acute intermittent porphyria. *Intractable Rare Dis Res* **9**, 196-204, doi:10.5582/irdr.2020.03082 (2020).

35 Andersson, C., Floderus, Y., Wikberg, A. & Lithner, F. The W198X and R173W mutations in the porphobilinogen deaminase gene in acute intermittent porphyria have higher clinical penetrance than R167W. A population-based study. *Scandinavian journal of clinical and laboratory investigation* **60**, 643-648, doi:10.1080/003655100300054891 (2000).

36 Fu, Y. *et al.* Systematically Analyzing the Pathogenic Variations for Acute Intermittent Porphyria. *Frontiers in pharmacology* **10**, 1018-1018, doi:10.3389/fphar.2019.01018 (2019).

37 Chung, J., Chen, C. & Paw, B. H. Heme metabolism and erythropoiesis. *Current opinion in hematology* **19**, 156-162, doi:10.1097/MOH.0b013e328351c48b (2012).

38 Brennan, M. J. & Cantrill, R. C. Delta-Aminolaevulinic acid and amino acid neurotransmitters. *Molecular and cellular biochemistry* **38 Spec No**, 49-58, doi:10.1007/bf00235687 (1981).

39 Laafi, J. *et al.* Pro-oxidant effect of ALA is implicated in mitochondrial dysfunction of HepG2 cells. *Biochimie* **106**, 157-166, doi:10.1016/j.biochi.2014.08.014 (2014).

40 Huang, M. L., Lane, D. J. & Richardson, D. R. Mitochondrial mayhem: the mitochondrion as a modulator of iron metabolism and its role in disease. *Antioxid Redox Signal* **15**, 3003-3019, doi:10.1089/ars.2011.3921 (2011).

41 Onuki, J. *et al.* Mitochondrial and nuclear DNA damage induced by 5-aminolevulinic acid. *Arch Biochem Biophys* **432**, 178-187, doi:10.1016/j.abb.2004.09.030 (2004).

42 Dowman, J. K. *et al.* Liver transplantation for acute intermittent porphyria is complicated by a high rate of hepatic artery thrombosis. *Liver Transplantation* **18**, 195-200, doi:https://doi.org/10.1002/lt.22345 (2012).

43 Dowman, J. K., Gunson, B. K., Bramhall, S., Badminton, M. N. & Newsome, P. N. Liver transplantation from donors with acute intermittent porphyria. *Annals of internal medicine* **154**, 571-572, doi:10.7326/0003-4819-154-8-201104190-00015 (2011).

44 Matkovic, L. B., D'Andrea, F., Fornes, D., San Martín de Viale, L. C. & Mazzetti, M. B. How porphyrinogenic drugs modeling acute porphyria impair the hormonal status that regulates glucose metabolism. Their relevance in the onset of this disease. *Toxicology* **290**, 22-30, doi:https://doi.org/10.1016/j.tox.2011.08.014 (2011).

45 Collantes, M. *et al.* Glucose metabolism during fasting is altered in experimental porphobilinogen deaminase deficiency. *Human molecular genetics* **25**, 1318-1327, doi:10.1093/hmg/ddw013 (2016).

46 García-Diz, L. *et al.* Assessing nutritional status of acute intermittent porphyria patients. *European journal of clinical investigation* **42**, 943-952, doi:https://doi.org/10.1111/j.1365-2362.2012.02673.x (2012).

47 Storjord, E. *et al.* Lifestyle factors including diet and biochemical biomarkers in acute intermittent porphyria: Results from a case-control study in northern Norway. *Molecular genetics and metabolism* **128**, 254-270, doi:https://doi.org/10.1016/j.ymgme.2018.12.006 (2019).

48 Wilcox, G. Insulin and insulin resistance. *The Clinical biochemist. Reviews* **26**, 19-39 (2005).

49 Andersson, C., Bylesjö, I. & Lithner, F. Effects of diabetes mellitus on patients with acute intermittent porphyria. *Journal of internal medicine* **245**, 193-197, doi:10.1046/j.1365-2796.1999.0448e.x (1999).

50 Lithner, F. Beneficial Effect of Diabetes on Acute Intermittent Porphyria. *Diabetes care* **25**, 797-798, doi:10.2337/diacare.25.4.797 (2002).

51 Waxman, A. D., Berk, P. D., Schalch, D. O. N. & Tschudy, D. P. Isolated Adrenocorticotrophic Hormone Deficiency in Acute Intermittent Porphyria. *Annals of internal medicine* **70**, 317-323, doi:10.7326/0003-4819-70-2-317 (1969).

52 Oliveri, L. M., Davio, C., Batlle, A. M. & Gerez, E. N. ALAS1 gene expression is down-regulated by Akt-mediated phosphorylation and nuclear exclusion of FOXO1 by vanadate in diabetic mice. *Biochem J* **442**, 303-310, doi:10.1042/bj20111005 (2012).

53 Ramanujam, V. S. & Anderson, K. E. Porphyria Diagnostics-Part 1: A Brief Overview of the Porphyrias. *Current protocols in human genetics* **86**, 17.20.11-17.20.26, doi:10.1002/0471142905.hg1720s86 (2015).

54 Berraondo, P., Martini, P. G. V. & Avila, M. A. Messenger RNA therapy for rare genetic metabolic diseases. **68**, 1323-1330, doi:10.1136/gutjnl-2019-318269 (2019).

55 Schmitt, C. *et al.* Recurrent attacks of acute hepatic porphyria: major role of the chronic inflammatory response in the liver. *Journal of internal medicine* **284**, 78-91, doi:10.1111/joim.12750 (2018).

56 Homedan, C. *et al.* Acute intermittent porphyria causes hepatic mitochondrial energetic failure in a mouse model. *The international journal of biochemistry & cell biology* **51**, 93-101, doi:10.1016/j.biocel.2014.03.032 (2014).

57 Homedan, C. *et al.* Mitochondrial energetic defects in muscle and brain of a Hmbs−/− mouse model of acute intermittent porphyria. *Human molecular genetics* **24**, 5015-5023, doi:10.1093/hmg/ddv222 (2015).

58 Solares, I. *et al.* Management of hyponatremia associated with acute porphyria-proposal for the use of tolvaptan. *Ann Transl Med* **8**, 1098-1098, doi:10.21037/atm-20-1529 (2020).

59 Pischik, E. & Kauppinen, R. An update of clinical management of acute intermittent porphyria. *Appl Clin Genet* **8**, 201-214, doi:10.2147/TACG.S48605 (2015).

60 Elder, G. H. & Hift, R. J. Treatment of acute porphyria. *Hospital medicine (London, England : 1998)* **62**, 422-425, doi:10.12968/hosp.2001.62.7.1613 (2001).

61 O'Malley, R., Rao, G., Stein, P. & Bandmann, O. Porphyria: often discussed but too often missed. **18**, 352-358, doi:10.1136/practneurol-2017-001878 (2018).

62 Soonawalla, Z. F. *et al.* Liver transplantation as a cure for acute intermittent porphyria. *The Lancet* **363**, 705-706, doi:10.1016/S0140-6736(04)15646-8 (2004).

63 Gilles, A. *et al.* Expert consensus statement on acute hepatic porphyria in Belgium. *Acta Clinica Belgica*, 1-7, doi:10.1080/17843286.2021.1961056 (2021).

64 Lissing, M. *et al.* Liver Transplantation for Acute Intermittent Porphyria. **27**, 491-501, doi:10.1002/lt.25959 (2021).

65 D'Avola, D. & Gonzalez Aseguinolaza, G. Prospect and progress of gene therapy in acute intermittent porphyria. *Expert Opinion on Orphan Drugs* **4**, 711-717, doi:10.1080/21678707.2016.1191346 (2016).

66 Yasuda, M. *et al.* RNAi-mediated silencing of hepatic Alas1 effectively prevents and treats the induced acute attacks in acute intermittent porphyria mice. *Proceedings of the National Academy of Sciences of the United States of America* **111**, 7777-7782, doi:10.1073/pnas.1406228111 (2014).

67 Chan, A. *et al.* Preclinical Development of a Subcutaneous ALAS1 RNAi Therapeutic for Treatment of Hepatic Porphyrias Using Circulating RNA Quantification. *Mol Ther Nucleic Acids* **4**, e263-e263, doi:10.1038/mtna.2015.36 (2015).

68 Sardh, E. *et al.* Phase 1 Trial of an RNA Interference Therapy for Acute Intermittent Porphyria. *New England Journal of Medicine* **380**, 549-558, doi:10.1056/NEJMoa1807838 (2019).

69 Jericó, D. *et al.* mRNA-based therapy in a rabbit model of variegate porphyria offers new insights into the pathogenesis of acute attacks. *Molecular Therapy - Nucleic Acids* **25**, 207-219, doi:10.1016/j.omtn.2021.05.010 (2021).

70 Unzu, C. *et al.* Porphobilinogen deaminase over-expression in hepatocytes, but not in erythrocytes, prevents accumulation of toxic porphyrin precursors in a mouse model of acute intermittent porphyria. *Journal of hepatology* **52**, 417-424, doi:10.1016/j.jhep.2009.09.003 (2010).

71 Meroni, M. *et al.* Mboat7 down-regulation by hyper-insulinemia induces fat accumulation in hepatocytes. *EBioMedicine* **52**, 102658, doi:10.1016/j.ebiom.2020.102658 (2020).

72 Longo, M. *et al.* TM6SF2/PNPLA3/MBOAT7 Loss-of-Function Genetic Variants Impact on NAFLD Development and Progression Both in Patients and in In Vitro Models. *Cellular and Molecular Gastroenterology and Hepatology* **13**, 759-788, doi:https://doi.org/10.1016/j.jcmgh.2021.11.007 (2022).

73 Li, C. & Samulski, R. J. Engineering adeno-associated virus vectors for gene therapy. *Nat Rev Genet* **21**, 255-272, doi:10.1038/s41576-019-0205-4 (2020).

74 Unzu, C. *et al.* Transient and intensive pharmacological immunosuppression fails to improve AAV-based liver gene transfer in non-human primates. *Journal of translational medicine* **10**, 122, doi:10.1186/1479-5876-10-122 (2012).

75 Unzu, C. *et al.* Helper-dependent adenovirus achieve more efficient and persistent liver transgene expression in non-human primates under immunosuppression. *Gene therapy* **22**, 856-865, doi:10.1038/gt.2015.64 (2015).

76 Unzu, C. *et al.* Sustained enzymatic correction by rAAV-mediated liver gene therapy protects against induced motor neuropathy in acute porphyria mice. *Molecular therapy : the journal of the American Society of Gene Therapy* **19**, 243-250, doi:10.1038/mt.2010.210 (2011).

77 Pañeda, A. *et al.* Safety and liver transduction efficacy of rAAV5-cohPBGD in nonhuman primates: a potential therapy for acute intermittent porphyria. *Human gene therapy* **24**, 1007-1017, doi:10.1089/hum.2013.166 (2013).

78 Rogers, G. L. *et al.* Plasmacytoid and conventional dendritic cells cooperate in crosspriming AAV capsid-specific CD8(+) T cells. *Blood* **129**, 3184-3195, doi:10.1182/blood-2016-11-751040 (2017).

79 Meliani, A. *et al.* Antigen-selective modulation of AAV immunogenicity with tolerogenic rapamycin nanoparticles enables successful vector re-administration. *Nature communications* **9**, 4098, doi:10.1038/s41467-018-06621-3 (2018).

80 Serrano-Mendioroz, I. *et al.* An Inducible Promoter Responsive to Different Porphyrinogenic Stimuli Improves Gene Therapy Vectors for Acute Intermittent Porphyria. *Human gene therapy* **29**, 480-491, doi:10.1089/hum.2017.056 (2018).

81 Serrano-Mendioroz, I. *et al.* Bioengineered PBGD variant improves the therapeutic index of gene therapy vectors for acute intermittent porphyria. *Human molecular genetics* **27**, 3688-3696, doi:10.1093/hmg/ddy283 (2018).

82 Jiang, L. & Berraondo, P. Systemic messenger RNA as an etiological treatment for acute intermittent porphyria. **24**, 1899-1909, doi:10.1038/s41591-018-0199-z (2018).

83 Ardaiz, N. *et al.* Insulin Fused to Apolipoprotein A-I Reduces Body Weight and Steatosis in DB/DB Mice. *Frontiers in pharmacology* **11**, 591293-591293, doi:10.3389/fphar.2020.591293 (2021).

84 Solares, I. *et al.* Understanding Carbohydrate Metabolism and Insulin Resistance in Acute Intermittent Porphyria. *International journal of molecular sciences* **24** (2023).

85 Székely, E., Szentmihályi, K., Tasnádi, G., Várnai, K. & Blázovics, A. Effect of alpha-lipoic acid on the porphyria cutanea tarda patients with type 2 diabetes mellitus and heavy drinkers. *Z Gastroenterol* **43**, 136, doi:10.1055/s-2005-869783 (2005).

86 Székely, E. *et al.* Secunder prevention with alpha-lipoic acid and vitamin E in porphyria cutanea tarda patients. *Z Gastroenterol* **46**, A103 (2008).

87 Shay, K. P., Moreau, R. F., Smith, E. J., Smith, A. R. & Hagen, T. M. Alpha-lipoic acid as a dietary supplement: molecular mechanisms and therapeutic potential. *Biochimica et biophysica acta* **1790**, 1149-1160, doi:10.1016/j.bbagen.2009.07.026 (2009).

88 Papanas, N. & Ziegler, D. Efficacy of α-lipoic acid in diabetic neuropathy. *Expert opinion on pharmacotherapy* **15**, 2721-2731, doi:10.1517/14656566.2014.972935 (2014).

89 Uusitupa, H. M. *et al.* Bifidobacterium animalis subsp. lactis 420 for Metabolic Health: Review of the Research. *Nutrients* **12**, doi:10.3390/nu12040892 (2020).

90 Caimari, A. *et al.* Heat-killed Bifidobacterium animalis subsp. Lactis CECT 8145 increases lean mass and ameliorates metabolic syndrome in cafeteria-fed obese rats. *Journal of Functional Foods* **38**, 251-263, doi:https://doi.org/10.1016/j.jff.2017.09.029 (2017).

91 Balaguer, F. *et al.* Lipoteichoic acid from Bifidobacterium animalis subsp. lactis BPL1: a novel postbiotic that reduces fat deposition via IGF-1 pathway. *Microbial Biotechnology* **15**, 805-816, doi:https://doi.org/10.1111/1751-7915.13769 (2022).

92 Urtasun, R. *et al.* A Combination of Apple Vinegar Drink with Bacillus coagulans Ameliorates High Fat Diet-Induced Body Weight Gain, Insulin Resistance and Hepatic Steatosis. *Nutrients* **12** (2020).

93 Hsiao, K. J., Lee, F. Y., Wu, S. J. & Chang, W. J. Determination of erythrocyte porphobilinogen deaminase activity using porphobilinogen as substrate. *Clinica chimica acta; international journal of clinical chemistry* **168**, 257-258, doi:10.1016/0009-8981(87)90296-8 (1987).

94 Lindberg, R. L. *et al.* Porphobilinogen deaminase deficiency in mice causes a neuropathy resembling that of human hepatic porphyria. *Nature genetics* **12**, 195-199, doi:10.1038/ng0296-195 (1996).

95 Najafi, N., Mehri, S., Ghasemzadeh Rahbardar, M. & Hosseinzadeh, H. Effects of alpha lipoic acid on metabolic syndrome: A comprehensive review. *Phytotherapy Research* **36**, 2300-2323, doi:https://doi.org/10.1002/ptr.7406 (2022).

96 Watanabe, Y. *et al.* Exogenous Glucose Administration Impairs Glucose Tolerance and Pancreatic Insulin Secretion during Acute Sepsis in Non-Diabetic Mice. *PLOS ONE* **8**, e67716, doi:10.1371/journal.pone.0067716 (2013).

97 Liu, Z., Patil, I., Sancheti, H., Yin, F. & Cadenas, E. Effects of Lipoic Acid on High-Fat Diet-Induced Alteration of Synaptic Plasticity and Brain Glucose Metabolism: A PET/CT and 13C-NMR Study. *Scientific reports* **7**, 5391, doi:10.1038/s41598-017-05217-z (2017).

98 Pedret, A. *et al.* Effects of daily consumption of the probiotic Bifidobacterium animalis subsp. lactis CECT 8145 on anthropometric adiposity biomarkers in abdominally obese subjects: a randomized controlled trial. *International Journal of Obesity* **43**, 1863-1868, doi:10.1038/s41366-018-0220-0 (2019).

99 Grundy, S. M. *et al.* Diagnosis and management of the metabolic syndrome: an American Heart Association/National Heart, Lung, and Blood Institute Scientific Statement. *Circulation* **112**, 2735-2752, doi:10.1161/circulationaha.105.169404 (2005).

100 Sprinz, C. *et al.* Effects of blood glucose level on 18F fluorodeoxyglucose (18F-FDG) uptake for PET/CT in normal organs: an analysis on 5623 patients. *Scientific reports* **8**, 2126, doi:10.1038/s41598-018-20529-4 (2018).

101 Maliszewska, K. & Kretowski, A. Brown Adipose Tissue and Its Role in Insulin and Glucose Homeostasis. **22**, doi:10.3390/ijms22041530 (2021).

102 Thorens, B. GLUT2, glucose sensing and glucose homeostasis. *Diabetologia* **58**, 221-232, doi:10.1007/s00125-014-3451-1 (2015).

103 Carreras, N. L. *et al.* Anti-obesity properties of the strain Bifidobacterium animalis subsp. lactis CECT 8145 in Zücker fatty rats. *Beneficial microbes* **9**, 629-641, doi:10.3920/bm2017.0141 (2018).

104 Stein, J. A. & Tschudy, D. P. Acute intermittent porphyria. A clinical and biochemical study of 46 patients. *Medicine* **49**, 1-16 (1970).

105 Sixel-Dietrich, F., Verspohl, F. & Doss, M. Hyperinsulinemia in acute intermittent porphyria. *Horm Metab Res* **17**, 375-376, doi:10.1055/s-2007-1013547 (1985).